Alma Mater Studiorum – Università di Bologna

DOTTORATO DI RICERCA IN

Ingegneria Civile, Chimica, Ambientale e dei Materiali

Ciclo XXXI

Settore Concorsuale: 09/D1

Settore Scientifico Disciplinare: ING-IND/22 Scienze e tecnologie dei materiali

Polyhydroxyalkanoates for advanced applications

Presentata da: Giacomo Foli

Coordinatore Dottorato Prof. Luca Vittuari

Supervisore Prof.ssa Paola Fabbri

Esame finale anno 2019

Abstract

Polyhydroxyalkanoates (PHAs) are a group of biobased, biodegradable and biocompatible polyesters, synthetized by bacterial enzymes through fermentation processes utilizing even agricultural wastes as feedstock, that represent a promising alternative to currently used petroleum-based polymers. Among various produced PHAs, poly(3-hydroxybutyrate) (PHB) and the copolymer poly(3-hydroxybutyarte-*co*-3-hydroxyvalerate-*co*-4-hydroxyvalerate) (PHBVV) are nowadays intensively studied. Such polyesters are intriguing candidates as fully biobased and biodegradable polymeric matrix, which can be reinforced to obtain composites with enhanced thermal and mechanical properties. Using a novel approach, water-suspended micro-fibrillated cellulose (MFC) was dispersed into a PHA matrix through thermo-mechanical mixing by using a suitable polymeric dispersing agent. SEM images confirms obtainment of good dispersion and encourage further investigation. Furthermore, considering biocompatibility of PHAs, realization of PHB and PHBVV scaffolds for tissue engineering, filled with osteoinductive inorganic particles, were prepared. Preliminary in vitro investigations showed promising results and further analyses are currently ongoing.

To improve and tune intrinsic excellent PHAs properties, and possibly extend polyesters applications, post-polymerization macromolecular chains modifications were attempted.

After a PHB and PHBVV fully characterization by conventional chromatographic, thermal and spectroscopic analyses, a more complete characterization has been achieved by end-groups analyses through a herein proposed new ^{19}F-NMR method, which allows to overcome typical disadvantages and drawbacks of traditional techniques. The ^{19}F-NMR method reveled to be a simple and fast analytical tool for characterizing PHB derivatives and planning further reactions to obtain useful PHB-based macromonomers, as the herein presented UV-sensible PHB-based segments. Following the successful utilization of PHB-based cross-linking agent mixed with a liquid commercial methacrylate monomer in stereolithography 3D printing, demonstrating the real possible application of the synthesized material, a new green solvent-free preparation procedure was established.

In this dissertation, a wide range of possible methodologies for PHAs properties modification have been proposed and all prepared materials can be envisioned in several various technological applications.

Summary

1. Introduction

Poly(hydroxyalkanoate)s, PHAs (**Figure 1**), are a group of polyesters characterized by impressive properties of biodegradability, biocompatibility and bioresorbability.[1] They was firstly recognized as natural polymers by the French biologist Lemoigne in 1927.[2]

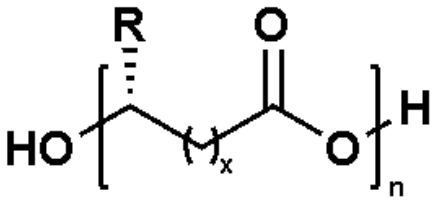

Figure 1. General structure of bacterial PHA: x = 1, Poly([R]-3-hydroxyalkanoate)s; x = 2, Poly([R]-4-hydroxyalkanoate)s.

At the time, he recognized that the β-hydroxybutyric acid, known also as 3-hydroxybutyric acid, obtained by autolysis of a studied bacterium was resulted from a depolymerization of an internal reservoir of carbon. It was the first reported observation of poly([R]-3-hydroxybutyrate), PHB, a particular PHA bearing a methyl moiety as lateral R group. It was later discovered that PHAs are a group of natural polyesters completely synthesized as enantiopure isotactic polymers by microorganisms from various substrates and accumulated as an intracellular carbon source.[3] (**Figure 2**)

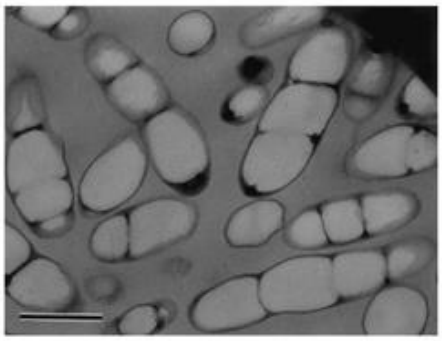

Figure 2. Transmission electron micrograph of thin sections of recombinant R. eutropha PHB$^-$ 4 cells containing large amounts (90% of the dry cell weight) of Poly(3HB-*co*-5mol% 3HHx). Bar represents 0.5 µm. Reproduced with permission of Elsevier from **[49]**.

Such a process is due to the presence, in many prokaryote bacteria, of PHA synthase,[4] the enzyme responsible for PHA biosynthesis.[5] As a consequence, the enzymatic catalyzed synthesis is totally accomplished in appropriate bioreactors through fermentative processes and an industrial production is nowadays achievable.[6] Usually, a two steps fed-batch cultivation is utilized.[7,8] In a first moment, cell population is allowed to grow without no nutrient limitation. When the desired cell concentration is

reached, microorganisms are exposed to a high carbon concentration with a concomitant limitation of the other elements (mainly oxygen, nitrogen, phosphorus and sulfur). This provoke the interruption of both protein synthesis and cell population growth. Consequently, a concomitant polymer granules production, namely a carbon source storage, began.[9] At the end of the fermentation, cell mass is separated from the liquid phase and polymer recovery, *i.e.* PHA downstream processing. Polymer extraction, that deeply affect overall polymer cost,[10] can be accomplished through various strategy (see **Figure 3**), but essentially there are two main possibilities.[11]

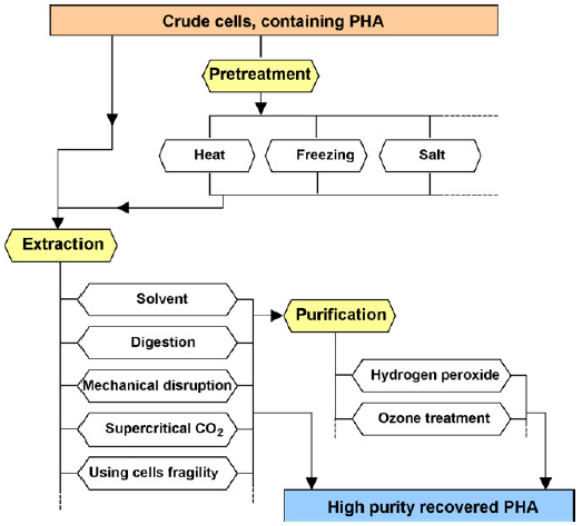

Figure 3. PHAs downstream strategies. Reproduced with permission of Elseviere from **[12]**.

One possibility consists in digestion and solubility of all non-PHA components. This can be made upon utilization of various chemicals (surfactants, sodium hypochlorite, hydrogen peroxide, …), even used in combination. The main disadvantage of such processes is they can affect polymer molecular weight and, lowering it, degrading the polyester.[12] On the other hand, the selective extraction, from the dry cell mass, of PHAs upon utilization of appropriate solvents is possible. In this case, highly pure and not degraded polymer is obtained. Regrettably, toxicity and hardness of mostly used solvents, mainly chlorinated, limit industrial application of these strategies.[13] Nevertheless, utilization of more green solvents was proposed and possible future industrial application of them is imaginable.[14]

Another aspect that strongly influence PHA total price is obviously the type of carbon source used to fed microorganism.[15] Currently, conventional and costly carbon source (glucose, sucrose, molasses, ...) are successively employed as feedstock for the bioconversion process.[16] Nevertheless, considering ethical concerns regarding utilization of food competitive resources, utilization of agri-food wastes appears to be a

suitable solution in a near future.[17,18] Even seaweeds, which production do not interfere with agricultural industry, metabolized by precise marine bacteria, can be used for PHAs production.[19] More recently, biomasses obtained from degradation processes of industrial textile dyes[20] or post-consumer agricultural polyethylene[21] were found suitable materials for PHAs enzymatic synthesis.

Interestingly, nature of the substrate and the bacterial strain are key-factors in order to obtain different types of hydroxyalkanoic monomers. Indeed, more than 150 different types of PHAs are known today and either homopolymer or copolymer can be produced.[22] According to the length of the hydroxy alkanoic acid's chain (R lateral group, see **Figure 1**), these linear biopolymers[23,24] may be classified in three macro-groups. Medium chain length (*mcl*PHAs), with monomeric units consisting of 6 to 14 carbon atoms and long chain length (*lcl*PHAs, more than 14 carbon atoms for monomeric unit) are usually characterized by low mechanical properties. On the contrary, short chain length PHAs (*scl*PHAs, 3 to 5 carbon atoms for monomeric unit) can be rigid and brittle materials.[25] Nevertheless, as previously stated, biosynthesis of copolymers can be achieved.[26] Foreseeably, presence of various types of hydroxyalkanoate monomeric units in the macromolecular chain sensibly affects material properties that vary accordingly.[27] For instance, the already cited PHB, universally recognized as the main and most promising representative of PHAs family,[28] is a crystalline material that melt at around 170 °C - 175°C. On the other hand, the copolymer poly([R]-3-hydroxybutyrate-*co*-[R]-3-hydroxyvalerate), PHBV, with an hydroxyvalerate content of 37mol%, display a lowering of the crystallization degree and consequently melts at lower temperature (roughly 75°C).[29] Biosynthesis of PHB and its copolymers with hydroxyvalerate have been intensively studied and are both long since industrially produced through biotechnological processes at industrial scale.[30] In addition, PHB is recognized to have some properties similar to other petroleum-based polymers, such as polypropylene,[31] making that biobased macromolecule even more attractive. For these reasons, in this work of thesis attention will be focused especially on PHB and on its terpolymer with [R]-3-hydroxyvalerate and [R]-4-hydroxyvalerate named PHBVV.

Regarding enzymatic synthesis of biopolymers, it is also worth mentioning that low specificity of PHA synthase catalytic active site, with respect to the substrate, allows even insertion of other monomeric units then hydroxyalkanoates. As a notably example, copolymer constituted by 3-hydroxyalkanoates and 3-mercaptoalkanoates (**Figure 4**)

can be enzymatically synthetized. Indeed, utilizing the same biotechnology, but upon utilization of proper feeding, copolymer as poly(3-hydroxybutyrate-*co*-3-mercaptopropionate) can be produced.[32] By employment of appositely engineered bacterial strain, such relatively new biomacromolecules can also be prepare as homopolymer,[33] named as polythioesters (PTEs), and possess an interesting property. Besides PTEs natural origin, all tested PHA depolymerase are not able to hydrolyze thioester bonds in polymer backbone chains, making such biopolymers not biodegradable.[34] If such polymers would result to be biocompatible, currently available biotechnologies would allow to prepare biopolymer for particular biomedical application where biodegradation is not desirable.

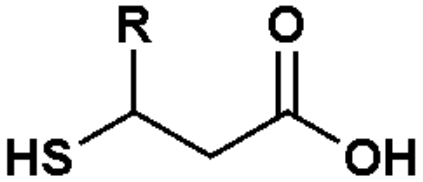

Figure 4. General structure of 3-mercaptoalkanoates (R = H, 3-mercaptoproprionate).

An issue that nowadays is limiting a wild spread utilization of PHAs is their thermal instability.[35] It is well known that a general ester functionality which presents hydrogens as substituents on the beta carbon, *i.e.* β-hydrogens, undergoes a thermal elimination through a six-membered transition state (**Scheme 1**).[36]

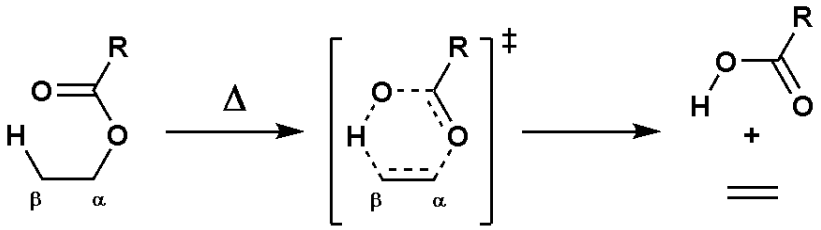

Scheme 1. Schematic representation of thermal cis-elimination in esters containing hydrogen in β position (Δ = heat source).

Independently of the type hydroxyalkanoic monomers, poly(hydroxyalkanoate)s backbone ester functionalities present hydrogen in beta position. Thus, the biopolyester undergoes thermal cis-elimination that result in a chain cleavage and, consequently, in an overall molecular weight reduction (see **Scheme 2**).

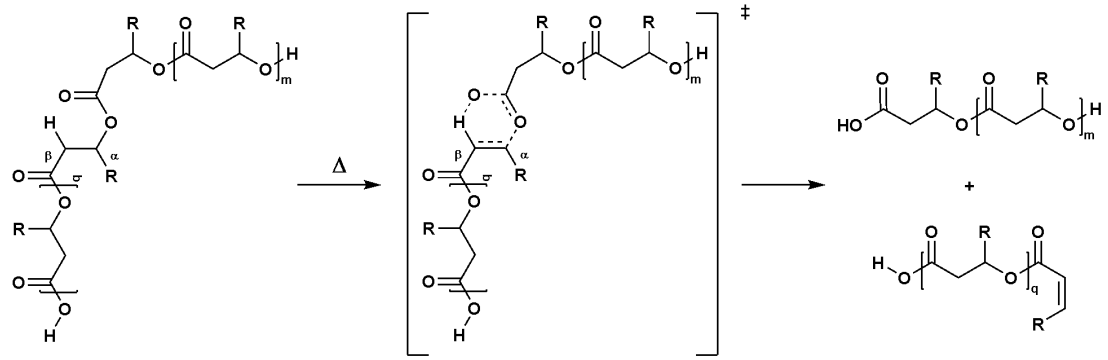

Scheme 2. Schematic representation of thermal cis-elimination (chain cleavage) in a general poly(hydroxyalkanoate)

Occurrence of those degradative processes began at around 180°C, a temperature slightly above the PHB melting temperature, and a significant molecular weight reduction is observed above 200°C.[37] This aspect represents a serious limitation for PHB processing and impose to work in a narrow window of temperature.[38] To overcome such a hurdle, effect of various plasticizers was deeply studied.[39] Indeed, a plasticizer, as defined by IUPAC, is a low molecular weight molecule that increase flexibility, workability or distensibility of a material.[40] In detail, penetrating in the amorphous phase, plasticizers have the effect to lower glass-transition temperature, melt viscosity and elastic modulus, making the material more flexible and processable. Obviously, due to the biobased origin of PHAs, plasticizers of natural origin have preferably been investigated.[41] Another possibility to increase PHB processability is act on the crystal phase with appropriate substances that, interacting with PHB chains, depress crystallizations phenomena. For instances, polymeric blends based on PHB and natural polyphenols display a decrease in melting temperature, allowing a good processability at temperature lower than pure PHB melting point.[42] Differently, PHB thermal stability could be achieved grafting unsaturated species onto backbone chain and increasing steric hindrances of degradative process.[43,44] Indeed, grafting onto polyester backbone molecules such as maleic anhydride, represent a hurdle to the formation of previously mentioned six-member ring intermediate and thermal degradation is inhibited.[45] A similar effect of chains mobility inhibition, known as nanoconfinement, can be accomplished even by certain fillers in nanocomposites. Such an effect was observed analyzing the improved thermal stability of polystyrene/clay nanocomposites.[46] During the first stages of the thermal degradation, newly formed degrading polymeric radical species are slowed, and eventually nanoconfined, by the clay nanonetworks. In such conditions, radicals can then recombine making the radical degradation process apparently reversible. As degradation proceeds, nanoconfinement effect ceases and

degradation reactions took place, restoring the irreversibility of the process. In order to evaluate possible clay thermal stabilization in PHB matrix, nanocomposites made of PHB and montmorillonite, a layered clay mineral, were prepared with a filler concentration varying from 0 to 5wt%.[47] As expected, thermogravimetric (TG) analyses evidence that fillers positively affect thermal stability, with higher stabilization utilizing 1wt% of montmorillonite. However, in this case, it was not elucidated if the observed behavior was effectively nanoconfinement or simply a mass barrier effect accomplished by thermally stable silicate layers. Indeed, the mass loss delay observed from TG analyses could be simply due to a labyrinth effect that retard loss of volatile degradation products. More detailed studies are required to understand if archived thermal stabilization is instead due to a fillers nanoconfinement effect that, penalizing conformational chains movements, prevents formation of the six-membered transition state.

As previously written, PHAs are recognized as biocompatible, biodegradable and bioresorbable materials.[1] Moreover, the main product of PHB enzymatic degradation consist practically only in its monomeric unit, 3-hydroxybutyrate.[48] Considering that PHB oligomers and monomers, in addition to be not toxic, could also have beneficial physiological effects,[1] the potential usage of PHB as biomaterial for the realization of medical devices is obviously to take into account. Indeed, in the last decades, possible usage of biocompatible and biodegradable polymers as biomaterials was deeply investigated.[49] As a matter of fact, polymers, compared to traditional biostable materials used for realization of medical devices (metals, alloys and ceramics) are more versatile materials. Indeed, through chemical syntheses or modifications, realization of totally synthetic or bioderived polymeric devices is possible. In addition, taking advantage of a huge library of possible reactive processes, biomaterials features and functions can be properly tailored.[50] Moreover, physiological environment responsive biopolymer-based systems, totally unimaginable utilizing traditional biomaterials, are today concrete tools. As an example, conjugation of a drug to specific polymers have surprisingly effects. When polyethylene glycol (PEG), a water soluble and biocompatible macromolecule, is used as conjugating polymer, PEGylated drug circulation half-life, immunogenicity and solubility improve.[51] Big efforts were made to develop increasingly sophisticated polymer-drug conjugates and nowadays an extensive array of elegant processes for realization of highly specific drug-delivery systems exists.[52] Parallel, different types of polymeric drug carriers were developed in search of a more and more specific delivery.

For instances, shell-crosslinking of methacrylate terminated triblock amphiphilic copolymers results in the preparation of a thermal-responsive potential drug-delivery system (**Figure 5**).[53] Copolymer aliphatic character was achieved by block copolymerizing hydrophilic and hydrophobic polymeric segment alternatively.

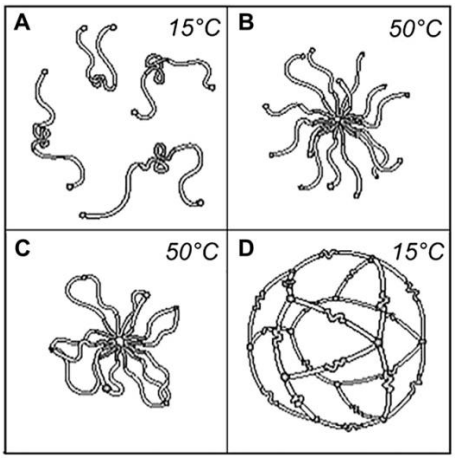

Figure 5. Formation and thermo-responsive behavior of the drug-delivery system. A: Triblock copolymers below critical micelle temperature; B: Micelles formation above critical micelle temperature; C: Shell-crosslinked micelles by reaction of methacrylate copolymers end-groups; D: Expanded crosslinked micelle bellow critical micelle temperature. Reproduced with permission of Elsevier from **[53]**.

In such a system, a hydrophobic drug, trapped in the core of a closed micelle, could be released on demand because of a thermal stimulus.[54]

Concerning realization of solid 3-dimensional medical devices, fabrication of polymer-based biomedical scaffold certainly opens the gates to a cascade of previously unreachable opportunities. Nowadays, the most attractive fashion to realize polymeric tissue scaffolds is though rapid prototyping technique (3D-printing).[55] Specifically, UV-assisted vat photopolymerization, Stereolithography (SLA) or Digital Light Processing (DLP) (**Figure 6**), is a technique characterized by an impressive resolution. As a result, object with an accuracy of 20µm can be produced.[56]

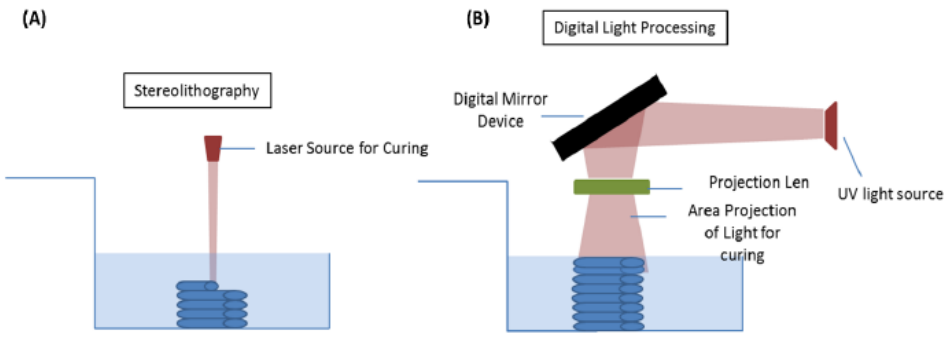

Figure 6. Vat Photopolymerization. A: Stereolithography; B: Digital Light Processing. Reproduced from **[57]**.

In details, vat photopolimerization allows the fabrication of solid objects through a photoinduced polymerization of a liquid formulation contained in a vat. The photo-curable formulation is then selectively irradiated with UV light, which promotes localized crosslinking process, resulting in the formation of a 2D solid structure with desired shape. After the curing of this first 2D structure, a platform moves in the opposite direction of the light source and the irradiation process is repeated. Layer by layer all the 2D structures are printed, leading to a 3D object with the tailored structure. Indeed, a rapid resin recoating of the last irradiated layer for an optimal photopolymerization of the next layer, an adequate viscosity is necessary. [58] The counterpart of such a step-by-step processing is the time required for realization of high-resolution objects. Nevertheless, development of new 3D printing methodologies, such as Continuous Liquid Interface Production,[59] consents to remarkably reduce objects time fabrication.[60] Photopolymerizable resins are usually based on low molecular weight acrylate terminated oligomers that, if solids, are dispersed in appropriate diluents.[61,62] In detail, the acrylate functionalities allowed to obtain a formulation that can be easily crosslinked under UV irradiation, whereas the low molecular weight play an important role imparting low viscosity to the photopolymerizable ink/resin. Also, realization of bioactive species releasing devices can be achieved by utilization of drug loaded photopolymerizable formulations.[63]

Depending on UV-sensible moieties concentration in the starting polymeric ink allows to realize 3D-printed devices characterized by different mechanical properties.[64] Due to the deep effect on cells of mechanochemical characteristics of scaffolds microenvironment,[65] vat photopolymerization could turn out to be a more and more powerful tool for the future realization of biomedical scaffolds. Considering the possibility to 3D print objects by utilization of high-resolution medical imaging data,[66] tremendous level of customization could be achieved. Additionally, polymeric nature of

prepared devices allow relevant post-realization chemical functionalization. As an example, surface functionalization with bioactive groups of polymeric films can be easily achieved through “click” chemistry reactions.[67] Furthermore, utilization of biodegradable polymeric materials allows to plan the gradual substitution of degrading scaffolds with newly formed tissues.[68] Such a process of tissue growth can obviously be enhanced by realization of composite scaffolds filled with adequate tissue stimulating species.[69] As a consequence, realization of polymer-based scaffolds for tissue engineering[70] filled with bioactive species[71] is a nowadays attractive research field.

Despite the nature of biobased polymers and the exceptional properties displayed by poly(hydroxyalkanoate)s, the most attractive aspect that concerns such biopolymers is their production. Indeed, at the present day, PHAs are the only macromolecules totally polymerized by enzymes on industrial scale. [72] Consequently, they can be considered the first polymers produced through “White Biotechnology”.[73] Obviously, various undeniable advantages derive from such a production. As a matter of fact, enzymatic catalysis is performed in moderate reaction conditions: atmospheric pressure, physiological temperature and water-based media.[74] Furthermore, fermentation processes inherently do not require utilization of toxic catalysts.[75] With a view to a more sustainable industrial production, that should minimize or avoid utilization of toxic chemicals,[76] use of safer natural catalysts instead of traditional systems have obviously to be preferred. Moreover, considering PHAs potential application in biomedical field, issues usually concerning the removing of post polymerization metal residues simply do not exist.[77,78] Besides such notably relevant aspects, White Biotechnologies, and related products, should be considered as part of a more complex and integrated systems: the Biorefinery.[79] Similarly to a traditional refinery, in a biorefinery fuels, chemicals and products are obtained from renewable resources instead of petroleum.[80] Considering the global growing attention toward a circular economy,[81] explore possibilities given by already currently available white biotechnolgical products is of extreme interest in a perspective of a future circular production. In the case of poly(hydroxyalkanoate)s such interest is undoubtedly amplified by the fact that the bioproduced good is a highly regular stereopolymer difficulty achievable with synthetic polymerizations.

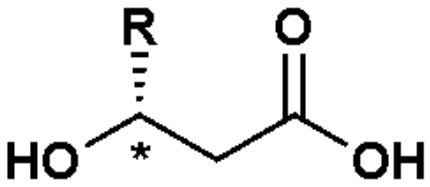

Figure 7. Chiral center in a general 3-hydroxyalkanoic acid, star indicate the chiral carbon.

Looking to the chemical structure of 3-hydroxyalkanoic acids, chiral nature of those organic compounds is easily recognizable (see **Figure 7**). Like all the macromolecules that present chiral center in the monomeric unit, poly(hydroxyalkanoate)s are tactic polymers.[82] Depending on the monomeric unit substituent orientation with respect to the orientation of the adjacent unit substituent, such macromolecules can be classified into three categories (**Figure 8**). If the units substituents are all oriented in the same direction with respect to the backbone chain, the macromolecule is called isotactic. Differently, a syndiotactic polymer is composed by monomers that present substituents alternatively oriented on both sides of the chain. Finally, if there is no correlation between the orientation of adjacent units substituents and all of these are randomly oriented with respect to the backbone chain, the polymer is defined as an atactic macromolecule.

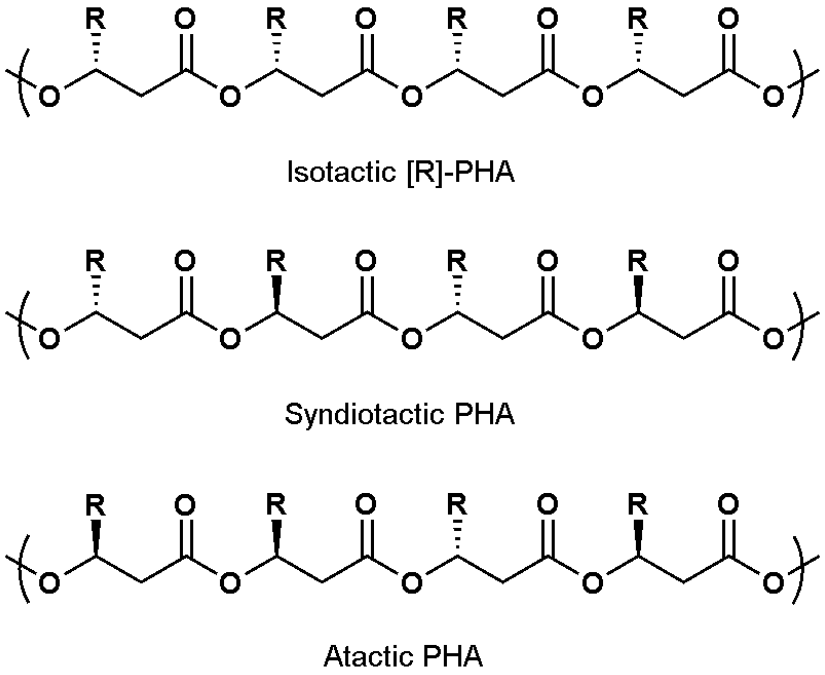

Figure 8. Representation of isotactic, syndiotactic and atactic poly(3-hydroxyalkanoate), PHA.

Enzymes are universally recognized as chiral biocatalyst[83] and increasingly used by chemists for the preparation of optically active compounds.[84,85] As a consequence, biocatalyzed synthesis of poly(3-hydroxyalkanoate)s allowed to obtain isotactic chains,

poly([R]-3-hydroxyalkanoate)s.[86] Obviously, depending on macromolecular tacticity, materials display variation in physical properties, such as melting temperature or crystallinity.[87] Nevertheless, in the case of PHB, the most notable effect of chains tacticity affect the enzymatic degradability.[88] Indeed, enzymatic PHB depolymerases seems to exhibit a specificity in hydrolyzed polymeric chain in the [R] configuration. As demonstrated by study conducted on PHBs single crystals,[89] bacterial PHB, with chain substituents only in the R configuration, can be completely enzymatically degraded. On the contrary, synthetic samples obtained from ring-opening polymerization of racemic β-butyrolactone, independently to their stereoconfiguration (iso-, syndio- or a-tactic), resulted to be not completely biodegraded. This behavior was ascribed to the presence, in all synthetic PHBs, of undegradable S units. Indeed, even the isospecific ring-opening polymerization, performed with a methylaluminoxane catalyst, leads to the obtainment of a mixture of poly([R]-3-hydroxybutyrate) and poly([S]-3-hydroxybutyrate) (**Scheme 3**). For the reason expressed above, it is clear that the 50% of the synthetic isotactic macromolecules have the absolute [S] configuration and are inaccessible to enzymes.

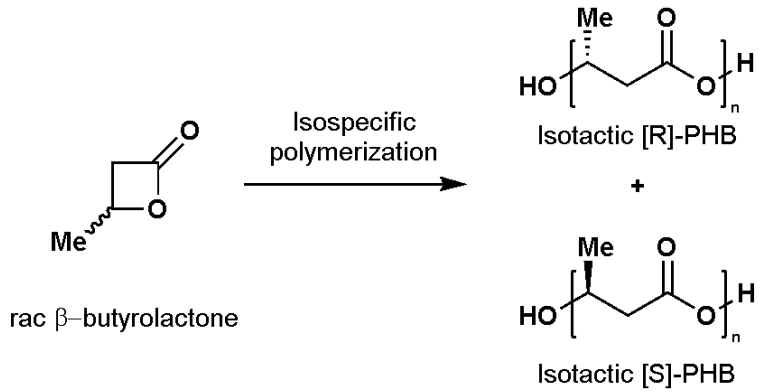

Scheme 3. Isospecific polymerization of racemic β-butyrolactone

At the present day, the only possibility to obtain a synthetic isotactic poly([R]-hydroxybutyrate) was the polymerization of the optically active [R]-β-butyrolactone.[90] However, obtainment of enantiomerically pure chemicals is usually a laborious task.[91] Therefore, natural PHB, enantioselectively produced through “White biotechnologies”, represents a unique opportunity. Indeed, availability of such products allow to establish a synergetic collaboration between nature and chemists. Indeed, being PHB a polyester, transesterification reactions with other hydroxyl bearing molecules could be planned. For instances, complete depolymerization of bacterial PHB with alcohols allow to obtain, in simple reaction conditions, the corresponding enantiomerically pure esters in extremely good yields[92] (**Scheme 4**).

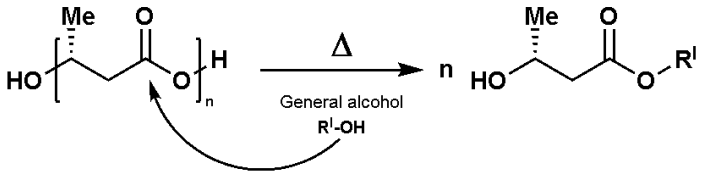

Scheme 4. Reaction of total alcoholysis of bacterial PHA

Nevertheless, avoiding the hypothesis to totally depolymerize the natural macromolecule, alcoholysis processes could turn out to be useful for the realization of PHB based oligomers. Indeed, while enzymes provide, in a sustainable way, a stereoregular macromolecular architecture, post-polymerization chemical modifications accomplished by chemists could lead to the obtainment of more useful materials. Considering the high molecular weight usually displayed by PHB[24], utilization of a substoichiometric amount of alcohol avoids a complete depolymerization and permits to obtain PHB-based low molecular weight derivatives. If, instead of a simple alcohol, alcoholysis is performed by a diol, di-hydroxyl-terminated PHB-based segment, PHB-diols, are obtained (see **Scheme 5**).[93] Such telechelic diols are effectively building-blocks which can be used as natural derived prepolymer for the realization of new PHB-based or PHB-containing materials.

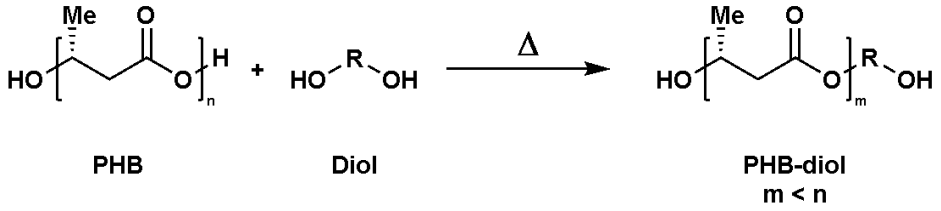

Scheme 5. Reaction of partial alcoholysis of natural PHB performed with a diol

Without any doubt, natural produced PHB is a material characterized by impressive properties that, at same time, present some limits. Despite the already mentioned thermal instability at melting temperature, other challenges are posed by this polyester. Indeed, even its high molecular weight and absence of chemical reactive moieties on the backbone deeply limit PHB utilization in a huge number of possible applications. Identify an industrially viable strategy to obtain, through reactive processes, bacterial PHB-based prepolymers more chemically attractive would probably help the biopolymer diffusion.

In this work of thesis, various possible approaches for the preparation of PHA-based materials employable in the realization of advanced devices are explored. Nowadays, it is well known that fillers, especially at nanoscale dimension, display a positive effect on

various polymer properties. It was recognized that even low amount of nanofiller have a deep effect on the polymer matrix and nanocomposites usually are characterized by improved thermal, mechanical and barrier properties.[94] In detail, opportunities to realize functionally tailored biopolyester composites are investigated. Considering poly(hydroxyalkanoate)s bio origin, utilization of natural fillers would eventually allow to obtain a 100% biobased polymeric composites. If, in addition to be naturally produced, utilized fillers are characterized even by good biocompatibility and biodegradability, resulting PHA-based composites would preserve all the attractive biopolyester original properties. Among various today available natural fillers, cellulosic materials are interesting candidate for realization of biocomposites.[95] Cellulose is a natural polymer that belong to the group of polysaccharides and is the main components of lignocellulosic biomass. Besides being a non-food competitive low-cost, abundant and renewable resource, cellulose is also a biocompatible and biodegradable materials.[96] In particular, MicroFibrillated Cellulose (MFC, cellulose fibers disintegrated into their structural components) is a promising material for the realization of biopolymer-based composites (**Figure 9**).[97,98]

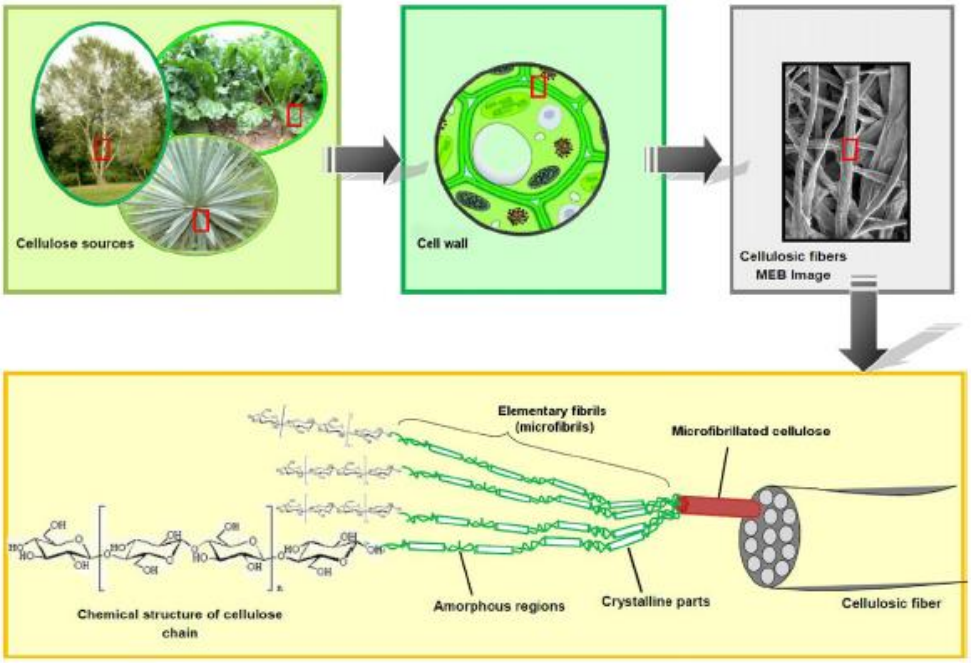

Figure 9. Obtainment of MFC from renewable cellulose sources, schematic representation. Reproduced with permission of Elsevier from **[99]**.

It is important to underline that, notwithstanding the Micro attribute, MFC fibrils are organized in a nanonetwork in which cellulose crystalline and amorphous domains are

present (see **Figure 10**).[100] Consequently, such a nanonetwork can deeply affect properties of the host polymer matrix.

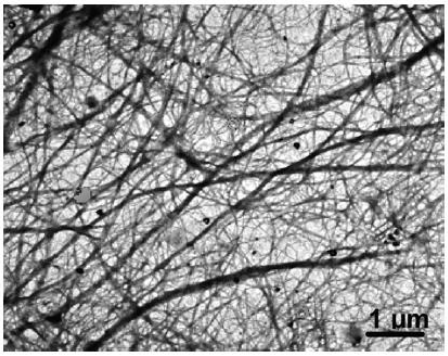

Figure 10. MFC nanonetwork. Reproduced with permission of Elsevier from **[101**]

For instances, bio-based poly(propylene carbonate) (PPC) mechanical properties and thermal stability are increased by the incorporation of MFC.[102] This result was attributed to the optimal dispersion of MFC into PPC-based composites, obtained from *N,N*-dimethylformamide solution casting. Nevertheless, in this case, a modified MFC was used. Indeed, prior composite realization, MFC was treated with an esterifying agent that, reacting with cellulose hydroxyl groups, increased fibrils lipophilicity. As observable from **Figure 9**, cellulose backbone chain present various pendant active hydroxyl groups that allows various type of chemical functionalizations.[103] Despite allowing easy and tailored functionalization, such hydroxyl groups are also responsible for the well-known ”hornification” effect.[104] In detail, cellulose, and more in general all polysaccharides, forms inter-macromolecular hydrogen bonds that, once established, result in an irreversible fibrils aggregation.[105] For this reason, after cellulose fibers disintegration, MFC is usually produced and commercialized as a diluted water suspension (2-3wt%).[100] At higher MFC concentration, or better lower water content, irreversible processes of agglomeration commence. Such a physical form of water-based suspension obviously poses sever problems concerning the insertion of MFC in a highly hydrophobic polymeric matrix, such as PHA.[106] Consequently, reported PHA/MFC composites, regardless good mechanical and biocompatibility properties displayed, were obtained only after increasing MFC lipophilicity by reaction with acetic anhydride (acetylation of hydroxyl groups). Such a modified MFC can be dispersed in organic solvent and PHA/MFC composites were obtained with solvent casting from chloroform solution.[107] Regrettably, such a procedure, characterized by the utilization toxic chemicals, does not seem to be viable for an industrial production. Indeed, possibility to realize PHA/MFC composite through mechanical mixing, *i.e.* extrusion, is investigated in

this work. Obviously, the hypothesis to introduce a diluted water suspension (MFC 2-3wt%) into an extruder operating at PHA processing temperature (above 170°C) is unrealistic. As previously stated, even the hypothesis of drying as-received-MFC suspension in oven has to be excluded due to the occurrence of agglomeration processes. On the other hand, utilization of a polymeric MFC dispersing agent could be an effective strategy.[108] Herein, the term polymeric MFC dispersing agent is used to refer to a water-soluble polymer that can be blended with PHAs and have the same properties of biocompatibility and/or biodegradability. Indeed, diluting MFC suspension with water, or with a polymer water solution, solution should not present particular issues. Rather, suitable homogenization should lead to an MFC suspension more diluted and less subjected to fibrils agglomeration. Subsequent water elimination accomplished with appropriate technique, to prevent concomitant cellulose agglomeration, would allow to produce a dry solid composed by polymer and MFC (see **Figure 11**).

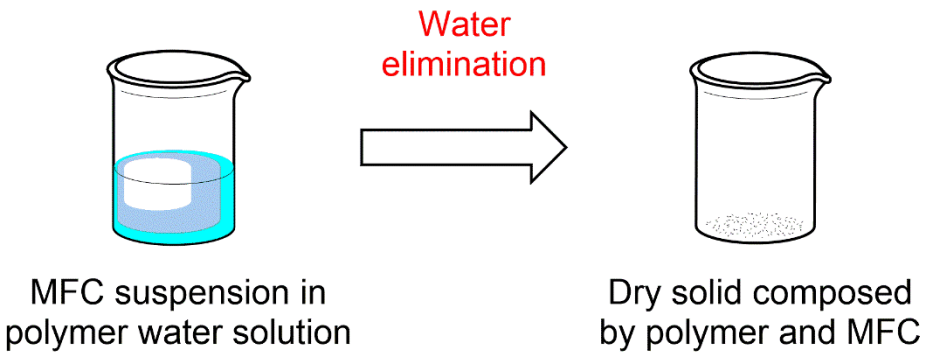

Figure 11. Schematic representation of polymer assisted drying of MFC water suspension.

In such a solid, the MFC nanonetwork, which agglomeration during water elimination phase is impeded choosing an appropriate drying technique, is maintained even at the solid state. Indeed, this preservation could be accomplished by a sort of fibrils polymer coating realized during the drying process. The polymer coating, avoiding direct interaction between distinct fibrils, would prevent the previously mentioned and irreversible “hornification” effect. Operating in this way, a dry-solid and agglomerates-free MFC composite, suitable for mechanical mixing, can be obtained without any kind of difficultly reliable chemical functionalization. Poly(ethylene glycol), PEG, is a non-biodegradable water soluble and biocompatible polymer[109] which can also be prepared from renewable resources.[110] Moreover, PHB/PEG blends were realized and the two polymers seem to display a certain degree of compatibility.[111] Regrading realization of dry PEG/MFC mixture, while dispersion of PEG water solution into MFC suspension

should not pose problems, particular attention is required in choosing appropriate suspension drying technique. Among various dehydration methods, freeze-drying seems to be the proper solution for realizing such a dry polyether/polysaccharide composite.[112] In detail, after freezing the suspension, water is then removed by sublimation by using appropriate vacuum-operating apparatus. Indeed, while pre-freeze treatment immobilizes MFC network, preventing undesired hornification, sublimation allow to maintain 3D structure during all the water elimination process. Summarizing, PEG presents all the characteristics to act as an MFC dispersing agent into a PHB-based matrix. Furthermore, the final resulting three components composite (PHA, PEG and MFC) would eventually be biobased and biocompatible. Such a composite could be characterized by improved properties with respect to original PHA. Achieving a good MFC dispersion into PHA polymeric matrix should results in an improvement of mechanical properties. Even a thermal stabilization effect could be reached and would be of extreme interest investigate the existence of an MFC-nanonetwork promoted nanoconfinement effect. Finally, the already mentioned presence of many active hydroxyl groups on cellulose backbone can turn out to be an attractive issue for drug conjugation.[113] Indeed, the PEG-based polymeric coating, that avoided fibrils aggregation during MFC drying and extrusion, once obtained a good MFC dispersion into PHA-matrix, is no more a composite essential component. MFC fibrils aggregation should be now prevent by PHA-matrix. Due to the fact that, among the species present in the three-component composite, only the polyether is water soluble, PEG removal can be accomplished by simple water leaching. The leached material would be characterized by a certain degree of porosity, generated by extracted PEG, and presence of free and functionalizable hydroxyl groups, derived from MFC fibrils uncoating. Such characteristics are of obvious interest for tissue engineering scaffolds and possible application of PHA/MFC composites in this field can be imagined.

A fundamental property for a potential biomedical material is obviously biocompatibility. Indeed, accurate studies regarding material cytotoxicity are a mandatory step. Additionally, even the ability to promote cells proliferation and induce cells differentiation are essentials information. These last properties, especially the latter one, are of extreme importance in the realization of scaffolds with tissue regenerative abilities.[114] In detail, Mesenchymal Stem Cells (MSCs) are widely used in such studies. Indeed, these multipotent cells, harvested from various post-natal tissues, are extremely useful due to their ability to precisely differentiate accordingly to specific stimuli.[115] Usually, *in-vitro*

biocompatibility studies are carried out by cells seeding of appositely prepared material-based object. By cells seeding, deposition of a low volume of an MSCs cellular suspension, characterized with a define concentration, is intended. In the case of cytotoxicity evaluation, in most of the cases a 2D shaped object is enough to evaluate cells compatibility and vitality on a potential biomaterial-based environment. For this reason, dealing with a possible biopolymer useful for medical applications, preliminary cytocompatibility tests are usually carried out on thin films obtained by solvent casting technique.[116] Such a technique, consists in complete solubilization of a defined amount of materials in a proper solvent. After a slow evaporation of the liquid, a homogenous thin film is finally obtained (see **Figure 12**). As imaginable, such methodology is a low-cost procedure easily accomplishable at laboratory scale, extremely useful for a preliminary materials screening.

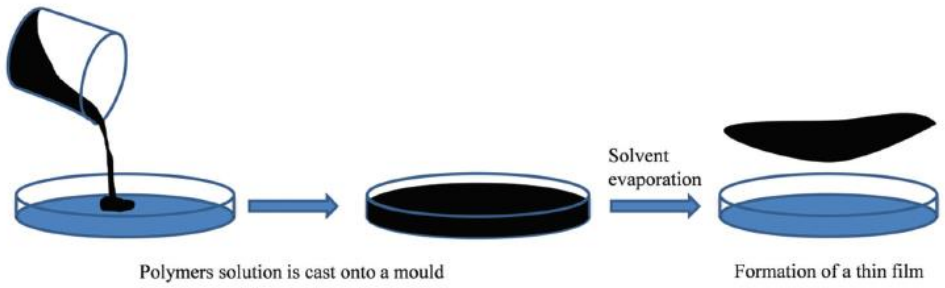

Figure 12. Schematic representation of solvent casting technique for obtainment of a polymeric film. Reproduced with permission of RCS from **[116]**.

For further evaluation, such as the osteoinductive activity of the materials, analyses are more informative when conducted on 3D shaped objects.[117] A structured and porous architecture could be obtained with various laboratory viable technique.[118] Among them, Thermally Induced Phase Separation (TIPS) is probably one of the most easily realizable (see **Figure 13**). Indeed, it requires common solvents and instrumentations routinely used in most laboratories. As for solvent casting, the first step consists in the solubilization of the material utilizing an appropriate solvent (solvent A). The choice of solvent A stands on its capacity to totally solubilize the solid only at high temperature. By allowing the system to cool down, a thermally induced solidification, *i.e.* phase separation, occurs. The solvent capacity of A is no more effective and high temperature achieved solution turn to be a swelled polymeric “sponge”. To enhance such a phase separation, *i.e.* polymer precipitation, utilization of cooling equipment, such as fridge or freezer, can be extremely useful. Successively, solvent A is removed from the swelled polymeric sponge by conventional drying technique or by leaching with an appropriately

chose solvent B, a polymer non-solvent. In this way, a 3D scaffold, characterized by porosity resulted from the free volume left by the removed solvent A, is obtained.

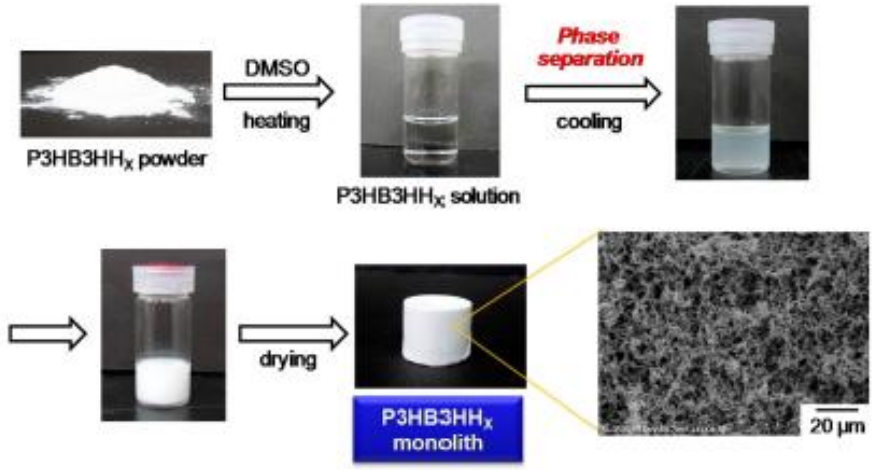

Figure 13. Schematic representation of thermally induced phase separation technique for obtainment of a polymeric porous 3D scaffold. Reproduced from **[119]**.

Osteogenic differentiation of hMSCs is influenced, beside the architecture and mechanical characteristics of the scaffold, also by the presence of bone-mimicking components.[120] Incorporation of these substances lead to realization of composite scaffolds with great potential application in tissue regeneration. Indeed, hydroxyapatite (HA)[121] and β-tricalcium phosphate (β-TCP)[71] are calcium phosphate-based substances that promote osteogenic differentiation. For this reason, in an attempt to realize a PHA-based 3D structured composites for bone tissue regeneration, biocompatibility studies were done. PHA-based films, filled with HA and β-TCP, were realized by solvent casting technique for cytocompatibility tests. Successively, 3D composite scaffolds realized by TIPS technique were used to evaluate cells proliferation and differentiation. Due to the already mentioned effect of morphological[120] and mechanical[65] properties on instruct cells differentiation, two different type of PHAs, characterized by different mechanical properties, were used as polymeric matrix. As aforementioned, presence on backbone chain of 3-hydroxyvalerate units deeply affect overall polymer properties. Consequently, the copolymer PHB-*co*-HV, PHBV, display extremely different physical characteristics with respect to the homopolymer PHB.

As previously mentioned, vat photopolymerization (VP) is emerging as a powerful tool for realization of customized biomedical scaffolds.[122,123] Indeed, this UV-assisted 3D printing technology not only permit realization of customized geometry, but it is also characterized by a high printing resolution.[58] Due to the resin characteristics expressed

above, it is clear that the neat biosynthesized PHB can not be employed in vat photopolymerization. The usually achieved molecular weight (over then 50 000 g·mol^{-1})[124] unlikely would allow to obtain, utilizing an adequate diluent, a sufficiently PHB concentrated resin with appropriate viscosity (1 Pa·s).[125] Moreover, PHB is a polyester characterized by the presence of only methyl lateral group and no photo sensible moieties are present on the natural polymer structure. Notwithstanding, as previously described, post-biosynthesis chemical modifications can turn to be a reliable strategy for realization of a PHB-based ink for VP printers. Summarizing what stated above, taking advantage of PHB ester functionalities present on backbone chains, transesterification reactions could be accomplished. Utilization of a diols as alcohol allows an overall lowering of polymer molecular weight accompanied by the insertion of a new terminal group. Due to the reactivity of hydroxyl groups toward various functional groups, conversion of oligomers terminals into methacrylic groups, UV sensible moieties, should not be challenging. It is reasonable to retain that such α,ω-di-methacrylate-terminated PHB-based oligoesters should be subjected to UV induced cross-linking. Moreover, considering that oligomers solutions usually display lower viscosity with respect to their high molecular weight counterpart,[126,127] dispersions with VP-suitable viscosities can be prepared. Finally, it has to be underlined that such modifications should be accomplished with solvent free processes that avoid utilization of expensive and toxic solvent. Indeed, analogues polyesters depolymerizations are successively performed through reactive extrusion processes.[128] Regrettably, previously mentioned PHB thermal instability could poses issues regarding polymer chemical modification carried out in the molten phase. However, at relatively low temperature, PHB degradation do not significantly affect polymerization degree.[129] Furthermore, utilization of non-toxic[130] titanium catalyst can deeply speed up transesterification reactions.[131,132] It can be expected that combination of relatively low temperature with short reaction time should result in a *quasi*-neglectable degradation. Concerning following functionalization, low molecular weight PHB derivatives, with $\boldsymbol{M_n}$ < 10 000 g·mol^{-1}, are characterized by lower melting point, far enough from polymer degradation temperature.[133] Indeed, react in the molten such oligomers to accomplish terminals methacrylation should not be challenging. To sum up, establishment of a process in which a sustainably-produced biobased and biodegradable polymer is green-chemically converted to useful macromonomers is of undeniable attractiveness. Indeed, expanding the concept of

biorefinery, a future production in which post-consume organic matter, natural or synthetic, is converted into highly advanced devices is imaginable.

Obviously, before plan any kind of chemical modifications, a complete chemical characterization of the starting PHB is mandatory. Proton Nuclear Magnetic Resonance (^{1}H-NMR) spectroscopy, both mono or bidimensional, is a long since recognized technique for accurate studies regarding polymers chemical structure.[134,135] Indeed, due to its sensitivity,[136] chemical nature of backbone repeating units could be easily studied. Moreover, protons belonging to terminal monomeric units, due to their position on the backbone chain, experience a diverse magnetic environment with respect to their backbone analogous. Such a diversity affects the nuclear magnetic response and end-groups protons have a different NMR chemical shift. Consequently, enabling to distinguish them from other peaks, NMR spectroscopy is suitable even for the end-groups characterization. Nevertheless, identification and correct interpretation of terminal groups signals could be quite challenging. In fact, NMR signals concentration dependency combined with the inherently terminal groups low concentration do not allow a clear characterization of these reactively interesting polymeric moieties. Indeed, such a difference in terms of concentration lead to an adverse spectral signal/noise ratio. This is even more true for high molecular weight polymers as natural PHB.[124] Consequently, interpretation of signals produced by terminal moieties is difficult and an uncomplete macromolecule characterization is usually achieved. For this reason, polyesters terminals, that theoretically consist only in equally present carboxylic and hydroxyl groups (**Figure 14**), are quantified by acid/base titration technique. Specifically, terms Acid Value (***AV***) and Hydroxyl Value (***OHV***), expressed in moles of carboxylic/hydroxyl groups for gram of polymer, are respectively used to refers to such quantities.

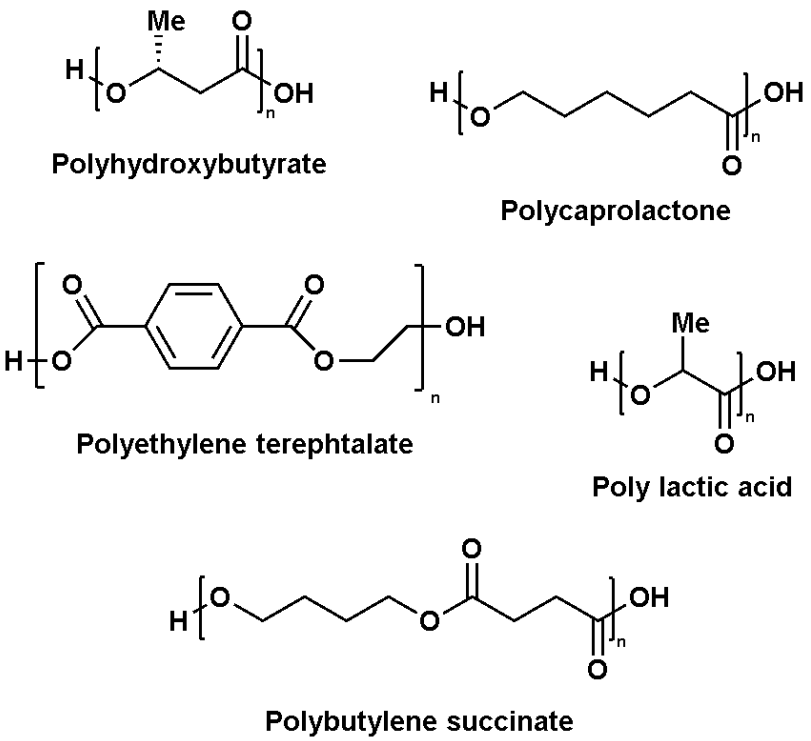

Figure 14. Structure of mostly diffused liner polyesters theoretically terminated with a hydroxyl and a carboxylic group.

Carboxylic terminals, due to their acid character, can be easily determined by simple acid/base titration.[137] The only limitation arise when mono carboxylic terminated polyester, as PHB is, are investigated. Indeed, these macromolecules present carboxylic moieties only as terminal group and due to such a low concentration, big amount of sample are required for an acceptable $\boldsymbol{AV}$ determination. On the other hand, $\boldsymbol{OHV}$ is usually determined after proper chemicals functionalization. For instance, hydroxyl moieties can be completely converted into acid species by reaction with succinic anhydride (see **Scheme 6**).[138] Modified end-groups can then be quantified by acid/base titration.

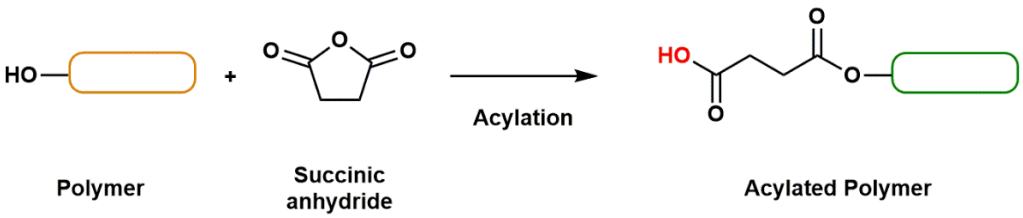

Scheme 6. Acylation of a general hydroxyl bearing polymer performed with Succinic anhydride. OH moieties are converted into acid/base titratable (*i.e.* quantifiable) carboxylic groups.

Another possibility is the quantitative acetylation of hydroxyl end-groups carried out by acetic anhydride.[139]. In such a derivatization, every acylated hydroxyl group produces a molecule of acetic acid (see **Scheme 7**). At the end of the functionalization, excess of

anhydride is hydrolysed to acetic acid by water addition. Overall acetic acid content is then quantified by acid/base titration and, knowing the initial amount of utilized anhydride, hydroxyl groups concentration is determined by appropriate calculation. Obviously, in both cases presence of original acid functionalities on the non-modified polymer has to be considered during calculation.

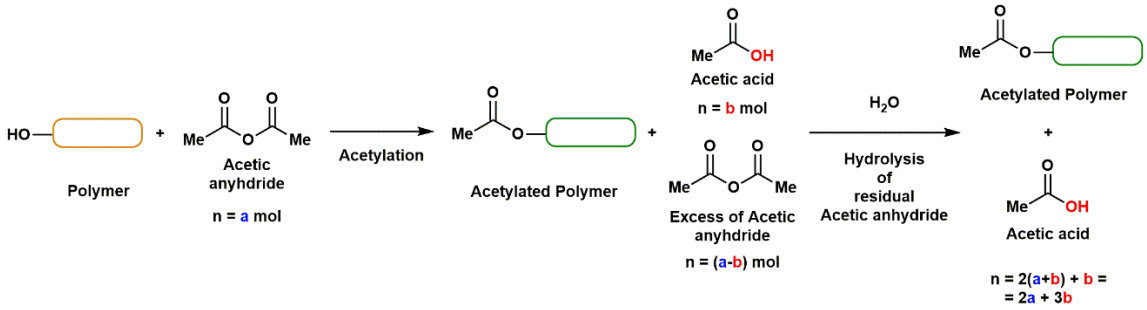

Scheme 7. Acetylation of a general hydroxyl bearing polymer with acetic anhydride. OH moieties are acetylated with concomitant generation of acid/base titratable (*i.e.* quantifiable) Acetic acid molecules.

Regrettably, evaluation of ***OHV*** accordingly to these procedures requires time-consuming functionalization processes and utilization of toxic solvents and reagents, even in big amount. Moreover, OH derivatization reaction conditions, that usually required long-time reaction at high temperature, can affect the temperature sensible PHAs chain structure. Such processes, even if marginal, in addition to possibly deep affect final recorded ***OHV***, could also occur systematically and be difficulty detectable. Obviously, this make such issues even more deleterious. For these reasons, in the last decades, spectroscopic methods for the ***OHV*** determination have been developed.[140,141,142] As stated above, NMR spectroscopy is a highly sensitive technique with potentially enormous applications in the determination of minute quantities, otherwise determined with doubtful accuracy.[143] Due to the already reported fact that they generate different NMR signals, hydroxyl bearing end-groups amount with respect to backbone repeating units can be determined by regular ^{1}H-NMR spectroscopy.[144] Therefore, by a simple integral values comparison, the ^{1}H-NMR determined ***OHV*** (^{1}H - ***OHV***), can be easily calculated. Specifically, ratio of end-groups and repeating units NMR signals integral values, respectively $\boldsymbol{I_{eg}}$ and $\boldsymbol{I_{ru}}$, correspond to their molar ratio.[145] Hence, from PHB hydroxyl bearing end-group and repeating units molecular weight, $\boldsymbol{MW_{eg}}$ = 87 g·mol-1 and $\boldsymbol{MW_{ru}}$ = 86 g·mol^{-1} respectively, ***OHV*** could be determined according to **Equation 1.**

$$OHV = \left(MW_{ru}\frac{I_{ru}}{I_{eg}} + MW_{eg}\right)^{-1} = \frac{I_{eg}}{MW_{ru}I_{ru}+MW_{eg}I_{eg}} \qquad \textit{(Equation 1)}$$

The main limitation of this technique is related to high molecular weight polymers. As previously reported, in high molecular weight polymer hydroxyl end-groups concentration sensibly decreases leading to an adverse signal/noise ratio. Moreover, a general quantitative NMR experiments require an adequate relaxation time to obtain trustworthy integral values, making this technique highly time-consuming and unsuitable to obtain reliable results. On the other end, quantitative conversion of polymeric hydroxyl moieties into functional groups containing NMR active heteroatoms is a valuable approach. Herein, by heteroatom (ha), an atom not present in the initial polymer chain is intended. Following this approach, the only signal present in ^{ha}NMR spectrum (the selected heteroatom NMR spectrum) would be produced by converted hydroxyl groups. An undoubtedly simplification of the resulting spectra interpretation is achieved. Quantification of functionalized terminals is then achieved by recording spectrum in presence of a well determined amount of internal standard. Utilization of an appropriate amount of standard would avoid also issues related to signa/noise ratio. Such an internal standard consists in a heteroatom containing molecules that obviously produces an ^{ha}NMR signal. By comparison of functionalized polymer and internal standard signals integrals values, moles of hydroxyl terminal polymer present in the NMR tube can be determined. If the mass concentration of ^{ha}NMR analyzed polymer was accurately determined prior the analysis, $\boldsymbol{OHV}$ can be determined by the hydroxyl groups moles/polymer weight ratio. Dealing with PHB, or a general poly(hydroxyalkanoate)s, fluorinated chemicals seem to be perfect candidate to perform such functionalization. Indeed, in addition to be not present in PHAs backbone chains, ^{19}F nuclei, the NMR active fluorine isotope, have a natural abundance of 100%. Furthermore, ^{19}F relative NMR sensitivity is comparable with the ^{1}H nuclei, which allows fast spectra acquisitions.[146] Consequently, many analyses based on ^{19}F-NMR quantitative spectroscopy are reported.[147,148,149] Thus, a poly(hydroxyalkanoate)s $\boldsymbol{OHV}$ quantification based on ^{19}F-NMR spectroscopy can be established. In a first moment, polyester hydroxyl groups are quantitatively trifluoroacetylated with a complete and fast *ex situ* reaction performed upon utilization of trifluoroacetic anhydride (**Scheme 8**).

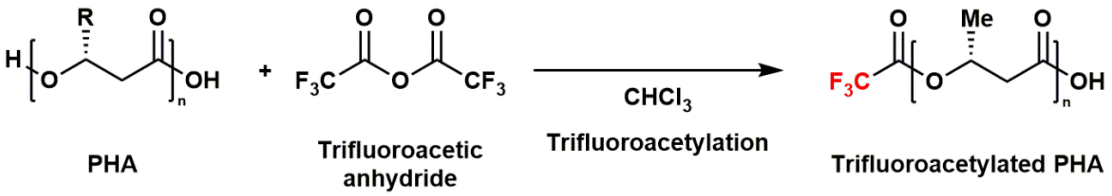

Scheme 8. Trifluoroacetylation of a general PHA performed with trifluoroacetic anhydride and hydroxyl groups conversion into ^{19}F-NMR titratable moieties.

OHV is then determined recording the quantitative ^{19}F-NMR spectrum of an accurately weighted quantity of functionalized polymer in presence of a known amount of trifluorotoluene as internal standard. The herein proposed approach offers several advantages such as the sharp and easily integrable trifluoroacetyl esters ^{19}F-NMR signals.[150] In addition, due to the presence of three heteroatoms for each derivatized hydroxyl groups, a remarkably improved signal/noise ratio can be achieved.

It has to be mentioned that possibility to perform an *in situ* functionalization, *i.e.* directly in the NMR tube, was excluded due to the usually long acquisition time required. [151] This is necessary in order to counter the deleterious effect of functionalization reagent excess on spectra interpretability. On the other hand, applying an optimized procedure, the complicated polymer isolation procedures, typically required by *ex situ* functionalization,[138] can be impressively minimized. Indeed, the previously schematized uncatalyzed reaction, requires only utilization of trifluoroacetic anhydride (T_b = 40°C) and solvent (chloroform, $CHCl_3$, T_b = 61°C), extremely volatile species. Furthermore, even the only reaction by-product, trifluoroacetic acid, is characterized by a low boiling point (T_b = 72°C). Consequently, instead performing laborious polymer isolation procedures, polymer sample can be accurately weighted in an analytical vial in which functionalization is performed. At the end of the functionalization, all the non-polymeric species could be rapidly eliminated by a gentle flux of gaseous nitrogen. The resulted solid, *i.e.* the trifluoroacetylated PHA, would then be easily solubilized in deuterated chloroform and transferred into an NMR tube for ^{19}F analysis. Low-molecular weight PHBs (Mn < 4000 mol·g^{-1}), herein named low MW PHBs, obtained after acid hydrolysis of neat PHB,[152] were used as model compounds. The ***OHV***s of such oligomers are calculated from ^{19}F-NMR spectra and compared with values obtained by already established method based on ^{1}H-NMR measurements. In this way, reliability of the proposed approach was verified. Successively, high molecular weight PHAs were analysed using the optimized conditions. In detail, samples of (PHB) and poly([R]-3-hydroxybutyrate-co-3-hydroxyvalerate) (PHBVV) were used in this study. The obtained

OHVs were validated with the corresponding Acid Values, determined by acid/base titration. Specifically, titration of high molecular weight PHAs chloroform solutions would be potentiometric titrated by utilization of a microtitrator. A diluted methanolic solution of potassium hydroxide (KOH) would be used as titrant after normalization upon titration of a benzoic acid chloroform standard solution. Indeed, accordance among ***OHV*** and ***AV*** determined for the same PHA sample would confirm, as a first step, reliability of trifluoroacetylation. Secondly, even the bacterial PHA nature of regular and linear polyester, resulted never accomplished at the best of our knowledge, would be proved.

2. Experimental section

2.1 Realization of PHA composites filled with MFC by extrusion

2.1.1 Materials

The PHA used for thermo-mechanical mixing is kindly provided by Bio-on SpA (Bologna, Italy) and produced with BioOn's fermentation process. Polyester is purchased as additivated pellets and dried overnight at 70°C prior to be used. Poly(ethylene glycol) 4000 is purchased by Sharlau Chemicals and before to be used dried in an desiccator at reduced pressure. MFC (Suzano, Brasil) is received as a white and creamy suspension (3wt% in water) and stored at 4°C.

2.1.2 Samples preparation

2.1.2.1 PEG/MFC water suspension

A uniform PEG/MFC suspension (80/20 by weight) is obtained by sonication. A typical preparation consists in the solubilization of PEG in water (5wt% solution) at room temperature. After achievement of a clear and transparent solution, mixture is poured in the proper amount of 3.1wt% MFC suspension. Finally, a complete and stable homogenization is obtained after1 hour of sonication utilizing an ULTRA-TURRAX® disperser operating at 8.5x1000min^{-1}.

2.1.2.2 PEG/MFC suspension drying by freeze-drying

To perform freeze-drying, the as-previously-described prepared PEG/MFC water suspension is transferred in aluminum plates and frozen by keeping sample at -18°C for 48 hours. Plates are then placed in a Liotop® K 105 freeze dryer. A complete drying process, operating at reduced pressure (0.14 mmHg), requires 72 hours.

2.1.2.3 Realization of PHA/PEG blend and PEG/MFC dispersion in PHA by extrusion

PEG and PEG/MFC powder are incorporated into PHA matrix by extrusion. Materials are extruded with respect to the following composition: PHA 80wt% and PEG 20wt%. When PEG/MFC was used, content of fibrils in the final obtained materials corresponds to 5wt% with respect to the whole polymeric matrix PHB-PEG(80-20). Thermo-mechanical mixing is performed using a single-screw bench extruder (AX Plastic LAB-16) equipped with a mixing element maddock. The temperature profile was 120, 155, 160, 160°C and a screw rotation speed of 40rpm was used.

2.1.3 Characterization

2.1.3.1. Scanning Electron Microscopy (SEM)

The phase morphology of all the prepared samples are examined using SEM. The images are obtained using a FEI Inspect F50 electron microscope. The lyophilized PEG/MFC powder is examined without any pre-treatment while PHA-PEG(80-20)/MFC(5wt%) pellets are hot pressed (1 minute at 190°C and a load of 500Kg) in aluminum molds (20 x 10 x 2 mm) and fractured in liquid nitrogen after 5 minutes of immersion. All samples are sputter coated with platinum prior to SEM.

2.2 PHA nanocomposites for bone tissue engineering

2.2.1. Materials

PHB and PHBVV are kindly provided by Bio-on SpA (Bologna, Italy) and produced with BioOn's fermentation process. All the films and scaffolds are realized only with purified PHA. The purification procedure consists in the selective precipitation of the pure polymer. It is obtained by solubilizing in a 500ml 2-neck round-bottomed flask, 10.0g of polymer powder in 250ml of chloroform. After 1 hour and 30 minutes at reflux condition, solution is vacuum filtered upon utilization of a filter aid (Celite). Obtained viscous, clear and yellow solution is poured in three volumes of ice cold MeOH vigorously stirred. After 15 minutes of stirring, white polymeric precipitate is vacuum filtered and pure white PHA is obtained after drying the solid at least 2 hours in oven at 85°C. All biocompatibility tests have been conducted at Istituto Ortopedico Rizzoli (IOR) laboratories. Procedures followed and relative utilized materials and reagents are reported together in section 2.2.3. All chemicals purchasing information are below descripted.

2.2.2. Samples preparation

2.2.2.1. PHA films casting

The compositions of the prepared films are reported in section *3.1.2*. The filler content is calculated on the polymer matrix (polymer or polymer and plasticizer when used) as 10% w/w (90% of polymer matrix and 10% of filler). Due to its lower flexibility compared to PHBVV, a plasticizer is used. 1,2-cyclohexane dicarboxylic acid diisononyl ester (Hexamoll® DINCH) is a non-phthalate plasticizer purchased by BASF and used

as received. In details, 10 Parts per Hundred Rubber (PHR) with respect to PHB amount are used. The polymer matrix concentration is 250 mg of polymer matrix (polymer or polymer and plasticizer) in 20 ml of solvent. Specifically, in a 50 ml round-bottom flask, 250 mg of polymer are solubilized in 20 ml of warm $CHCl_3$ (hot plate at 50°C). When PHB is used, the correct amount of plasticizer (25 mg) is added. When a clear and colorless solution is achieved, mixture is transferred into a glass Petri dish. Thin films are obtained after a slow solvent evaporation. For the preparation of composite films, before transferring mixture in the Petri dish, correct amount of filler is added to the flask. In detail, 5wt% or 10wt% (with respect to 250mg of PHBVV or 275mg of PHB + plasticizer) of HA or β-TCP are added and the mixture is sonicated for 30 minutes using a Hielscher UP50H homogenizer equipped with a MS2 sonotrode operating at 100% of amplitude (continuous sonication, Cycle 1). Suspension is then quickly transferred into glass Petri dish and solvent slowly evaporated. Drying is concluded overnight in oven at 50°C. Prior clinical trials, materials are properly dimensioned.

2.2.2.2. PHA-based 3D scaffold preparation by Thermally Induced Phase Separation (TIPS) procedure

The compositions of the prepared scaffolds are reported in section *3.1.2*. The filler content is calculated on the polymer matrix (polymer or polymer and plasticizer when used) as 10% w/w (90% of polymer matrix and 10% of filler). As for the preparation of 2D films, PHB-based samples have to be plasticized and 10 PHR of DINCH are used. The polymer matrix concentrations 1.2 g of polymer matrix (polymer or polymer and plasticizer) in 34 ml of solvent. Specifically, for 3D scaffolds preparation, 1.10 g of polyester and 32 ml of 1,4-dioxane are added in a 100 ml 2-neck round-bottom flask. The mixture is heated in a silicon hot bath (hot plate set at 103°C) under magnetic stirring. For PHB-based scaffolds, when a clear and colorless solution is achieved, correct amount of DINCH (0.11 g), solubilized in 2 ml of 1,4-dioxane, is added to the flask. Otherwise, when PHBVV is used, 2 ml of 1,4-dioxane are added. After 2-3 minutes, magnet is removed, and, maintaining heat source, hot solution is sonicated for 1 hour and 30 minutes using a Hielscher UP50H homogenizer equipped with a MS2 sonotrode operating at 100% of amplitude (continuous sonication, Cycle 1). Solution is then transferred into a disposable aluminum dish and solvent is allowed to solidify at -18°C overnight. Extraction of 1,4-dioxane is accomplished immersing the frozen mixture in 200 ml of cold ethanol. Extraction is repeated twice. Excess of ethanol is then removed firstly with a clean piece of paper and, successively, immerging in a deionized

water containing beaker. An as-before sonication is conducted for 1 hour and, after removal from the beaker, scaffolds are completely dried overnight in oven at 50°C. For the preparation of composite scaffolds, a very similar procedure is followed. After achievement of 1,4-dioxane clear solution, and potential plasticizer addition, but before the 1 hour and 30 minutes sonication, correct quantity of filler (0.13 g of HA or β-TCP) is added. After 10 minutes of stirring, magnet is removed, and suspension sonicate with the homogenizer. Composite scaffolds are then obtained operating as before. Prior clinical trials, materials are properly dimensioned.

2.2.3. Characterizations

2.2.3.1. hMSCs isolation and culture

Primary human Mesenchymal Stromal Cells (hMSCs) were isolated from bone marrow aspirates obtained from Rizzoli's patients during routine orthopedic surgical procedures. The study was approved by the Rizzoli Orthopedic Institute Ethics Committee (Bologna, Italy), and all patients provided an informed consent. hMSCs isolation, expansion and characterization was performed as previously described.[153,154]

2.2.3.2. Cells seeding on prepared materials

Materials were sterilized in a 70% ethanol bath for 2 hours, then washed twice in Dulbecco Modified Buffered Saline solution (D-PBS, Life-technologies), and conditioned for 24 h in complete culture medium: α-modified minimum essential medium (α-MEM; BioWhittaker, Lonza, Verviers, Belgium) supplemented with 20% fetal bovine serum (FBS; Lonza, Basel, Switzerland). For cell seeding they were transferred in an Ultra Low Attachment 24-well plate (Corning Costar) and air-dried under the laminar flow of a tissue culture hood. Then a small volume (10-20 µL) of cell suspension was placed over the film and incubated at 37°C, 5% CO_2 for 2 h, to permit cell adhesion. After the seeding step, 500 µL of fresh medium was added to each well.

2.2.3.3. Cells viability and adhesion on PHA films

The presence of viable cells on prepared films was qualitatively observed with Live and Dead staining (Life Technologies, Monza, Italy) after 24 hours after the seeding of $1x10^4$ MSCs ($\cong 2 \cdot 10^4$ cells/cm^2). Briefly, an aliquot of microcarriers was incubated with 2.5 µM of Calcein-AM and 10 µM of Ethidium Homodimer-1 in saline solution for 15 min at 37°C and 5% CO_2. After two washes with saline solution, images were acquired using an epifluorescence microscope (Nikon Eclipse TE2000-U inverted epifluorescence microscope) using filter for Calcein-AM: excitation 465–495 nm,

emission 515–555 nm; Ethidium Homodimer-1: excitation 510–560 nm, emission 590 nm).

2.2.3.4. Metabolic cell activity (cell proliferation study)

Six replicates for each material were seeded with $2 \cdot 10^3$ hMSCs (≅ $4x10^3$ cellule/cm^2). Evaluation of the metabolic activity of adherent hMSCs was performed by Alamar Blue Assay (Life-Technologies). In details, cell-seeded materials were treated with 10% v/v Alamar Blue solution in complete medium for 4 h at 37°C. The fluorescence of the obtained solution (excitation/emission 560/590 nm) was measured in a multi-well reader (Synergy HT, Bio-Tek). The same protocol was applied to cells cultured on traditional cell culture plastic 24-well plates as reference sample.

2.2.3.5. Osteogenic differentiation on PHA 3D structures

3D scaffolds were sterilized in a 70% ethanol bath overnight, then washed twice in Dulbecco Modified Buffered Saline solution (D-PBS, Life-technologies), and conditioned for 24 h in complete culture medium (αMEM+20%FBS). For cell seeding they were transferred in an Ultra Low Attachment 24-well plate and excess fluid was removed with a pipette. Then 20µL containing $2x10^5$ MSCs were placed on the upper surface of the scaffold and incubated at 37°C, 5% CO_2 for 2 h, to permit cell adhesion. After the seeding step, 1.5 mL of fresh medium was added to each well. MSCs were allowed to proliferate and colonize the scaffolds for 1 week prior to start the osteogenic induction. Then complete culture medium was replaced with an osteoinductive medium composed of α-MEM supplemented with 2% FBS, 10 mM β-glycerophosphate, 50 µg/ml ascorbic acid and 100 nM dexamethasone (Sigma, St. Louis, MO, USA). To assess osteoinductive intrinsic property of the materials, scaffold seeded under the same conditions were maintained in a non-inducing medium (α-MEM + 2% FBS). Media were changed twice per week. After 21 days, the samples were fixed in 70% ethanol for 90 min, then stained with 40 mM pH 4.0 Alizarin Red-S solution (ARS, Sigma) to reveal the deposition of a calcium-rich mineralized matrix. The bound ARS was then quantified by extraction with 10% (w/v) cetylpyridinium chloride (CPC; Sigma) solution in 10 mM sodium phosphate, pH7, for 30 min at RT. The colored solution of each well was then measured at 570 nm in an ELISA reader. (Synergy HT, Bio-Tek). ARS staining and extraction was performed also on cell-free scaffolds and the results were used as background signal.

2.2.3.6. Statistical analysis

The effect of the scaffold composition on cell proliferation was assessed at indicated timepoint by one-way analysis of variance (ANOVA), followed by Tukey's or Dunnet's multicomparison tests to compare all pairs of groups, or to compare each group to control group, respectively.

2.3 Chemical modification of bacterial PHA

2.3.1. Materials

All the materials were used as received, except where specified. Trifluoroacetic anhydride (TFAn), α,α,α-trifluorotoluene ($PhCF_3$), 1,4-butanediol, p-toluenesulfonic acid monohydrate (PTSA), benzoic acid (BzOH), chloroform ($CHCl_3$), 1,2-dichloroethane (previously dried over molecular shives), tetrabutylammonium hydroxide (TBAOH, methanolic solution), methanol (MeOH), Propylene carbonate (99%) and all the used solvents were purchased from Sigma Aldrich. Deuterated chloroform ($CDCl_3$) was purchased from VWR. Titanium(IV) butoxide (TBT, 97%), dibutyltin dilaurate (DBTDL, 95%), 2-isocyantioethyl methacrylate (98%) and 2-hydroxyethyl methacrylate (98%) were purchased by Aldrich while utilized photoinitiator (PI) Irgacure® 819 by BASF. All PHBs and PHBVVs were kindly provided by Bio-on SpA (Bologna, Italy) and produced with BioOn's fermentation process. In this work, all the reactions were conducted only on purified PHA. The purification procedure consists in the selective precipitation of the pure polymer. It is obtained by solubilizing in a 500ml 2-neck round-bottomed flask, 10.0g of polymer powder in 250ml of. After 1 hour and 30 minutes at reflux condition, solution is vacuum filtered upon utilization of a filter aid (Celite). Obtained viscous, clear and yellow solution is poured in three volumes of ice cold MeOH vigorously stirred. After 15 minutes of stirring, white polymeric precipitate is vacuum filtered and pure white PHA is obtained after drying the solid at least 2 hours in oven at 85°C.

2.3.2. Samples Preparation

2.3.2.1. Preparation of low molecular weight PHBs

Low molecular weight PHBs were prepared following a previously reported procedure.[152] Specifically, in a twin-neck round bottom flask equipped with a bulb-condenser and magnetic stirrer, approximately 2.5 g of purified PHB (M_n = 84700 $g \cdot mol^{-1}$ by GPC) were added to 90mL of 1,2-dichloroethane under nitrogen atmosphere and the mixture was heated at 70°C. According to the desired final polymer molecular

weight, the amount of PTSA with respect to PHB weight and the reaction time were varied. Specifically, for Low MW PHB (**1**) reaction was conducted for 17 hours in presence of 35 wt.% of PTSA. On the other hand, 20wt% of PTSA and a reaction time of 17 and 5 hours were necessary to prepare Low MW PHB (**2**) and Low MW PHB (**3**) respectively. The reaction products were precipitated in a large excess of ice-cold MeOH under vigorous stirring for 15 min. In the case of extremely low molecular weight PHB (Low MW PHB (**1**), $\boldsymbol{M_n}$ < 1500 g·mol^{-1}), oligomers were isolated as follows. The reaction solvent was removed under vacuum at 35°C and the residual dark-red oily solution was quickly solubilized in 100 mL of hot MeOH up to obtain a clear solution. The still warm MeOH solution was then precipitated in a large excess of vigorously stirred ice-cold water. In both cases the precipitated white solid was recovered by vacuum filtration over sintered disk filter funnel (porosity P4) and dried overnight at 70°C. Molecular structures were confirmed by ^{1}H-NMR. Low MW PHB (^{1}H-NMR, $CHCl_3$, δ): 5.25ppm (-O-C***H***(CH_3)-CH_2-CO-, backbone protons), 4.17 ppm (HO-C***H***(CH_3)-CH_2-CO-, terminal protons), 2.60-2.46 ppm (-O-C**H**(CH_3)-C***H***$_2$-CO-, backbone protons), 1.26 ppm (-O-CH(C***H***$_3$)-CH_2-CO-, backbone protons), 1.21 ppm (HO-CH(C***H***$_3$)-CH_2-CO-, terminal protons).

2.3.2.2. Preparation of low molecular weight PHB-diols in solution

In a twin-neck round bottom flask equipped with a bulb-condenser and magnetic stirrer, 2.5 g of purified PHB (M_n = 84700 g·mol^{-1} by GPC) and 6.8 mL of 1,4-butanediol were added to 80 mL of 1,2-dichloroethane (DCE) under nitrogen and the mixture was heated at selected reaction temperature. Specifically, alcoholysis was conducted for 5 hours at 75°C and 80°C for PHB-diol (**1**) and PHB-diol (**2**) respectively. When a pale milky-white solution was obtained, 875mg of PTSA (35wt% with respect to PHB weight) were added to the mixture in order to start the reaction. The product was recovered by precipitation following the same procedure aforementioned in the section 2.3.2.1. Molecular structures were confirmed by NMR spectroscopy. PHB-diol (**1**, **2**) (^{1}H-NMR, $CHCl_3$, δ): 5.25ppm (-O-C***H***(CH_3)-CH_2-CO-, backbone protons), 4.17 ppm (HO-C***H***(CH_3)-CH_2-CO-, 3-hydroxybutyric terminal protons), 4.12 ppm (HO-CH_2-CH_2-CH_2-C***H***$_2$-CO-, 4-hydroxybutyl terminal protons), 3.66 ppm (HO-C***H***$_2$-CH_2-CH_2-CH_2-CO-, 4-hydroxybutyl terminal protons), 2.60-2.46 ppm (-O-C**H**(CH_3)-C***H***$_2$-CO-, backbone protons), 1.71-1.63 ppm (HO-CH_2-C***H***$_2$-C***H***$_2$-CH_2-CO-, 4-hydroxybutyl terminal protons), 1.26 ppm (-O-CH(C***H***$_3$)-CH_2-CO-, backbone protons), 1.21 ppm (HO-CH(C***H***$_3$)-CH_2-CO-

, 3-hydroxybutyric terminal protons). PHB-diol (**1**, **2**) (^{13}C-NMR, $CHCl_3$, δ): 172.1 ppm (HO-CH_2-CH_2-CH_2-CH_2-***C***O-, 4-hydroxylbutyl terminal protons), 169.29 ppm (-O-CH(CH_3)-CH_2-***C***O-, backbone protons), 67.75 ppm ((-O-***C***H(CH_3)-CH_2-CO-, backbone protons), 64.68 ppm (HO-***C***H_2-CH_2-CH_2-CH_2-CO-, 4-hydroxylbutyl terminal protons), 64.51 ppm (HO-***C***H(CH_3)-CH_2-CO-, 3-hydroxybutyric terminal protons), 62.34 ppm (HO-CH_2-CH_2-CH_2-***C***H_2-CO-, 4-hydroxylbutyl terminal protons), 43.37 ppm (HO-CH(CH_3)-***C***H_2-CO-, 3-hydroxybutyric terminal protons), 40.92 ppm (-O-CH(CH_3)-***C***H_2-CO-, backbone protons), 29.20 ppm (HO-CH_2-CH_2-***C***H_2-CH_2-CO-, 4-hydroxylbutyl terminal protons), 25.20 ppm (HO-CH_2-***C***H_2-CH_2-CH_2-CO-, 4-hydroxylbutyl terminal protons), 22.65 ppm (HO-CH(***C***H_3)-CH_2-CO-, 3-hydroxybutyric terminal protons), 19.90 ppm (-O-CH(***C***H_3)-CH_2-***C***O-, backbone protons).

2.3.2.3. Trifluoroacetylation of terminal hydroxyl groups

Approximately 25 mg of a given sample were solubilized in 1.5 mL of $CHCl_3$ on a hotplate at 50°C. The so-obtained solution was cooled down at room temperature and 0.15 mL of TFAn was added under stirring. After 30 minutes at room temperature, volatiles were quickly removed under nitrogen flow. 0.4 mL of toluene was added to the residue and once again volatiles were removed under nitrogen flow. Toluene addition was necessary in order to totally remove the possible residual trifluoroacetic acid by-product.

*2.3.2.4. Preparation of PHB-MA (**1**) starting from PHB-diol (**1**)*

In a 2-neck round-bottomed flask immersed in an oil bath at 80°C, equipped with a stirring magnet and a bulb-condenser, 1.00g of PHB-diol (**1**) is solubilized in 50ml of DCE in a nitrogen atmosphere. 88µl (1.2 equivalent with respect to oligomer hydroxyl groups) of 2-isocyantoethyl methacrylate and 1wt% of DBTDL (10mg) and course of the reaction *on line* monitored by FTIR spectroscopy (isocyante peak at 2227 cm^{-1}). After 30 minutes, observation of a peak constant intensities indicates achievement of a complete process. Solution is transferred into 250ml of ice cold MeOH and white precipitated isolated by vacuum filtration. ^{1}H-NMR spectroscopy confirms accomplishment of a complete end-capping process. Achievement of a complete end-capping process is confirmed by observation of ethyl methacrylate (EtMA) characteristic ^{1}H-NMR peaks and shift of polymer chain terminal protons signals. PHB-MA (**1**) (^{1}H-NMR, $CHCl_3$, δ): 6.12-5.59 ppm (C***H***$_2$-C(CH_3)-CO-O-CH_2-CH_2-NH-, EtMA terminal protons), 5.25ppm (-O-C***H***(CH_3)-CH_2-CO-, backbone protons), 5.05 ppm (CH_2-C(CH_3)-

CO-O-CH_2-CH_2-N***H***-, EtMA, terminal protons), 4.22-3.49 ppm (CH_2-C(CH_3)-CO-O-C***H***$_2$-C***H***$_2$-NH-, EtMA, terminal protons), 4.10 ppm (EtMA-CO-C***H***$_2$-CH_2-CH_2-C**H**$_2$-CO-, tetramethylene segment protons and EtMA-O-C***H***(CH_3)-CH_2-CO-, 3-hydroxybutyric terminal protons), 2.60-2.46 ppm (-O-C**H**(CH_3)-C***H***$_2$-CO-, backbone protons), 1.94 ppm ((CH_2-C(C***H***$_3$)-CO-O-CH_2-CH_2-NH-, EtMA terminal protons), 1.68-1.62 ppm (EtMA-CO-CH_2-C***H***$_2$-C***H***$_2$-CH_2-CO-, tetramethylene segment protons), 1.26 ppm (-O-CH(C***H***$_3$)-CH_2-CO-, backbone protons), 1.21 ppm (EtMA-O-CH(C***H***$_3$)-CH_2-CO-, 3-hydroxybutyric terminal protons).

*2.3.2.5. Preparation of low molecular weight PHB-diols with solvent-free process: PHB-diols (**sf**)*

In a 2-neck round-bottomed flask, 1.00g of purified PHB powder and 400µl of 1,4-butanediol are added. Flask is connected to a Hei-TORQUE Value 100overhead stirrer equipped with properly dimensioned PTFE stirring blade. After passing the system in a nitrogen atmosphere, flask is immersed in an oil bath at 190°C. Stirring is initiated at 15rpm and slowly increased to 100rpm in 15 minutes. This time is also necessary to achieve a properly melted and homogenized polymeric mass. Proper quantity (0.1wt%) of TBT, solubilized in 100µl of Toluene, is added and reaction conducted at 190°C for 5 minutes. At the end of the process, flask is removed from the oil bath and quickly immersed in an ice bath to quench transesterifications. Final PHB-diol (**sf**) are isolated stirring the obtained solid in 25ml of deionized water at room temperature for 30 minutes. ^{1}H, ^{13}C and ^{1}H-^{13}C-HSQC NMR experiments confirmed structure of prepared telechelic diol. Molecular structures were confirmed by NMR spectroscopy. PHB-diol (**sf**) (^{1}H-NMR, $CHCl_3$, δ): 5.25ppm (-O-C***H***(CH_3)-CH_2-CO-, backbone protons), 4.17 ppm (HO-C***H***(CH_3)-CH_2-CO-, 3-hydroxybutyric terminal protons), 4.12 ppm (HO-CH_2-CH_2-CH_2-C***H***$_2$-CO-, 4-hydroxybutyl terminal protons), 3.66 ppm (HO-C***H***$_2$-CH_2-CH_2-CH_2-CO-, 4-hydroxybutyl terminal protons), 2.60-2.46 ppm (-O-C**H**(CH_3)-C***H***$_2$-CO-, backbone protons), 1.71-1.63 ppm (HO-CH_2-C***H***$_2$-C***H***$_2$-CH_2-CO-, 4-hydroxybutyl terminal protons), 1.26 ppm (-O-CH(C***H***$_3$)-CH_2-CO-, backbone protons), 1.21 ppm (HO-CH(C***H***$_3$)-CH_2-CO-, 3-hydroxybutyric terminal protons). PHB-diol (**sf**) (^{13}C-NMR, $CHCl_3$, δ): 172.1 ppm (HO-CH_2-CH_2-CH_2-***C***O-, 4-hydroxylbutyl terminal protons), 169.29 ppm (-O-CH(CH_3)-CH_2-***C***O-, backbone protons), 67.75 ppm ((-O-***C***H(CH_3)-CH_2-CO-, backbone protons), 64.68 ppm (HO-***C***H_2-CH_2-CH_2-CH_2-CO-, 4-hydroxylbutyl terminal protons), 64.51 ppm (HO-***C***H(CH_3)-CH_2-CO-, 3-hydroxybutyric terminal protons), 62.34 ppm (HO-CH_2-CH_2-CH_2-***C***H_2-CO-, 4-hydroxylbutyl terminal protons), 43.37 ppm (HO-CH(CH_3)-

CH_2-CO-, 3-hydroxybutyric terminal protons), 40.92 ppm (-O-CH(CH_3)-***C***H_2-CO-, backbone protons), 29.20 ppm (HO-CH_2-CH_2-***C***H_2-CH_2-CO-, 4-hydroxylbutyl terminal protons), 25.20 ppm (HO-CH_2-***C***H_2-CH_2-CH_2-CO-, 4-hydroxylbutyl terminal protons), 22.65 ppm (HO-CH(***C***H_3)-CH_2-CO-, 3-hydroxybutyric terminal protons), 19.90 ppm (-O-CH(***C***H_3)-CH_2-***C***O-, backbone protons).

*2.3.2.6. Preparation of PHB-MA with solvent-free process: PHB-MA (**3sf**)*

In a 5ml cylindrical Schlenk flask, equipped with a cross-shaped magnetic stirrer, 360mg of PHB-diol (**3sf**) are added. Flask is connected to nitrogen source and, after immersion in a oil bath at 150°C, solid allowed to suitably melt (roughly 5-10 minutes). 71µl (1.1 equivalent with respect to oligomer hydroxyl groups) of 2-isocyantoethyl methacrylate are added and reaction carried out. Performing *on line* monitoring of isocyanate FTIR peak intensity, reaction is considered complete after 10 minutes. Slight excess of isocyanate is removed applying high vacuum at 150°C for 5 minutes. ^{1}H-NMR spectroscopy confirms accomplishment of a complete end-capping process. PHB-MA (**3sf**) (^{1}H-NMR, $CHCl_3$, δ): 6.12-5.59 ppm (C***H***$_2$-C(CH_3)-CO-O-CH_2-CH_2-NH-, EtMA terminal protons), 5.25ppm (-O-C***H***(CH_3)-CH_2-CO-, backbone protons), 5.05 ppm (CH_2-C(CH_3)-CO-O-CH_2-CH_2-N***H***-, EtMA, terminal protons), 4.22-3.49 ppm (CH_2-C(CH_3)-CO-O-C***H***$_2$-C***H***$_2$-NH-, EtMA, terminal protons), 4.10 ppm (EtMA-CO-C***H***$_2$-CH_2-CH_2-C**H**$_2$-CO-, tetramethylene segment protons and EtMA-O-C***H***(CH_3)-CH_2-CO-, 3-hydroxybutyric terminal protons), 2.60-2.46 ppm (-O-C**H**(CH_3)-C***H***$_2$-CO-, backbone protons), 1.94 ppm ((CH_2-C(C***H***$_3$)-CO-O-CH_2-CH_2-NH-, EtMA terminal protons), 1.68-1.62 ppm (EtMA-CO-CH_2-C***H***$_2$-C***H***$_2$-CH_2-CO-, tetramethylene segment protons), 1.26 ppm (-O-CH(C***H***$_3$)-CH_2-CO-, backbone protons), 1.21 ppm (EtMA-O-CH(C***H***$_3$)-CH_2-CO-, 3-hydroxybutyric terminal protons).

2.3.3. <u>Characterizations</u>

2.3.3.1. Determination of M_n and M_w by gel permeation chromatography

Molecular weights as M_n of the used and synthetized polymers were determined by gel permeation chromatography (GPC) with an Agilent 1260 Infinity instrument (G1322A 1260 Degasser, G1310B 1260 Isocratic Pump, G1316A 1260 TCC Thermostatted Column Compartment, G1362A 1260 RID Reflective Index Detector, G1328C 1260 Manual Injector); RID and column compartment were thermostatically controlled at 35°C ± 0.2°C. The instrument was equipped with a PLgel MiniMIX-A column (20 µm particle

size, 4.6x250 mm) coupled with a Tosoh TSKgel SuperMultipore HZ-M column (4 µm particle size, 4.6x150 mm); columns were preceded by a low dispersion in-line filter (frit porosity 0.2 µm). $CHCl_3$ was used as mobile phase at a flow rate of 0.2 mL·min^{-1} and toluene was used as internal standard (0.1 µL·mL^{-1}), run time of 37 minutes. Sample concentration of approximately 2 mg·mL^{-1}. Data were processed with Agilent GPC/SEC software, version A.02.01 using a calibration curve obtained with monodispersed polystyrene standards (EasiCal PS-1 Agilent kit).

2.3.3.2. Differential Scanning Calorimetry (DSC)

Thermal behavior is evaluated by Differential Scanning Calorimetry (DSC, Q10), fitted with a standard DSC cell and equipped with a Discovery Refrigerated Cooling System (RCS90) (all TA Instruments). Samples of about 7 mg are placed into aluminum pans and subjected to two heating cycles from −40°C to +195°C, hold for 6 and 4 minutes respectively, with heating and cooling rates of 10°C·min^{-1}. For glass transition temperatures ($\boldsymbol{T_g}$) evaluation, after second heating, a fast cooling to -40°C is accomplished. $\boldsymbol{T_g}$ are then observed performing a final heating to +195°C at 10°C·min^{-1}. The DSC cell was purged with dry nitrogen at 50 mL·min^{-1}. The system was calibrated both in temperature and enthalpy with Indium standard. DCS curves were processed with TA Universal Analysis 2000 software in order to extrapolate melting temperature ($\boldsymbol{T_m}$), crystallization temperature ($\boldsymbol{T_c}$) and glass transition temperature ($\boldsymbol{T_g}$) from the second heating scan. For melt and crystallization enthalpy ($\boldsymbol{\Delta H_m}$ and $\boldsymbol{\Delta H_c}$ respectively) are calculated integrating thermogram peaks. Where multiple endotherms were observed, the melting point from the higher temperature was taken as the true melting temperature. Crystallization degree are calculated according to:

$$X_c = \frac{\Delta H_m \cdot 100}{\Delta H_0 \cdot W_{PHB}} \qquad \textbf{(Equation 2)}$$

where $\boldsymbol{\Delta H_0}$ from melting enthalpy of PHB single crystal (literature: $\boldsymbol{\Delta H_0}$ = 146 J·g^{-1}) and $\boldsymbol{W_{PHB}}$ correspond to the weight fraction of PHB present in the sample. When PHBVV samples are analyzed, $\boldsymbol{X_c}$ is valued according to **Equation 2** utilizing the $\boldsymbol{W_{PHB}}$ determined by ^{1}H-NMR analyses.

2.3.3.3. Nuclear Magnetic Resonance (NMR) measurements

^{1}H-NMR and ^{19}F-NMR experiments were carried out at room temperature on a Varian Unity 400 spectrometer operating at 400MHz with a flip-angle of 45° while ^{1}H-^{13}C-HSQC experiments were carried out on Varian Inova 600 MHz equipped with an indirect triple resonance probe. $CDCl_3$ was used as solvent in order to reach a polymer

concentration in the range of 25 - 30 mg·mL^{-1}. Chemical shifts (δ) are reported in ppm relative to residual solvent signal $CHCl_3$ for ^{1}H-NMR (7.26 ppm) and ^{13}C-NMR (77.16 ppm) analyses and to $PhCF_3$ signal (-62.61ppm)[155] used as internal standard in ^{19}F-NMR measurements. Preliminary studies were performed in order to optimize the NMR acquisition conditions for each nucleolus. ^{1}H-NMR spectra were acquired with 28 scans and a T_1 of 1 sec. For the ^{19}F-NMR evaluation of ***OHV*** a T_1 of 5 sec and a flip-angle of 30° were used. ^{19}F-NMR spectra were recorded with 28 scans and a T_1 of 10 seconds. When the ***OHV*** content was lower than < 10^{-5} mol·g^{-1}, 52 scans were used in order to increase the signal/noise ratio. All the spectra were processed with VnmrJ software (Varian, Inc.).

*2.3.3.4. Determination of **OHV** by ^{19}F-NMR spectroscopy*

After derivatization, trifluoroacetylated polymer was dissolved directly in the functionalization vessel with 800 µL of $CDCl_3$, and 60 µL of trifluorotoluene (0.0407M in $CHCl_3$). The solution was stirred at room temperature for 10 minutes to ensure a complete solubilization. Afterwards, 600 µL of this solution were transferred in an NMR tube and ^{19}F-NMR spectrum was recorded. ^{19}F-***OHV*** expressed in mol·g^{-1} was calculated by the following equation:

$$^{19}\mathrm{F} - OHV = (I_{OH(F)} \cdot n_{STD} / I_{STD}) \cdot 1/m_T \qquad \textbf{(Equation 3)}$$

where $\boldsymbol{I_{OH(F)}}$ and $\boldsymbol{I_{STD}}$ are the integral value recorded for the fluorinated hydroxyl terminals and for the internal standard respectively. $\boldsymbol{n_{STD}}$ is the number of moles of internal standard added in the NMR tube (1.704·10^{-3} mmol). $\boldsymbol{m_T}$ is the mass of polymer contained in the NMR tube and is calculated as follows:

$$m_T = 0.75 \cdot m_{Pol} \qquad \textbf{(Equation 4)}$$

where $\boldsymbol{m_{Pol}}$ is the amount of polymer weighed at the beginning of the procedure and 0.75 is the volume ratio of the polymer solution in the NMR tube and initially prepared solution (600 µL/800 µL).

2.3.3.5. Determination of carboxylic end-groups concentrations by titration

Carboxylic end-groups are quantified by a potentiometric titration using a Mettler Toledo DL53 titrator. All analysed samples are previously dried overnight in oven at

70°C. The electric potentials are valuated with a CRISON 52 03 electrode. A MeOH solution of TBAOH (0.005M) is used as titrant and standardized titrating 10 mL of a BzOH/$CHCl_3$ solution (0.0007408 M). Approximately 300 mg of a given sample are solubilized in 40 mL of $CHCl_3$ and potentiometric titrated with the standardized TBAOH solution.

*2.3.3.6. Determination of **OHV** by ^{1}H-NMR spectroscopy*

Low molecular weight PHBs and PHB-diols obtained as described in section 2.2.1 and 2.2.2 were analysed by ^{1}H-NMR in order to confirm the structure of the obtained oligomers. Moreover, from ^{1}H-NMR spectra, Hydroxyl Value was determined by comparison of the relative intensities of PHB backbone signal at 5.26ppm ($\boldsymbol{I_{5.26}}$) and the secondary hydroxyl end-groups at 4.18ppm ($\boldsymbol{I_{4.18}}$) according to **Equation 5**:

$$^1\mathrm{H} - OHV = (I_{5.26}/I_{4.18} \cdot 86 + 87)^{-1} \qquad \textbf{(Equation 5)}$$

where 86 and 87 are the molar mass, in g·mol^{-1}, of hydroxy butyric repetitive units and secondary hydroxyl end-group bearing terminal unit, respectively.

*2.3.3.7. Determination of $\boldsymbol{M_n}$ by **OHV** in hydroxyl terminated polymers*

Dealing with hydroxyl-terminated polymer with hydroxyl groups as end-groups only, $\boldsymbol{M_n}$ of mono-hydroxyl-terminated polymers can be easily obtained from the reciprocal of the determined ***OHV***, based on its mathematical definition.

$$M_n = 1/OHV \qquad \textit{(Equation 6)}$$

For bi-hydroxyl-terminated polymers, where the polymeric chain bears two hydroxyl groups, the relationship between $\boldsymbol{M_n}$ and ***OHV*** has to be expressed by the following equation.

$$M_n = 2/OHV \qquad \textit{(Equation 7)}$$

2.3.3.8. FTIR analyses

FTIR spectra are recorded on a PerkinElmer Spectrum Two spectrometer equipped with a diamond crystal in Attenuated Total Reflectance (ATR) mode. Measurements are performed in the range of 4000 to 400 cm-1 at room temperature; the spectral resolution

was 4 cm^{-1} and the number of scans was 64 for each spectrum. Spectral data were processed with Spectrum 10 software (PerkinElmer).

*2.3.3.9. Preparation of PHB-MA (**1**)-based resin diluted in 2-HEMA and vat photopolymerization*

In a 100ml backer, equipped with a stirring bar, PHB-MA(**1**) and 2-HEMA are added in the appropriate ratio in order to obtain a mixture composition of 5wt% of PHB-MA(**1**) in 2-HEMA. Achievement of a homogeneous resin (milky white) is accomplished by stirring the mixture on a hot plate at 40°C to speed up the process. After addition of an appropriate amount of PI,[156] 2wt% with respect to PHB-MA (**1**), 3D printing is attempted using a PICOplus39, Asiga, with an X-Y resolution of 39 μm and light intensity of 30 $mW \cdot cm^{-2}$. The digital model of structure is designed and converted to stereolithography (STL) file format for 3D printing. The 100 printed layers thickness is set to 100 nm and an exposure time of 2 seconds is used, except for the first 5 layers irradiated for 7 seconds each. For the determination of the gel content, roughly 25mg of the printed object, accurately weight, are immersed in 10ml of $CHCl_3$ and leave at room temperature for 5 days. After that time, the insolubilized solid is filtered and dried in hoven at 70°C for 24 hours. The negligible weight-loss observed indicate achievement of a cross-linked resin.

*2.3.3.10. UV-irradiation of PHB-MA (**1sf**)*

UV-irradiation experiments are conducted utilizing a Hamamatsu Lightingcure LC8 (intensity 100%). Specifically, 10-15mg of PHB-MA (**3sf**) are placed on a microscope glass slide and the proper amount of Propylene Carbonate (40wt%) and PI (2wt%) is added. Glass is placed on a hot plate at 90°C and a macroscopically sufficient viscous resin is achieved in few minutes. The glass slide, maintained on the hot plate, is covered with an appositely realized polypropylene lid bearing three holes. While UV lamp is connected to the central hole, a nitrogen flux is allowed to enter from one of the other two holes and consequently exiting from the last hole. This is made in order to purge the cross-linking environment from all the traces of oxygen that have a well-known deleterious effect in quenching radical reaction.

3. Results and Discussions

3.1. Bacterial PHA for advanced applications

3.1.1. Realization of PHA composites filled with MFC by reactive extrusion

As illustrate in the introduction, the aim of this section is the realization of PHA based composite filled with MicroFibrillated Cellulose (MFC) by extrusion. Due to the physical nature of water-based suspension and to the problematics associated to its drying, prior MFC insertion into extruder appropriate modifications are required. Utilization of an MFC dispersing agent, a macromolecule that prevent fibrils "hornification" during suspension drying and facilitate MFC dispersion into a PHA-based matrix, could be a suitable solution. Considering water-solubility and PHA affinity of Polyethylene Glycol (PEG), such a polyether could be a good dispersing agent candidate. Nevertheless, earlier any kind of investigations into this direction, extrusion conditions to mix in the melt PHA and PEG must be identified. In detail, for this *ab initio* study, a 20wt% of PEG is used for realizing a PHA-based blend (PHA, 80wt%). Indeed, using a four-temperature zone single-screw extruder, conditions for obtain a good 80/20 blend are determined (**Figure 15**).

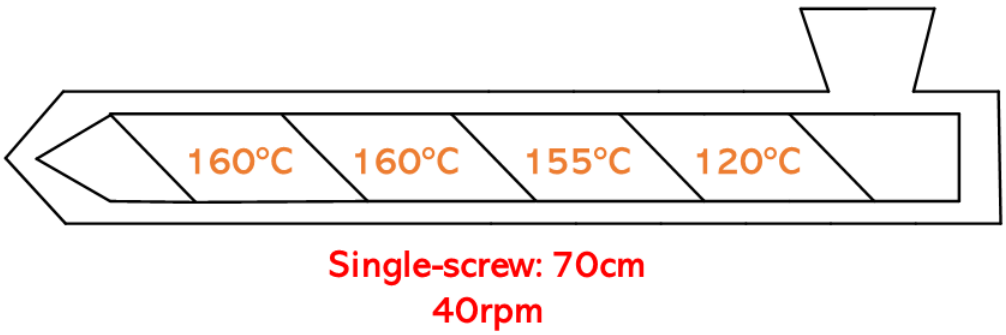

Figure 15. Extrusion condition for thermo-mechanical mixing of the 80/20 blend composed by PHA and PEG.

Once established correct parameters to extrude the 80/20 blend, MFC fibrils incorporation into PEG is faced. Thus, PEG is easily solubilized in water and the clear and colorless solution is added to a proper amount of MFC suspension. Specifically, quantity of MFC is chosen in order to obtain a final 80/20 polymeric blend filled with 5wt% of MFC. Dispersion of the polymer solution into polysaccharide suspension is

achieved upon utilization of an ULTRA-TURRAX® disperser. Homogenized dispersion is finally transferred in metal petri dish and freeze-dried. The obtained white porous sponge is milled to powder and SEM images are realized to exclude occurrence of agglomeration phenomena (**Figure 16**).

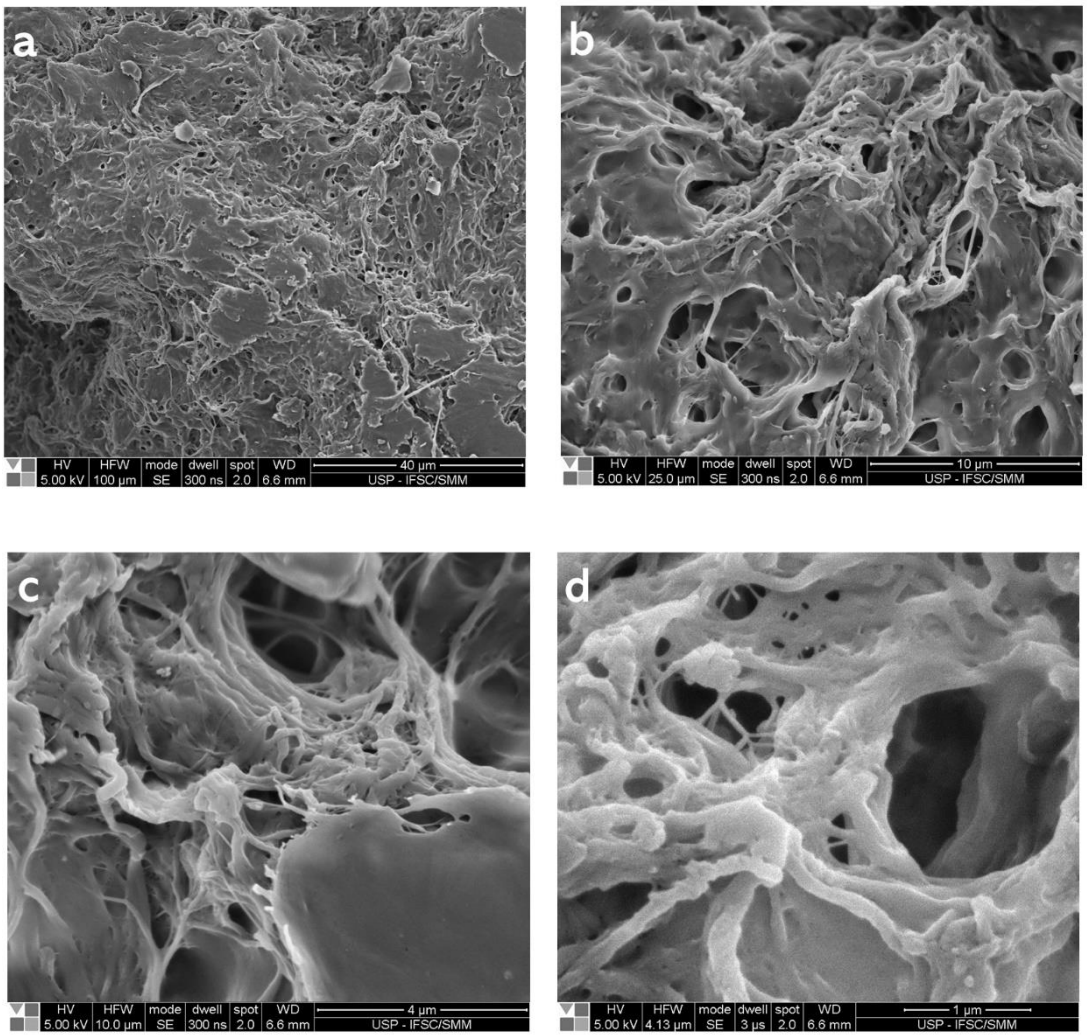

Figure 16. SEM images of the PEG/MFC mixture obtained by freeze-drying.

Collected SEM images highlight how PEG act as a coating agent for MFC fibrils. In detail, PEG covering seems to actually prevent drying induced “hornification” effect. Such a hypothesis seems to be confirmed by the presence of nano-dimensioned fibers reasonably ascribed to cellulose (**Figure 16d**). The prepared dried material consists in an easily handled powder perfectly suitable for being processed in a conventional extruder. Indeed, keeping constant the previously investigated PHA/PEG ratio and extrusion parameters (**Figure 15**), distribution of MFC fibrils into PHA matrix is

attempted. Even in this case, morphology of cryo-fractured surfaces is analyzed by SEM images (**Figure 17**).

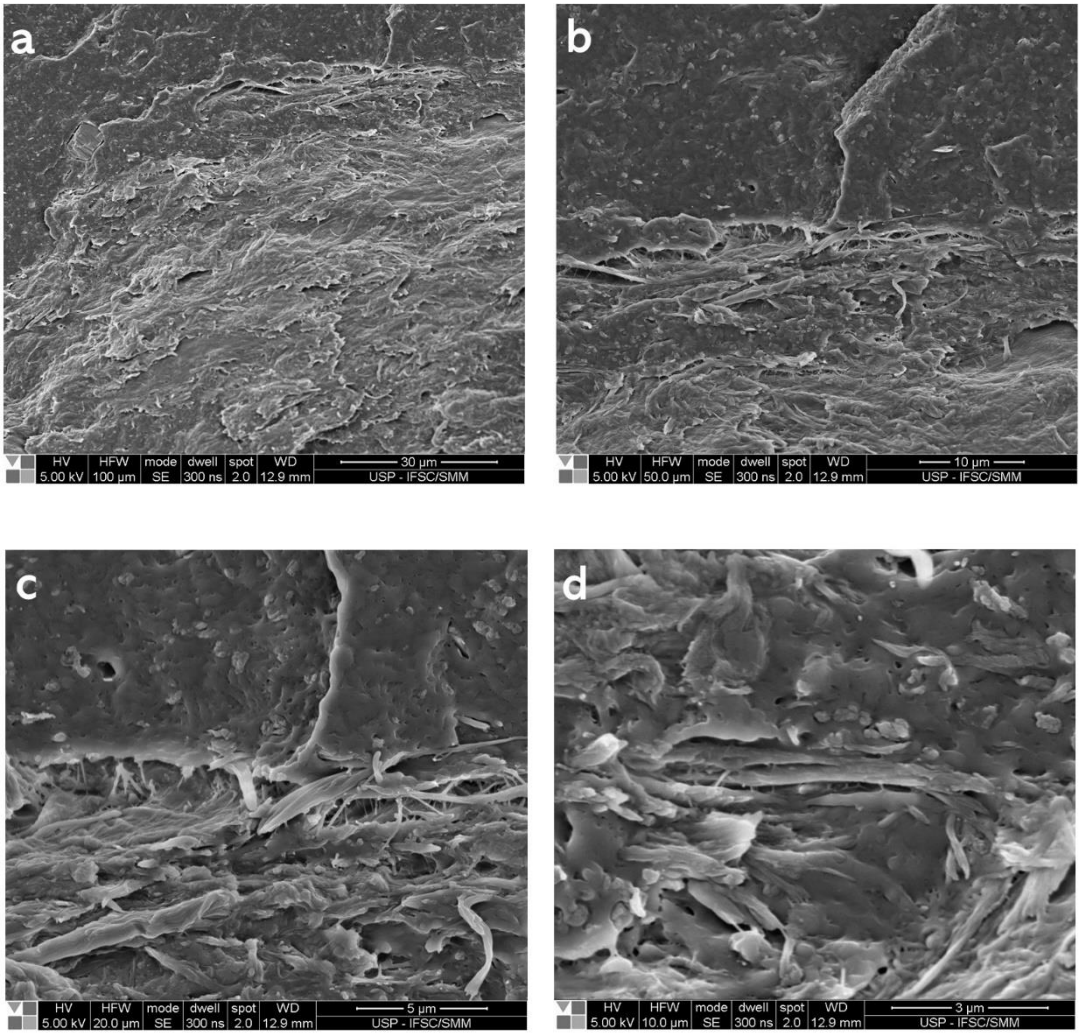

Figure 17. SEM images of the prepared blend: PHB and PEG (80/20 in wt%) filled with 5wt% of MFC.

As it is possible to observe from images in **Figure 17** a good level of fibers dispersion seems to have been achieved. Especially in **Figure 17c** and in **Figure 17d** nanometric fibers seems to be present and well-accommodate into the polymeric matrix. Thus, from such a very preliminary study, obtained satisfying results endorse further research in these field. Indeed, in addition to verify possible prepared material melioration ascribed to MFC presence, such as mechanical and thermal stability improvement, composite composition should be varied. Reasonably, utilization of a different PHA/PEG weight ratio or a change in MFC content would affect final materials properties.

3.1.2. PHA nanocomposites for bone tissue engineering

As above stated, a fundamental parameter to consider dealing with potential biomaterials is biocompatibility and, more specifically, cytotoxicity. For this reason, thin polymeric films based on PHB and PHBVV are prepared by previously mentioned Solvent Casting technique. In detail, polymer is solubilized in chloroform (1.25wt%) and, after solution transfer in a petri dish, thin films are obtained carrying out a slow solvent evaporation. Composites films are realized employing Hydroxyapatite (HA) and β-Tricalcium phosphate (β-TCP) as fillers, well-known osteogenic promoting inorganic materials. A slightly different procedure is followed for the preparation of these composites. Specifically, before transfer the as-before-realized polymer chloroform solution into the petri dish, solvent-insoluble inorganic fillers are added in the desired amount. Therefore, homogenization of the suspension is then achieved upon sonification. The inorganics well-dispersed suspension is finally poured into a petri dish and, analogously to pure polymer, thin films obtained. Thus, with a view to next differentiation studies, even cytotoxicity of PHA based composite is studies (**Table 1**).

Table 1. Composition of sample prepared for preliminary biocompatibility trials.

PHB-based films		**PHBVV-based films**	
Polymer matrix	**Filler**	**Polymer matrix**	**Filler**
PHB (**1**) + DINCH (10phr)	-	PHBVV (**1**)	-
PHB (**1**) + DINCH (10phr)	HA (5wt%)	PHBVV (**1**)	HA (5wt%)
PHB (**1**) + DINCH (10phr)	HA (10wt%)	PHBVV (**1**)	HA (10wt%)
PHB (**1**) + DINCH (10phr)	β-TCP (5wt%)	PHBVV (**1**)	β-TCP (5wt%)
PHB (**1**) + DINCH (10phr)	β-TCP (10wt%)	PHBVV (**1**)	β-TCP (5wt%)

Two different type of PHAs are used in the realization of polymeric matrix. As mentioned in the introduction, material mechanical properties could have an effect on instruct cells differentiation. Properties of rigid and brittle PHB can be easily varied, and potentially tailored, by the enzymatic realization of copolymers as PHBVV. Specifically, PHBVV (**1**) display very different properties with respect to PHB (**1**) in terms of melting, crystallization and crystallinity (see **Table 3**). As a technical consequence, utilization of a plasticizer (DINCH) is required for the realization of thin films based on rigid PHB (**1**). From the prepared thin films (**Figure 18**), small disks are realized for cytotoxicity trials.

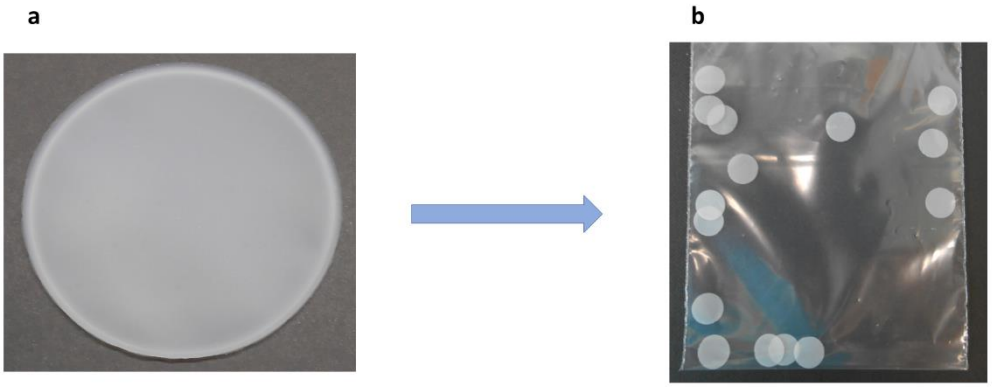

Figure 18. a) General example of PHA-based thin film prepared by Solvent Casting technique; b) Small disks prepared for preliminary biocompatibility trials.

Prepared small disks were analyzed at the Istituto Ortopedico Rizzoli (IOR) laboratory. In details, films are seeded with $1x10^4$ human Mesenchymal Stem Cells (hMSCs), as described in *2.2.3.2* section (**Figure 19**).

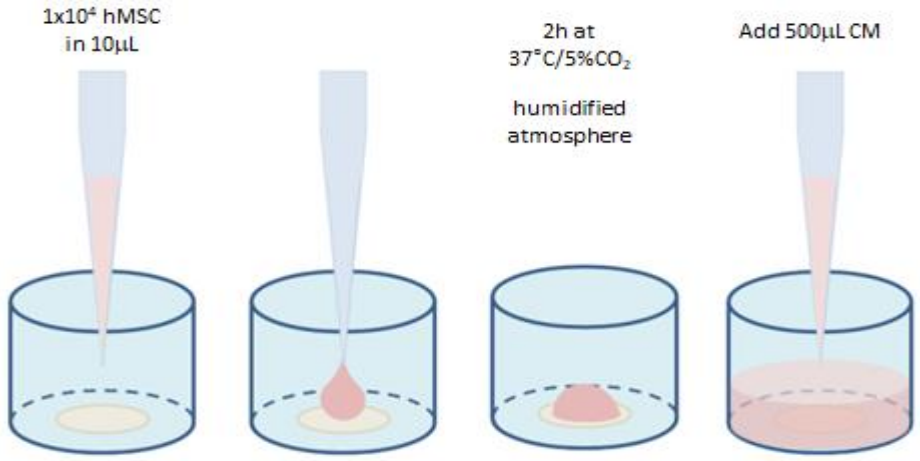

Figure 19. General procedure for the seeding of prepared materials. a) Seeding of hMSCs solution; b) Cell adhesion on seeded materials: 2 hours at 37°C in humidified atmosphere with 5% of CO_2; c) Addition of 500µl of Culture Media.

After 24 hours, cells adhesion is evaluated staining hMSCs using the Live&Dead viability/cytotoxicity assay. Operating in this manner, a simultaneous identification of live and dead cells can be accomplished. Indeed, viable cells are stained in green, while dead cells in red. It can be concluded that all the tested materials exhibited little or no toxicity towards hMSCs (**Figure 20**).

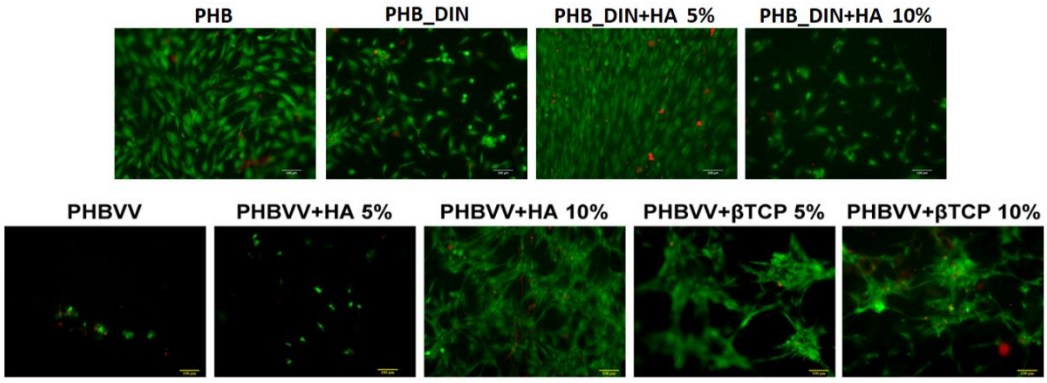

Figure 20. Representative images of Live/Dead assay of hMSCs seeded on various PHAs-based thin film 24 hours after the seeding. Bar represents 100 µm.

One more interesting result is derived from cells morphologies in the fluorescence images in **Figure 20**. The observable spindle shape, typical of healthy cells, further proves biocompatibility of the tested materials. Even proliferation studies highlight positive results. Metabolic state of the cells attached on different films is assessed by using Alamar Blue proliferation assay (**Figure 21**).

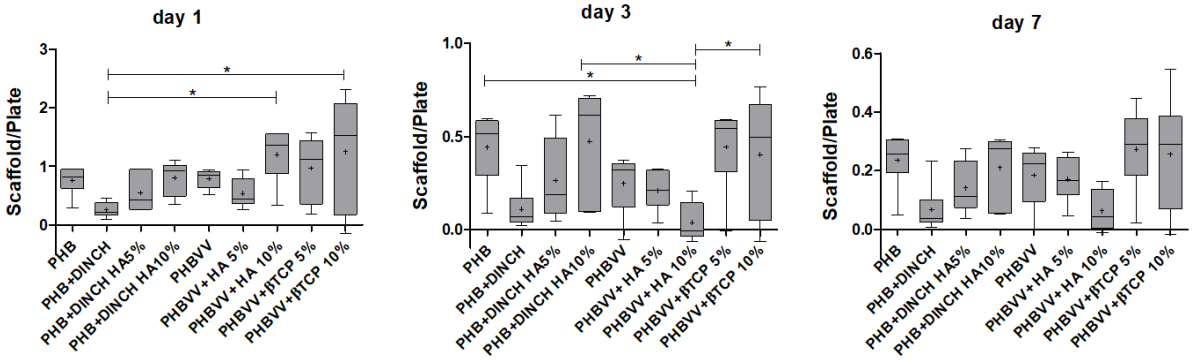

Figure 21. Cell number obtained from interpolation of Alamar blue fluorescence with a standard curve are normalized against cell number in the reference sample (cell culture flask). Data are presented as box plot indicating median (horizontal line), interquartile range (box) and minimum/maximum values (error bars). Mean values are also reported (cross). One Way ANOVA was performed, followed by Tukey multiple comparison test to check for significant differences (*P<0.05; **P<0.01).

From these results is possible to compare how the composition of each materials affect cell growth on the films. Specifically, a significative lower result of PHB + DINCH compared to PHBVV + HA10% (P <0.05) and PHBVV + β-TCP10% (P <0.01) at 24 hours after seeding is highlighted. After 3 days in culture, however, only PHBVV + HA10% shows a lower proliferation than other materials. Other comparisons are not statistically significant, but it is interesting to note that the PHBVV added with β-TCP, both at 5% and at 10%, has the highest values at all the considered timepoints.

Concerning cells differentiation, potential materials osteogenic differentiation is valued on 3 dimensional scaffolds, for reasons stated in the introduction. Indeed, a series of PHB and PHBVV based scaffolds is prepared utilizing Thermally Induced Phase Separation (TIPS) technique. Even in this case, utilization of a plasticizer (Dinch) is necessary for PHB based scaffolds **Table 2**.

Table 2. Composition of sample prepared for preliminary biocompatibility trials.

PHB-based scaffolds		**PHBVV-based scaffolds**	
Polymer matrix	**Filler**	**Polymer matrix**	**Filler**
PHB (**1**) + DINCH (10phr)	-	PHBVV (**1**)	-
PHB (**1**) + DINCH (10phr)	HA (10wt%)	PHBVV (**1**)	HA (10wt%)
PHB (**1**) + DINCH (10phr)	β-TCP (10wt%)	PHBVV (**1**)	β-TCP (5wt%)

According to the utilized procedure, a clear and colorless polymer solution (3wt%) in hot 1,4-Dioxane. As for thin films, when composites scaffolds are prepared, insoluble inorganics are homogenously suspended in 1,4-Dioxane hot solution by means of sonification. Solution was then poured in an aluminum plate and phase separation achieved freezing solvent at -18°C. After repeated solvent extraction carried out with ethanol, a PHAs non-solvent, and a final drying in oven, 3D porous scaffolds are obtained (**Figure 22**).

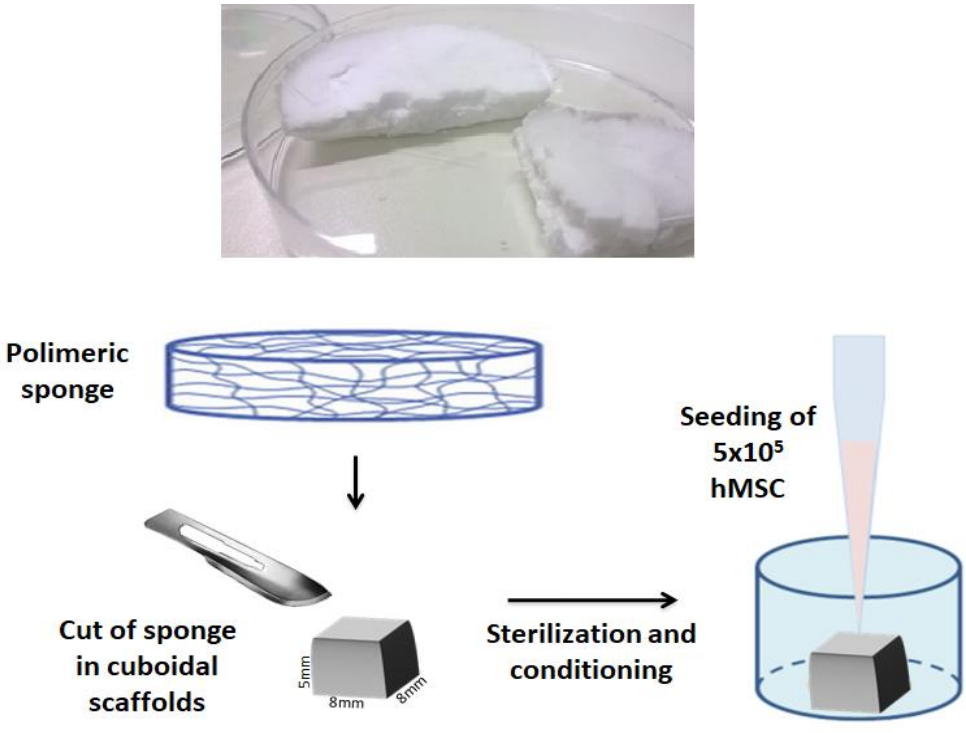

Figure 22. General example of PHA-based scaffolds prepared by TIPS technique. Graphic representation of 3D scaffold preparation for cell culture.

After appropriate samples preparation and sterilization, seeded materials are analyzed in order to point out evidence of cell differentiation towards osteogenic lineage., Under osteogenic stimuli MSCs engage a molecular reprogramming that lead the cell to become a functional osteoblast. One of the hallmark of this lineage commitment is the ability to produce mineralized nodules. For this reason the mineralization level of the extra-cellular matrix produced by the MSCs seeded on the different types of biomaterials has been evaluated using the Alizatin Red S dye. Indeed, it forms stable precipitates with calcium ions which can subsequently be dissolved and quantified by optical density measurements (**Figure 23**).

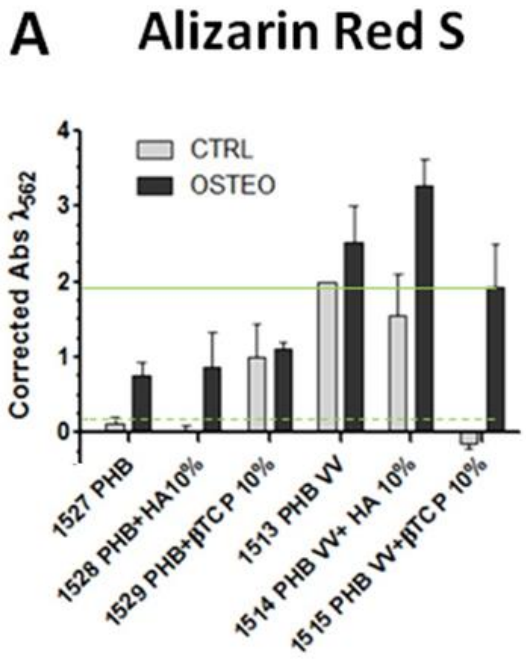

Figure 23. hMSC mineralization was quantified by Alizarin Red-S. Results are the mean of standard deviation from triplicate values per condition.

Differentiation tests are conducted in triplicates. Control condition results are accompanied by results obtained utilizing an osteogenic media (CTRL and OSTEO respectively, **Figure 23**). In control conditions, it is interesting observe that an opposite cellular response is produced by neat PHB and PHBVV. While it is recognizable how PHB alone do not has an osteoinductive behavior, addition of 10wt% β-TCP clearly leads to calcium deposition by hMSCs. Interestingly, such effect is not observed by the addition of 10wt% HA. On the other hand, dealing with PHBVV, pure polyester is unambiguously able to induce osteogenic cell differentiation. Such an induction is maintained even when PHBVV composites filled with 10wt% HA are studied. Surprisingly, utilization of 10wt% β-TCP as osteoinductive inorganic additive for PHBVV

based matrix results in a total suppression of hMSCs differentiation. As expected, trials performed exposing the materials to osteogenic medium leads in all the analyzed cases to cell differentiation. Among all materials, improvement due to osteogenic media effect is registered for PHB + 10wt% β-TCP and for PHBVV + 10wt% HA. In particular, results obtained for PHBVV based materials are extremely interesting. Indeed, neat PHBVV films and PHBVV based composite with 10wt% HA exhibit good osteogenic differentiation both in control condition and in presence of osteogenic media. However, cell differentiation total suppression carried out by β-TCP in control condition, is completely restored exposing composite to osteogenic media.

3.2. Chemical modification of bacterial PHA

3.2.1. Characterization and quantification of enzymatic PHB and PHBVV terminals

Gel Permeation Chromatography (GPC) and Differential Scanning Calorimetry (DSC) are widespread used techniques for thermoplastic polymer characterization and give an insight over various characteristic of materials as PHAs (see **Table 3**). Specifically, information about macromolecules molecular weights (MW) distribution and correlation between phase transition and heat exchanges are obtained respectively.

Table 3. Properties of some PHAs samples: GPC determined number average (M_n) and mass average (M_w) molecular weight; DSC

Sample	GPC analyses[a]		DSC analyses[b]					
	M_n [g·mol^{-1}]	M_w [g·mol^{-1}]	T_c† [°C]	ΔH_c† [J·g^{-1}]	T_m‡ [°C]	ΔH_m‡ [J·g^{-1}]	X_c‡,*	T_g†† [°C]
PHB (1)	126 300	655 100	87	68	173	83	57%	2
PHB (2)	84 900	288 600	82	62	173	82	56%	2
PHB (3)	45 500	122 700	81	67	172	83	57%	2
PHBVV (1)	237 300	639 100	-	-	130	3	-	-3
PHBVV (2)	107 300	253 700	74‡	30‡	170	27	-	-1

[a] See Experimental section for details. [b] General DSC run (heating and cooling rate 10°C/min): first heat to 195°C, cooling to -40°C; second heat to 195°C; † From cooling; ‡ From second heating; †† Determined by DSC after a fast cooling from melt phase (195°C) and subsequent heat at 10°C/min to 195°C.

On the other end, macromolecules chemical structure, as other chemical species, can be easily studied through ^{1}H-NMR spectroscopy. For instances, NMR peaks produced by monomeric unit protons of PHB (**1**) are easily recognized and from integral relative intensities chemical structure can be confirmed (**Figure 24**). Moreover, dealing with copolymers as PHBVV, integral relative intensities could lead to determination of different monomers concentration, *i.e.* copolymer composition. Indeed, chemically different monomers, as different species, would present distinct NMR signals. In such a case, by integral relative intensities comparison of properly selected peaks and adequate calculation, a monomers molar, and also mass, ration can be determined.

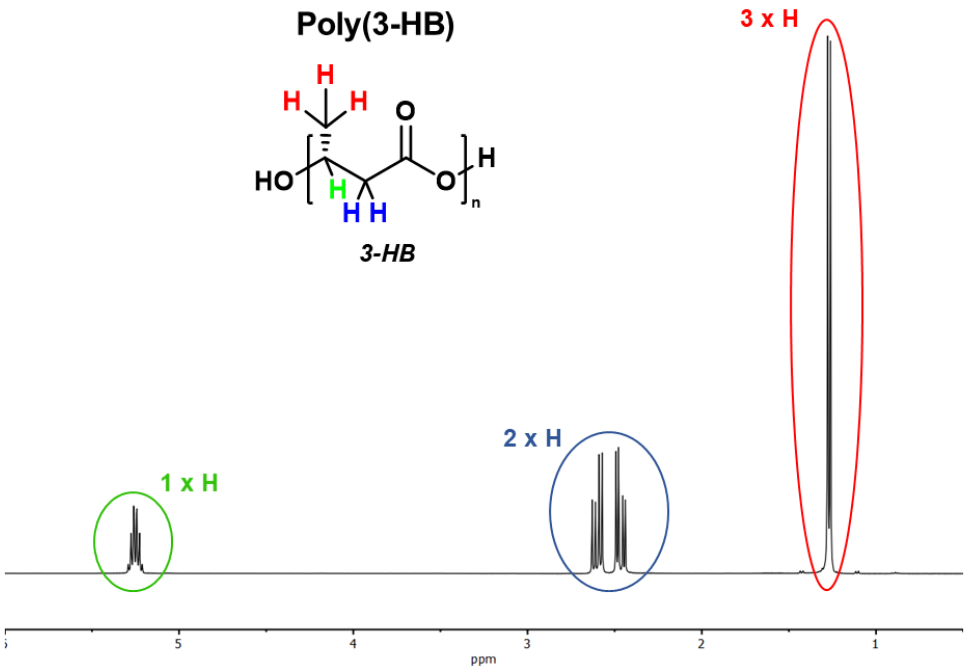

Figure 24. ^{1}H-NMR spectrum of PHB (**1**). In the spectrum, signals produced by hydroxybutyrate (***3-HB***) monomeric units are clearly visible. Comparison of integral relative intensities confirms molecular structure.

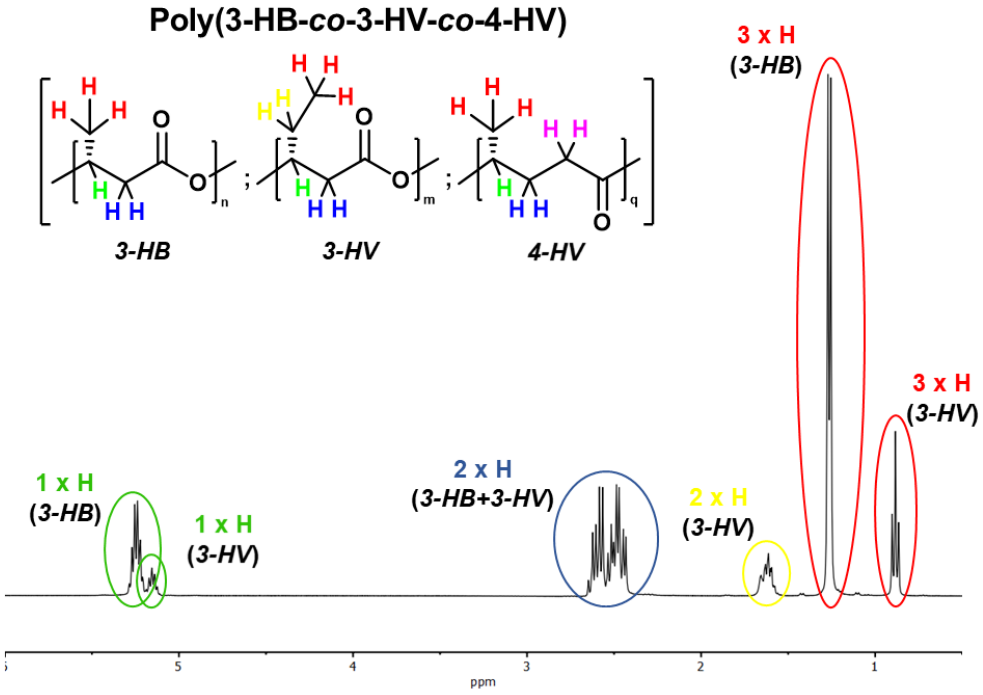

Figure 25. ^{1}H-NMR spectrum of PHBVV (**1**). In the spectrum, signals produced by hydroxybutyrate (***3-HB***) and hydroxyvalerate (***3-HV***) monomeric units are clearly visible. Comparison of integral relative intensities confirms molecular structure and allow to evaluate copolymer composition. In this case, peaks indicating presence of 4-hydroxyvalerate (***4-HV***) units are not visible.

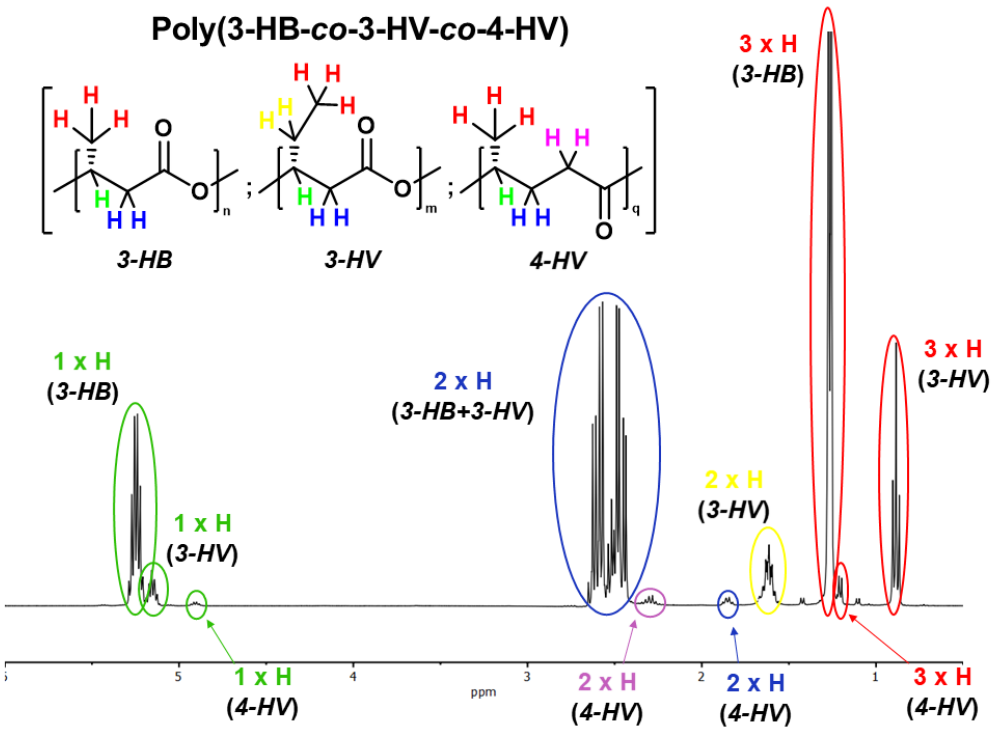

Figure 26. ^{1}H-NMR spectrum of PHBVV (**2**). In the spectrum, signals produced by hydroxybutyrate (***3-HB***), hydroxyvalerate (***3-HV***) and 4-hydroxyvalerate (***4-HV***) monomeric units are clearly visible. Comparison of integral relative intensities confirms molecular structure and allow to evaluate copolymer composition.

In details, signals produced by backbone methine protons (green labelled protons in **Figure 25** and **Figure 26**) can used to determine monomers relative concentration and, consequently, copolymer composition. Indeed, hydroxybutyric (***3-HB***) methine protons produce a multiplet centered at 5.25ppm, labelled 1xH (***3-HB***) in **Figure 24**, **Figure 25** and **Figure 26**. On the other hand, signal due to hydroxyvaleric (***3-HV***) methine protons, marked on **Figure 25** and **Figure 26** as 1xH (***3-HV***), has a chemical shift of 5.15ppm. Analogously, presence of 4-hydroxyvalerate (***4-HV***) repeating units is confirmed by multiplet centered at 4.90 and named 1XH (4-HV) in **Figure 26**. These signals are well distinguishable and relative integral intensities can be calculated. It is well-known that comparison of NMR relative intensities ($\boldsymbol{I}$), when correctly normalized with respect to number of magnetic equivalent protons ($\boldsymbol{H}$) that generate each signal, leads to molar ration ($\boldsymbol{X}$) determination. Dealing with PHBVV terpolymer, ***3-HV*** molar content ($\boldsymbol{X_{3HB}}$) can be calculated according to **Equation 8**.

$$X_{3HB} = \frac{I_{3HB}/H_{3HB}}{I_{3HB}/H_{3HB}+I_{3HV}/H_{3HV}+I_{4HV}/H_{4HV}} \qquad \textit{(Equation 8)}$$

Knowing ***3-HB***, ***3-HV*** and ***4-HV*** monomeric unit molecular weight ($\boldsymbol{MW}$: 86, 100 and 100 g·mol^{-1} respectively), copolymer mass composition ($\boldsymbol{m}$), derived from molar ratio, can be

easily calculated according to **Equation 9**. Clearly, molar and mass ratio of other PHBVV monomeric units can be similarly derived.

$$m_{3HB} = \frac{X_{3HB}MW_{3HB}}{X_{3HB}MW_{3HB}+X_{3HV}X_{3HV}+X_{4HV}X_{4HV}} \qquad \textit{(Equation 9)}$$

Specifically, analyzing PHBVV (**1**), no signal ascribed to 4-hydroxyvalerate units is visible (**Figure 25**). Indeed, it is reasonably to conclude that such PHA is composed only by 3-hydroxybutyrate and 3-hydroxyvalerate units. On the other hand, ^{1}H-NMR spectrum acquisition of PHBVV (**2**) clearly highly terpolymeric nature of the sample (**Figure 26**). According to previously reported calculation, copolymers compositions have been derived and summarized in **Table 4**.

Table 4. Composition of studied PHBVV sample

Sample	Copolymers compositions					
	X_{3HB} mol%	m_{3HB} wt%	X_{3HV} mol%	m_{3HV} wt%	X_{4HV} mol%	m_{4HV} wt%
PHBVV (**1**)	78	75	22	25	-	-
PHBVV (**2**)	79	76	19	21	2	2

However, as extensively discussed in the introduction, NMR signals intensities concentration dependency do not allow to easily investigate chemical nature of high $\boldsymbol{MW}$ polymers end-groups. Thus, in order to have as much as possible spectroscopic information regarding the biopolyester, low molecular weight PHBs were prepared following a previously reported procedure. Indeed, a lower in a polymer molecular weight obviously correspond to terminals concentration increase. Consequently, due to the expected signal/noise ratio improvement, NMR terminals peaks should result easily construable. In details, acid catalyzed (para-Toluene Sulfonic Acid Monohydrated, pTSA·H_2O) hydrolysis of an enzymatic high molecular weight PHB sample was conducted in organic media (**Scheme 9**).

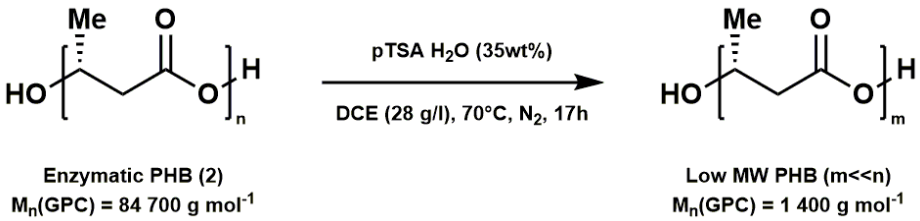

Scheme 9. Acid catalyzed molecular weight reduction of high molecular weight enzymatic PHB conducted in 1,2-dichloroethane (DCE).

Modulation of oligoesters molecular weight was obtained by varying reaction parameters. Specifically, a decrease in acid catalyst amount and reaction time corresponds to an increase in the oligomers molecular weights (**Table 5**).

Table 5. Molecular weight of prepared PHB oligoesters obtained by varying reaction conditions.

Entry	Starting PHB M_n by GPC	Reaction time	Catalyst amount	Low MW PHB M_n by GPC
1		17h	35wt%	1 400 g·mol^{-1}
2	84 700 g·mol^{-1}	17h	20wt%	1 700 g·mol^{-1}
3		5h	20wt%	2 100 g·mol^{-1}

As expected, NMR spectra of prepared low molecular weight polyester derivatives lead to additional information concerning terminal groups. As a general example, spectrum of low MW PHB (**1**) (entry **1**, **Table 5**) is reported (see **Figure 27a**). NMR signals due to protons of hydroxyl bearing end-group are highlighted by dashed/red circles. Specifically, multiplet attributed to terminal group methine proton, at 4.18ppm, is clearly observable and distinguishable from backbone analogues, at 5.25ppm (see box in **Figure 27a**). This allows to determine oligomers hydroxyl value, labelled ^{1}H-$\boldsymbol{OHV}$, according to **Equation 5**, that regarding low MW PHB (**1**) correspond to:

$$^1\mathrm{H} - \mathrm{OHV} = 7.69 \cdot 10^{-4}\ \mathrm{mol} \cdot \mathrm{g}^{-1}$$

Nevertheless, the most notably possibility offered by identification of such peaks is that reactive processes involving terminals functional groups could be easily investigated. Indeed, it is reasonable retain that any kind of hydroxyl derivatization would affect surrounding magnetic environment. Thus, NMR signals of end-group protons surely would spectroscopically fell the effect of such an event. Therefore, low MW PHBs can be used as model compounds for the study of a general hydroxyls involving reactive process. Consequently, the course of a PHB hydroxyl terminals general acylation reaction could be followed by valuing change in the relative intensity of the well-identifiable terminal methine peak. Specifically, reaction condition for a complete and not degradative trifluoroacetylation of PHAs hydroxyl groups would be defined though ^{1}H-NMR spectroscopy.

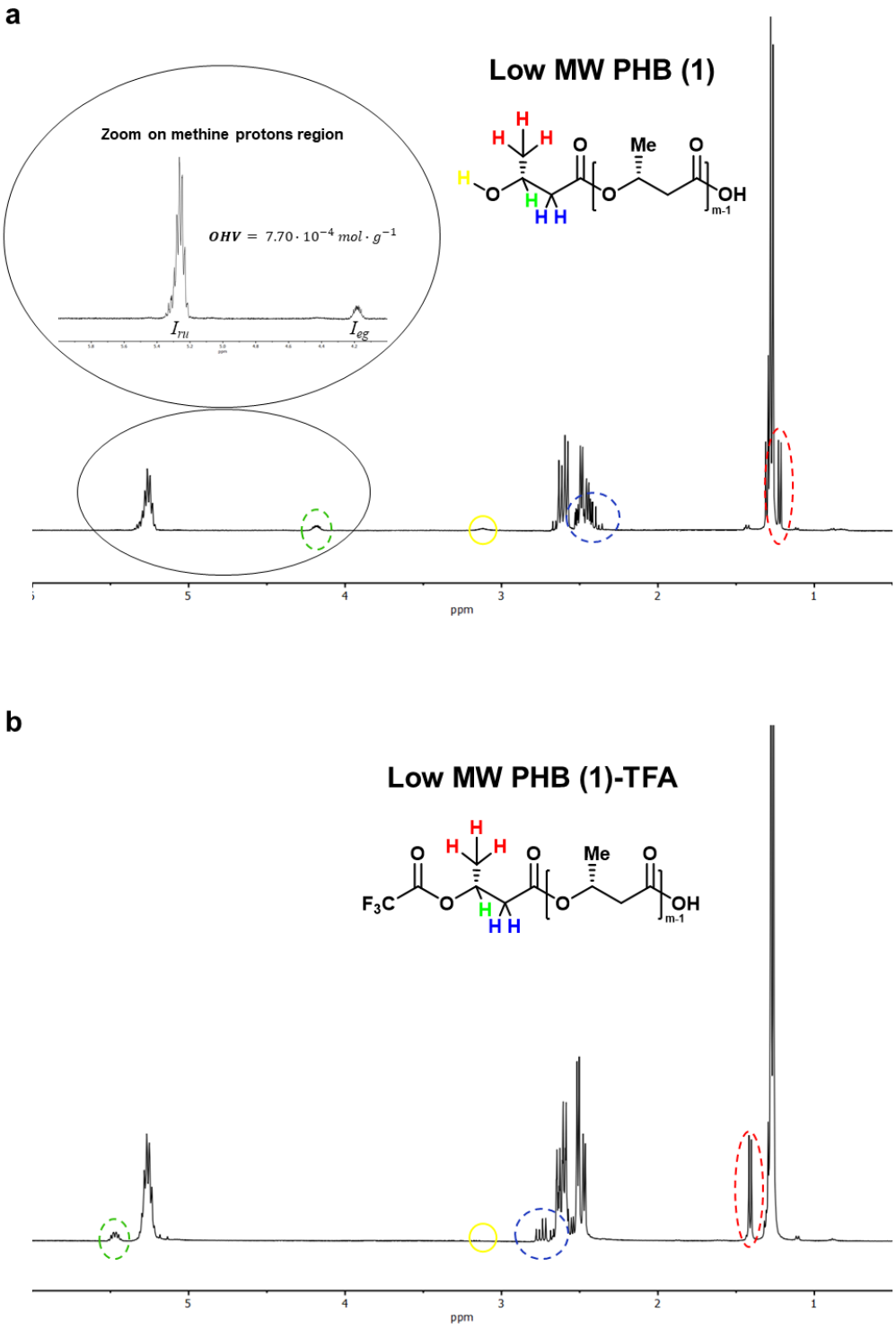

Figure 27. ^{1}H-NMR spectra. **a**) Low MW PHB (**1**), zoom on the methine protons region allow to easily calculate ***OHV*** according to **Equation 5**. **b**) Trifluoroacetylated low MW PHB (**1**). A shift to higher ppm is observed for all signals belonging to hydroxyl bearing end-group (dashed circles). Moreover, broad signal due to hydroxyl proton at roughly 3ppm (solid yellow circles) disappears.

As expected, a shift to higher ppm values, consequence of hydroxyl groups esterification, affect all the signals ascribed to terminal unit (see **Figure 27b**). Reasonably, the trifluoroacetyl electron withdrawing effect involves a downfield shift for all vicinal protons signals. Total disappearance of hydroxyl broad signal and complete shift of methine multiplet from 4.18ppm to 5.47ppm in the spectrum showed in **Figure 27b** proves the accomplishment of the process in the utilized reaction conditions (**Scheme 10**).

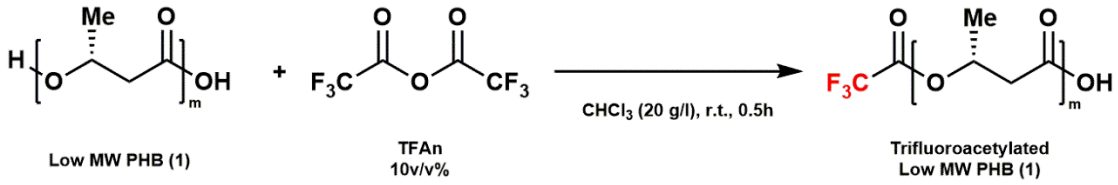

Scheme 10. Reaction condition for a complete trifluoroacetylation of low MW PHB (**1**) hydroxyl groups.

Confirms derived from ^{1}H-NMR spectra, regarding trifluoroacetylation reaction feasibility and completeness demand ^{19}F-NMR spectrum acquisition to continue the investigation. As stated in the introduction, complete hydroxyls trifluoroacetylation could be an interesting strategy to determine ***OHV*** in high molecular weight PHAs through ^{19}F-NMR titration. Obviously, in order to have a reliable NMR titration, a quantitative acquisition is required. Thereafter, determination of correct relaxation time T_1 and number of transients are fundamental parameters to carefully set in order to obtain reliable signals. For this reason, preliminary ^{19}F-NMR experiments were performed in order to find the appropriate conditions. In particular, T_1 of 10 seconds and 28 transients were found to be the most favourable parameters for obtaining reproducible integral values and acceptable signal/noise ratio. It has to be disclosed in advanced that for samples with an ***OHV*** lower then 10^{-5} mol·g^{-1}., *i.e.* characterized by an extremely low concentration of hydroxyl groups, 56 transients are required.

Returning to trifluoroacylated low MW PHB (**1**), named low MW PHB (**1**)-TFA, its fluorine NMR spectrum is simply acquired (see **Figure 28**). Indeed, the nowadays average available NMR technologies allow to investigate the most common studied nuclei (^{1}H, ^{13}C, ^{19}F, ^{31}P, …) utilizing the same instrument. Indeed, a simple switching command, operated from the workstation, is required. Performing ^{19}F-NMR acquisition of a precisely weighted amount of functionalized polymer (m_T) in presence of a known molar quantity of internal standard (n_{STD}), an easily interpretable spectrum is obtained (see **Figure 28**). Comparison of integrals relative intensities of the peaks produced by

trifluoroacylated polymer terminals and internal standard, $I_{OH(F)}$ and I_{STD} respectively, allows to calculate ***OHV***, according to **Equation 3**. For low MW PHB (**1**), calculated ^{19}F-***OHV*** is:

$$^{19}F - OHV = 7.70 \cdot 10^{-4}\, mol \cdot g^{-1}$$

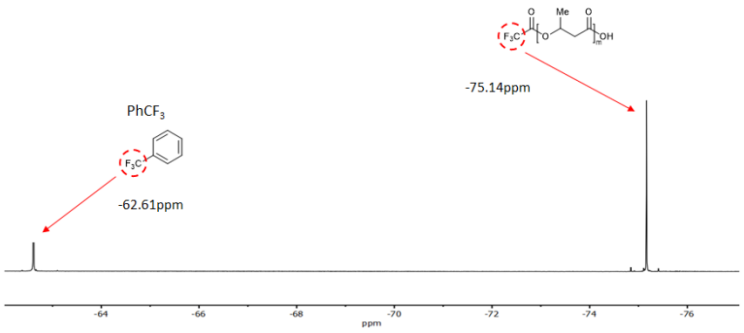

Figure 28. ^{19}F-NMR spectrum of low MW PHB (**1**)-TFA in presence of Trifluorotoluene ($PhCF_3$, internal standard).

The good accordance among the ^{1}H and ^{19}F determined ***OHV*** for low MW PHB (**1**), see **Table 6**, validates the reliability of the method, *i.e.* functionalization and subsequent acquisition of quantitative ^{19}F-NMR spectrum. After this preliminary study for optimizing the characterization method, other low MW PHBs (see **Table 5**) were analysed by means of the established procedure. Acquired ^{19}F-NMR spectra regarding low MW PHBs are reported in **Figure 29**. Even in these cases good concordance between ***OHV***s determined by ^{1}H-NMR and ^{19}F-NMR is observed (see **Table 6**) therefore consolidating the proposed method based on ^{19}F-NMR measurement.

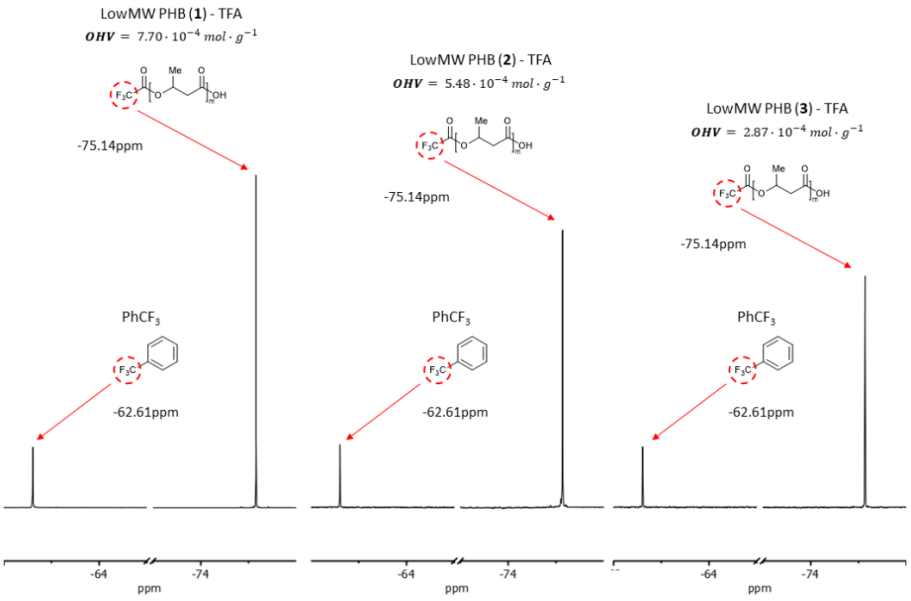

Figure 29. ^{19}F-NMR spectra recorded for the analyzed low molecular weight PHB derivatives and related OHV, calculated from integral values comparison.

Table 6. Data collected for Low MW PHBs. ***OHV*** obtained by ^{19}F-NMR, ***OHV*** by ^{1}H-NMR.

Sample	δ(OH^{II}-TFA)	^{19}F-***OHV*** [mol·g^{-1}]	^{1}H-***OHV*** [mol·g^{-1}]
Low MW PHB (**1**)	-75.14ppm	7.70·10^{-4}	7.69·10^{-4}
Low MW PHB (**2**)		5.48·10^{-4}	5.56·10^{-4}
Low MW PHB (**3**)		2.87·10^{-4}	3.03·10^{-4}

Such results are extremely important, making possible to conclude that the proposed functionalization, followed by ^{19}F-NMR spectroscopy, is a valid and easily reliable alternative to the conventional ^{1}H-NMR-based technique for ***OHV*** evaluation. As aforementioned, such information for high ***MW*** PHAs cannot be obtain by ^{1}H-NMR spectroscopy since the concentration of hydroxyl end-groups decreases significantly, therefore lowering the hydroxyl signal intensity in the spectrum. On the contrary, thanks to the more favourable signal/noise ratio, the herein proposed ^{19}F-NMR technique offers a very simple peaks individuation and integration, which allowed to characterize even samples with high ***MW***. Even in this case, the acetylation is initially studied and the sample PHB (**1**) (M_n = 126 300 mol·g^{-1}, see **Table 3**) is chosen for further optimizing this step. The trifluoroacetylation is performed with the previously found conditions varying the reaction times and the obtained products are consecutively analyzed by ^{19}F-NMR (**Figure 30a**). From the collected spectra at 30, 60 and 120 minutes of reaction, the ^{19}F-***OHV*** values are calculated. As show by **Figure 30b**, a quite constant value of ^{19}F-***OHV*** is

observed for all reaction times, indicating that 30 minutes of acetylation permit to reach a complete process as for low MW PHBs. Moreover, the constant ^{19}F-$\boldsymbol{OHV}$ recorded during the time is a first prove that no degradation processes took place during the functionalization. Indeed, a general acid promoted polyester degradation results in the formation of new hydroxyl terminals. Indeed, a hydrolytic chain cleavage, carried out by traces of water and catalysed by the reaction by-product trifluoroacetic acid, could occurs producing new carboxylic and hydroxylic end-groups. As the original polymer hydroxyl groups, these newly produced terminals would be functionalized by trifluoroacetic anhydride. Calculated ^{19}F-$\boldsymbol{OHV}$ would obviously be affected by these events, and an increasing value should be recorded during the time. Thus, a time constant ^{19}F-$\boldsymbol{OHV}$, in addition to demonstrate a complete acetylation achievement, demonstrate polymer stability in used acylation conditions, excluding occurrence of the only possible chain degradation process.

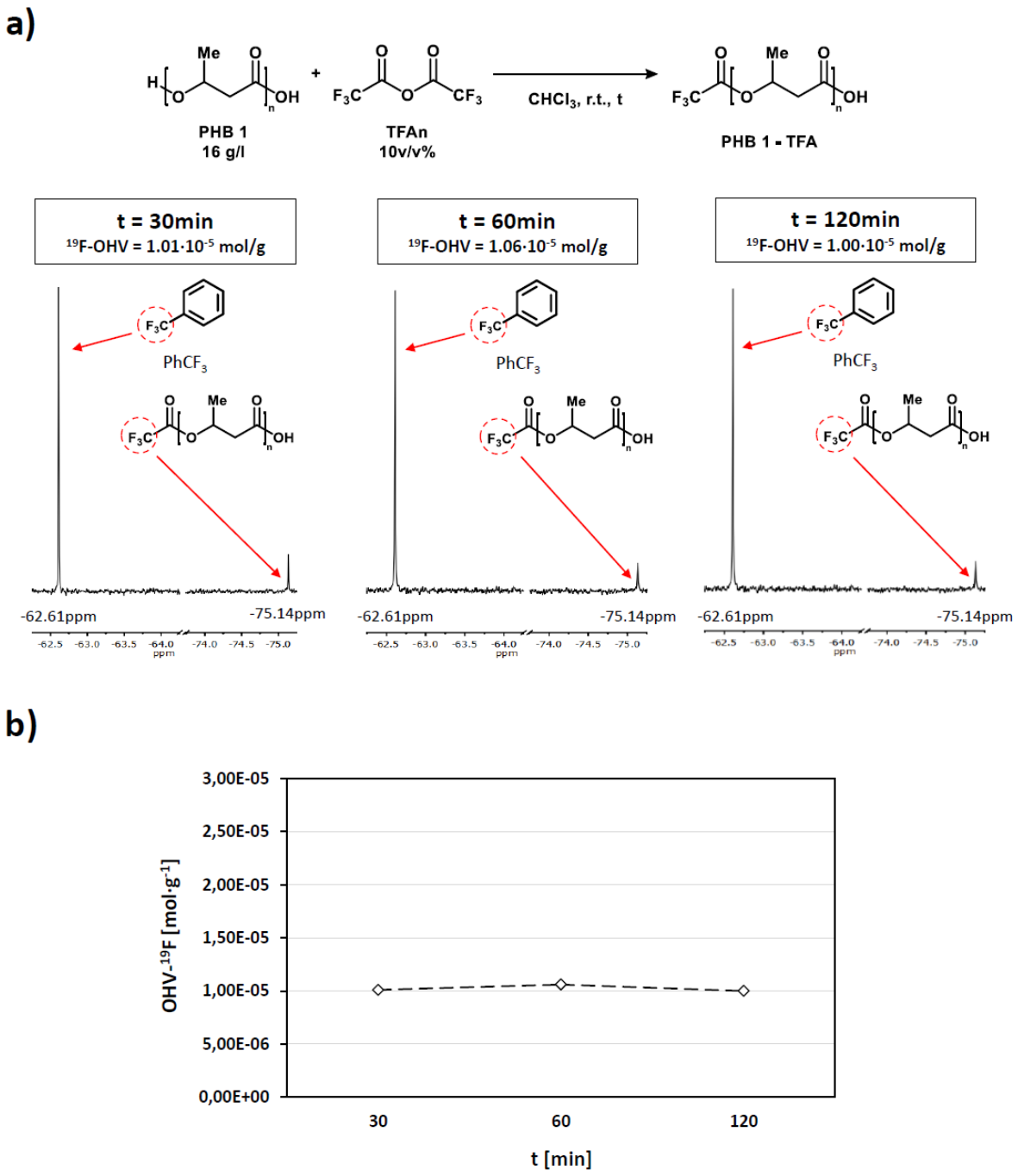

Figure 30. (a) ^{19}F-NMR spectra and corresponding calculated ^{19}F-***OHV*** of PHB 1-TFA obtained after 30, 60 and 120 minutes of trifluoroacetylation. **(b)** Graphical comparison of calculated ^{19}F-***OHV*** after 30, 60 and 120 minutes of trifluoroacetylation.

In order to further verify that the deliberately chosen mild reaction conditions do not induce any kind of polymer chains degradation, GPC analyses are conducted. In details, chromatogram of PHB (**1**) treated with trifluoroacetic anhydride for 2 hours was recorded and compared with chromatogram acquired for the bare PHB (**1**). As expected, comparing the chromatograms presented in **Figure 31**, it is clear that the two

curves do not present any significant difference. Such a result demonstrates that the acetylation process does not affect the molecular weight distribution even after 2 hours. Considering that a complete acetylation is achieved in a well lower time, 30 minutes, GPC results even more confirm that acylation conditions do not affect polymer structure.

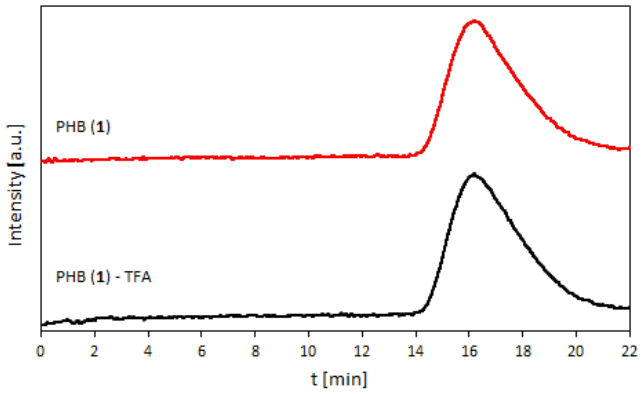

Figure 31. Chromatograms by GPC of bare PHB (**1**) (red line) and PHB (**1**)-TFA isolated after 2 hours in trifluoroacetylation reaction conditions (black line).

The possibility to extend the method to high $\boldsymbol{MW}$ PHAs was proved by comparing the results obtained by ^{19}F-NMR (spectra of high $\boldsymbol{MW}$ PHB and PHBV in **Figure 32** and **Figure 33** respectively) and titrimetric methods. Specifically, $\boldsymbol{AV}$s of all the analysed high molecular weight PHAs samples were determined by direct acid/base potentiometric titration of polymer chloroform solutions. The good matching between the data (**Table 7**) confirms the mono-hydroxyl terminated structure of bacterial PHAs polymers. Indeed, comparable $\boldsymbol{OHV}$ and $\boldsymbol{AV}$ recorded in a PHA sample, allows to exclude existence of other end-groups. Thus, according to **Equation 6**, a number average molecular weight ($\boldsymbol{M_n}$) of analysed PHA can be determined. Spectroscopically determined molecular weight are compared with results obtained by conventional GPC technique in **Table 6**. Such a result points out the efficiency of the proposed method. Indeed, after a simple and fast functionalization, many information can be determined by NMR spectra acquisition. Considering that for high molecular weight polymer the proposed functionalization does not affect ^{1}H-NMR spectra, due to the over and over again remembered signal/noise ratio, structural and composition data can be derived. Then, acquiring ^{19}F-NMR spectrum of the same sample results in calculation of sample $\boldsymbol{OHV}$ and $\boldsymbol{M_n}$. Tu sum up, a simple functionalization allows to access various information by utilization of a single spectroscopic technique.

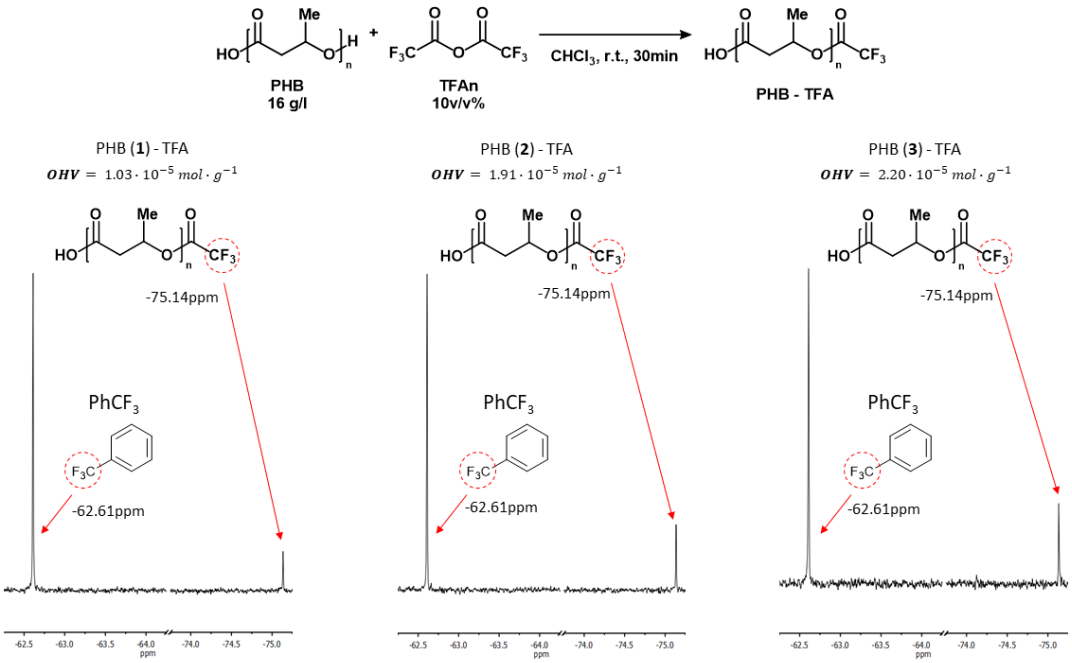

Figure 32. ^{19}F-NMR spectra and corresponding calculated ^{19}F-***OHV*** of three high molecular weight PHB after complete hydroxyl functionalization with trifluoroacetic anhydride.

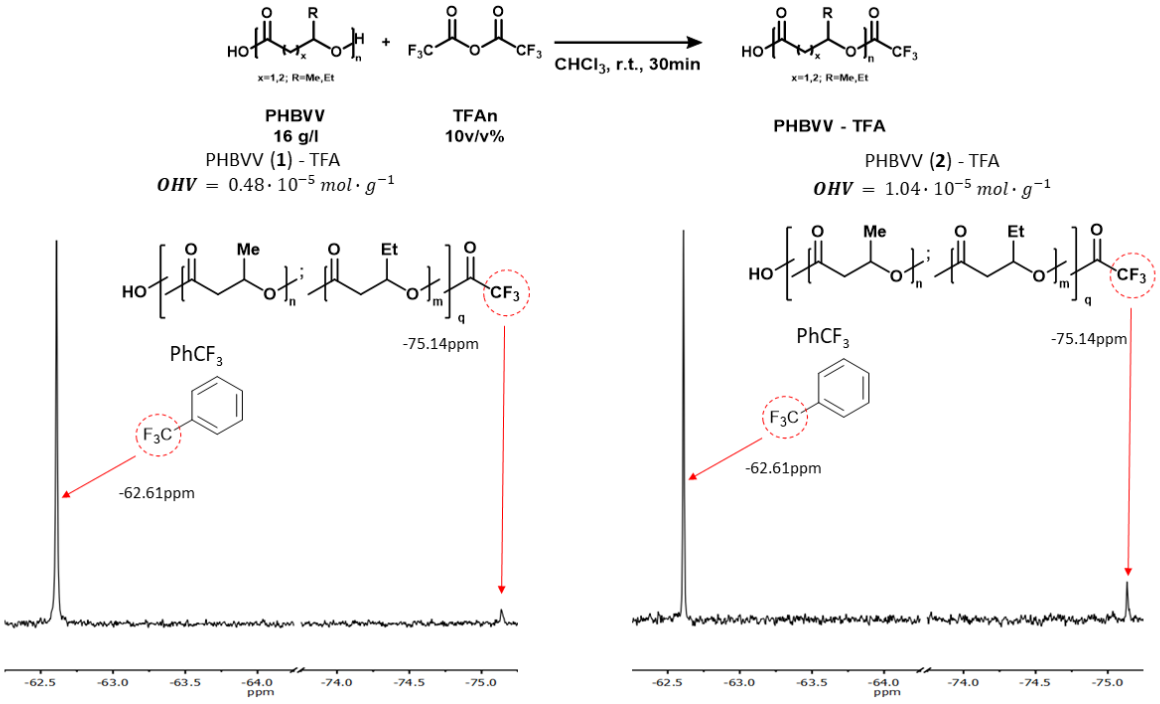

Figure 33. ^{19}F-NMR spectra and corresponding calculated^{19}F-***OHV*** of three high molecular weight PHBV after complete hydroxyl functionalization with trifluoroacetic anhydride.

Table 7. Data collected for high MW PHAs. ***OHV*** obtained by ^{19}F-NMR, Acid Value (AV) by titration, M_n by GPC and M_n by ***OHV*** analyses.

Sample	δ(OH^{II}-TFA)	^{19}F-***OHV*** [mol·g^{-1}]	***AV*** [mol·g^{-1}]	M_n by GPC [g·mol^{-1}]	M_n by ***OHV*** [g·mol^{-1}]
PHB (**1**)	-75.14ppm	$1.03 \cdot 10^{-5}$	$1.13 \cdot 10^{-5}$	126 300	97 100
PHB (**2**)		$1.91 \cdot 10^{-5}$	$1.78 \cdot 10^{-5}$	84 900	52 100
PHB (**3**)		$2.20 \cdot 10^{-5}$	$2.10 \cdot 10^{-5}$	45 500	45 700
PHBVV (**1**)	-75.14ppm	$0.48 \cdot 10^{-5}$	$0.63 \cdot 10^{-5}$	237 300	208 300
PHBVV (**2**)		$1.04 \cdot 10^{-5}$	$0.92 \cdot 10^{-5}$	107 500	96 200

An additional insight on the chemical nature of terminal hydroxyl groups can be obtained when the analysed polymer is terminated with different hydroxyl groups. This aspect was studied analysing the synthesized PHB-diol samples (**Scheme 11**) by ^{19}F-NMR, after an appropriate acylation (**Scheme 12**). It is worthy explicit that, for clarity reasons, PHB-diols structures have been sketched reverse with respect to previously reported PHAs structures. Regarding it, note opposite methyl substituent orientation in **Scheme 10** and **Scheme 11**.

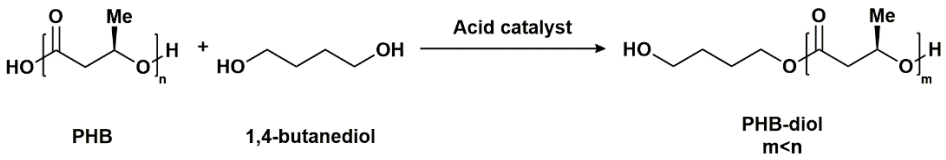

Scheme 11. General procedure for the synthesis of PHB-diols.

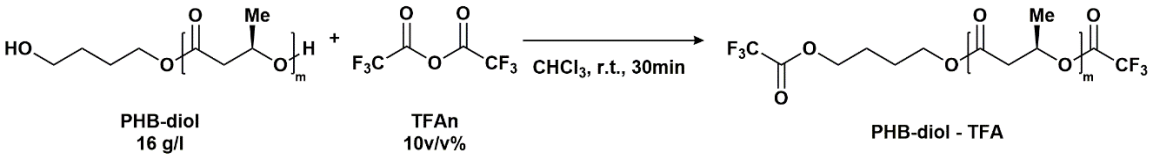

Scheme 12. Schematic representation of the trifluoroacetylation reaction and related conditions.

Due to the presence of primary and secondary hydroxyl groups, the ^{19}F-NMR acquisition shows two distinct signals (see **Figure 34** for PHB-diol (**1**)-TFA as a general example). Along with the previously observed peak at -75.14ppm, an additional peak at -74.92ppm is detected and assigned to the trifluoroacetylated primary terminal hydroxyl. Such singlet not previously observed in the spectra of trifluoroacetylated PHBs (**Figure 30a**), clearly appears in the spectra of PHB-diols-TFA. Moreover, by comparing the

relative intensities of the peaks, is also possible to estimate the molar concentration of the two types of hydroxyl groups (**Table 8**).

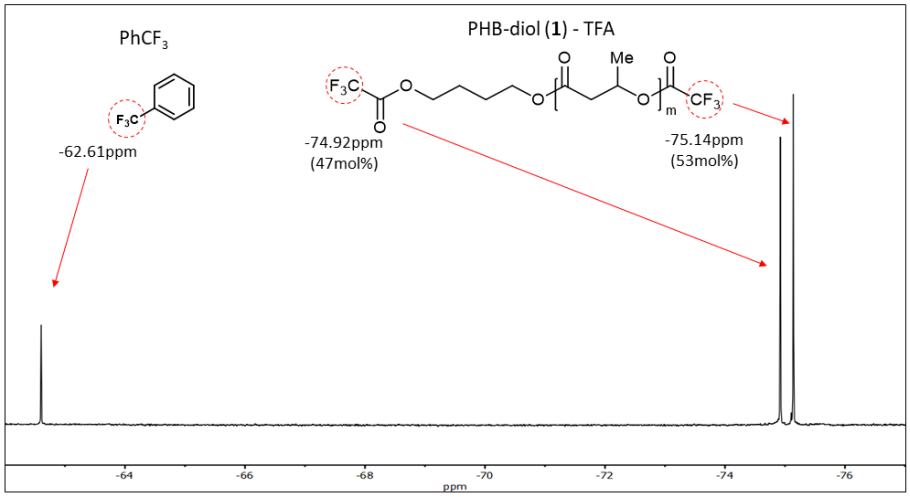

Figure 34. ^{19}F-NMR spectrum of trifluoroacetylated PHB-diol (**1**), named PHB-diol (**1**)-TFA.

Table 8. Hydroxyl content collected for PHB-diols samples. The chemically different hydroxyl groups present on the molecule are distinguished by the analysis.

Sample	δ(OH^{II}-TFA)	δ(OH^{I}-TFA)	Partial *OHV*		Total *OHV*	Molecular weight	
			^{19}F-$OH^{II}V$ [mol·g^{-1}]	^{19}F-$OH^{I}V$ [mol·g^{-1}]	^{19}F-*OHV* [mol·g^{-1}]	M_n by GPC [g·mol^{-1}]	M_n by OHV [g·mol^{-1}]
PHB-diol (**1**)	-75.14ppm	-74.92ppm	$2.28 \cdot 10^{-4}$	$2.02 \cdot 10^{-4}$	$4.30 \cdot 10^{-4}$	4300	4700
PHB-diol (**2**)			$3.38 \cdot 10^{-4}$	$2.93 \cdot 10^{-4}$	$6.31 \cdot 10^{-4}$	3000	3200

As for high molecular weight PHA, even for analyzed PHB-diol samples ***OHV*** can provides molecular mass information. Indeed, for regularly terminated PHB-diols in which each chain is di-end-terminated with hydroxyl groups, number average molecular weight ***Mn*** is calculated according to **Equation 7**. As expected, GPC determined molecular weight are comparable with the masses derived from ***OHV***s (**Table 8**).

3.2.2. *Realization of a PHB photopolymerizable resin with potential use for the realization of biomedical scaffolds through vat photopolymerization*

As stated in the introduction, polymer suitable for realization of vat photopolymerizable resins should be characterized by low viscosity, imparted by macromolecules low molecular weight. Moreover, presence of photosensible moieties, such as methacrylic groups, is clearly mandatory. Regrettably, natural PHB, as previously illustrated, do not present neither of these characteristics. Despite it, its polyester nature allows to easily prepare low molecular weight derivatives through alcoholysis reactions. In particular, the telechelic nature of the already mentioned PHB-diols makes such dihydroxyl-functionalized oligoesters attractive for preparation of various PHB-based "building blocks". Among them, macromonomers suitable for vat photopolymerization are of undeniable interest and PHB-diols are perfect starting point. Indeed, while their molecular weight can be modulated to very low value, according to preparation conditions, terminal hydroxyl moieties could be easily converted upon tailored reaction with specific chemicals. As an example, isocyanate display an interesting reactivity towards hydroxyl groups. Reasonably, α,ω-methacrylate terminated PHB-oligoesters (PHB-MAs) could be easily prepared reacting PHB-diol with a methacrylic bearing isocyante, such as 2-isocyantoethyl methacrylate (**Scheme 13**). The resulting oligomers could turn out to be suitable component in the preparation of a photopolymerizable resin.

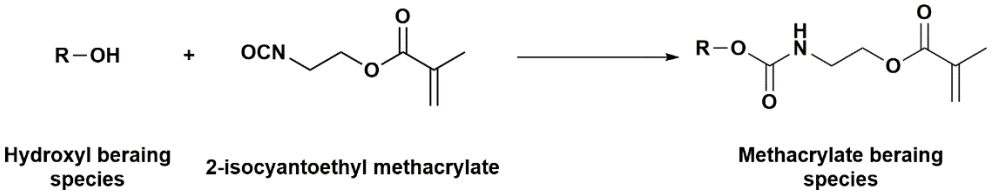

Scheme 13. General reaction between a hydroxyl bearing species and 2-isocyantoethyl methacrylate.

For these reasons, the previously analyzed PHB-diol (**1**) (**Table 8**) is used as starting point (see **Scheme 14** and for preparation).

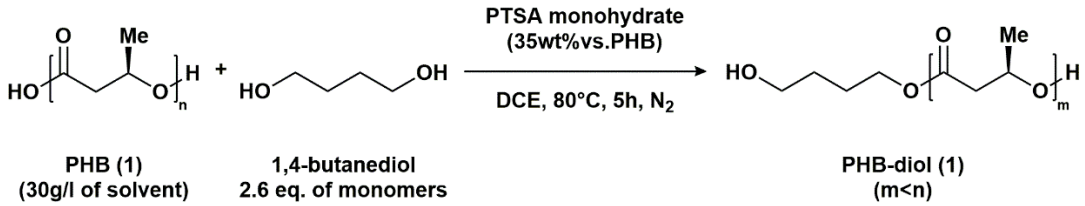

Scheme 14. Reaction condition for preparation of PHB-diol (**1**).

Looking to utilized amount of depolymerizing diol, quantity of 1,4-butnaediol is expressed in equivalent of monomers (2.6 eq. of monomers, **Scheme 14**). Dealing with alcoholysis, such a notation results to be extremely useful due to the fact that in addition to unequivocally define polyester/diol ratio also allows to visualize the conducted process. Indeed, total polyester depolymerization is theoretically accomplished upon utilization of one monomer equivalent of diol, as illustrated in **Scheme 15**.

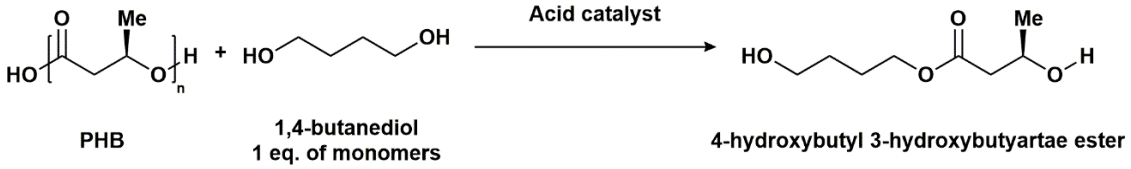

Scheme 15. Total PHB depolymerization theoretically achievable utilizing 1 monomers equivalent of 1,4-butanediol.

Utilization of such a notation allows to easily visualize the inefficiency of the process. Indeed, the preparation of PHB-diol (**1**) require a considerable excess of diol (2.6 equivalent of monomers). Thus, in addition to utilize toxic solvent and require long reaction time, realization of PHB-diol by processes conducted in solution suffers from one more drawback.

The isolated PHB-diol (**1**) was finally analyzed by NMR spectroscopy (**Figure 35**) to verify prepared oligomer structure. Indeed, an unambiguously increasing in intensity of the ***3-HV*** terminal methine protons signal clearly indicate achievement of molecular weight lowering (dashed and purple circles in **Figure 35a**). Moreover, ^{13}C-NMR and HSQC spectra, assigning detected carbon atoms (**Figure 35a** and **b**), confirm prepared oligoesters structure.

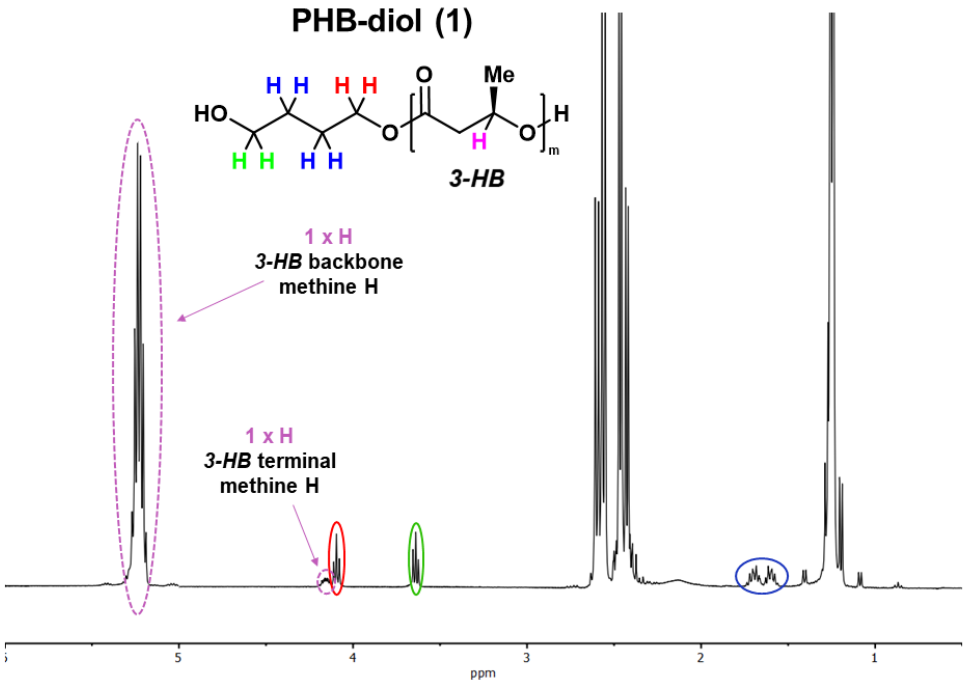

Figure 35a. ^{1}H-NMR spectrum of prepared PHB-diol (**1**). In the spectrum, signals belonging to newly introduced 4-hydrobutyl end-group and to ***3-HV*** methine proton, both in terminal and backbone positions, are highlighted.

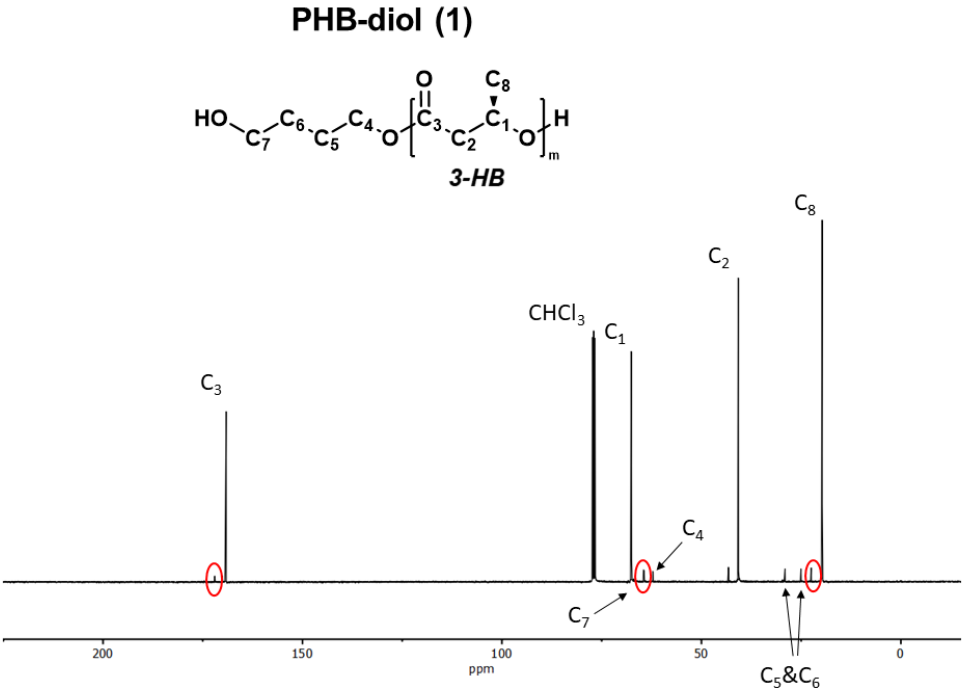

Figure 35b. ^{13}C-NMR spectrum of prepared PHB-diol (**1**). Presented spectrum, combined with HSCQ experiment (see **Figure 35c**), allows to assign carbon peaks and even identify signal produced by terminal group carbons (red circles, next to the signal of corresponding backbone analogous). Note that C_7 and terminal C_1 ^{13}C-NMR peaks has a very similar chemical shift (signals separation is not appreciable in reported spectrum.

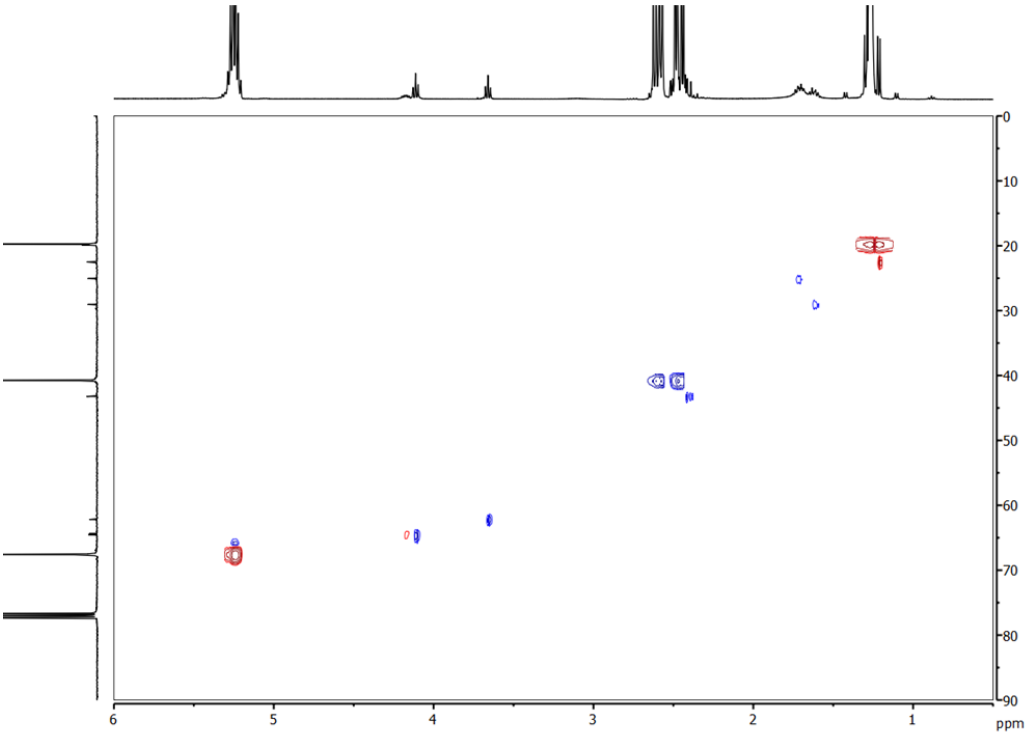

Figure 35c. HSQC spectrum of PHB-diol (**1**). HSQC experiments allow to distinguish secondary carbons (CH_2, red) from tertiary and primary carbons (CH and CH_3, blue). Correlating carbon and vicinal protons, such a technique is not able to identify quaternary carbons, as the carbonylic carbons. On the ^{13}C-NMR carbon axe, chloroform signal is observable (77.16ppm).

Finally, DSC analysis, reported in **Figure 36**, reveals an expected lowering in oligoesters melting temperature with respect to the staring high molecular weight biopolyemer (**Table 3**).

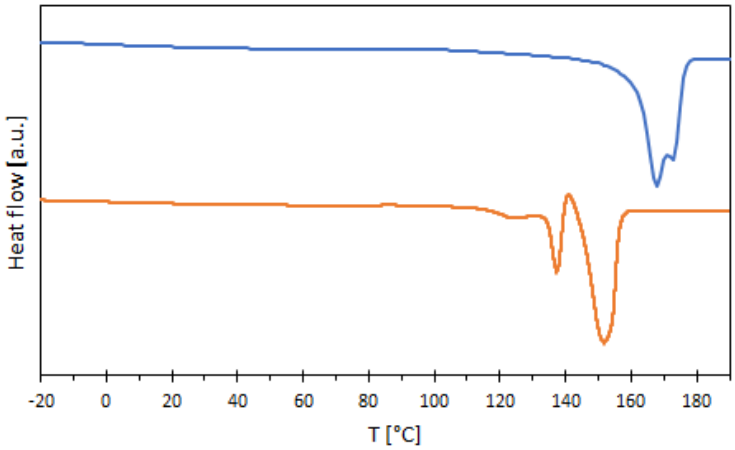

Figure 36. DSC thermogram (second heating) of starting PHB (**1**) (blue line) and prepared PHB-diol (**1**) (orange line).

The intent to derivatize PHB-diol hydroxyl terminals with proper chemicals forces an accurate determination of ***OHV*** in order to plan terminals methacrylation. In this case, ***OHV*** of prepared PHB-diol (**1**) was previously valued with the trifluoroacylation method

(**Table 8**). Thus, end-capping reaction of PHB-diol (**1**) hydroxyl groups with 2-isocyantoethyl methacrylate is performed (**Scheme 16**).

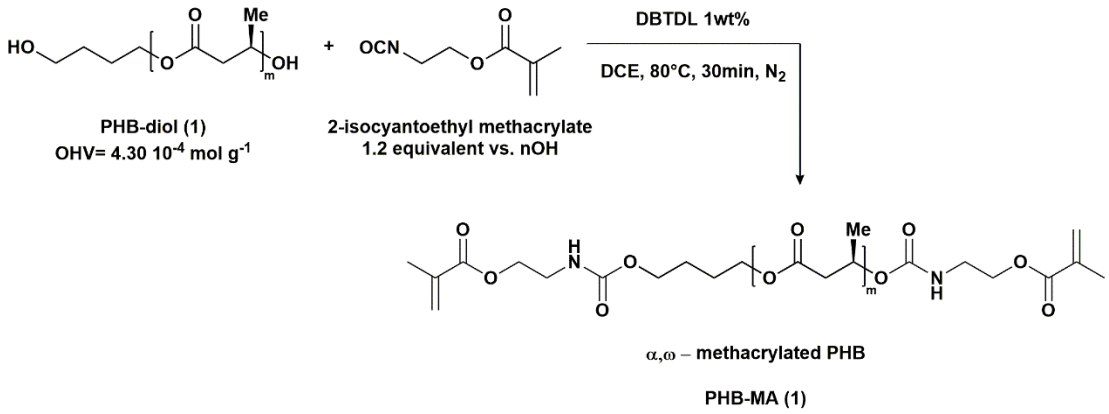

Scheme 16. Reaction condition for a complete hydroxyls end-cupping reaction.

Probably, due to PHB-diol (**1**) relatively high molecular weight (see **Table 8**), that impart low reactivity to terminal hydroxyl moieties, utilization of an acid catalyst is necessary to accomplish end-capping reaction. Kinetic of the process is studied through Fourier Transform Infrared Spectroscopy (FTIR). Specifically, an *on-line* monitoring of isocyante peak decreasing intensity (2227 cm^{-1}) proves the progress of the reaction. Indeed, as functionalization proceeds, isocyante groups are consumed by reaction with hydroxyl terminals that results in urethane bonds formation (**Figure 37**).

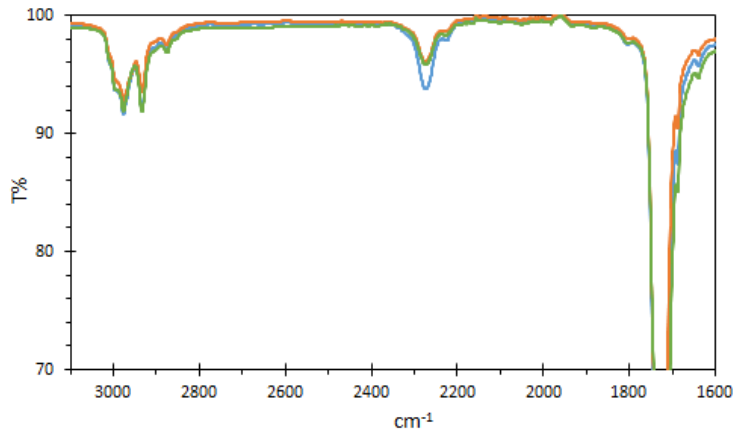

Figure 37. Kinetic study of PHB-diol (**1**) hydroxyl groups functionalization realized by FTIR spectroscopy (zoom on isocyanate peak region). Sample for analyses are collected after 15 minutes (blue line), 30 minutes (orange line) and 60 minutes (green line). Decrease of isocyanate peak at 2227 cm^{-1} is clearly observable.

Due to the utilization of a slight excess of isocyanate, reaction is considered complete when a time constant isocyante IR peak is detected. Achievement of α,ω-MethAcrylated PHB oligomers, PHB-MA (**1**), isolated by precipitation in cold methanol, is confirmed by proton NMR spectroscopy (**Figure 38**).

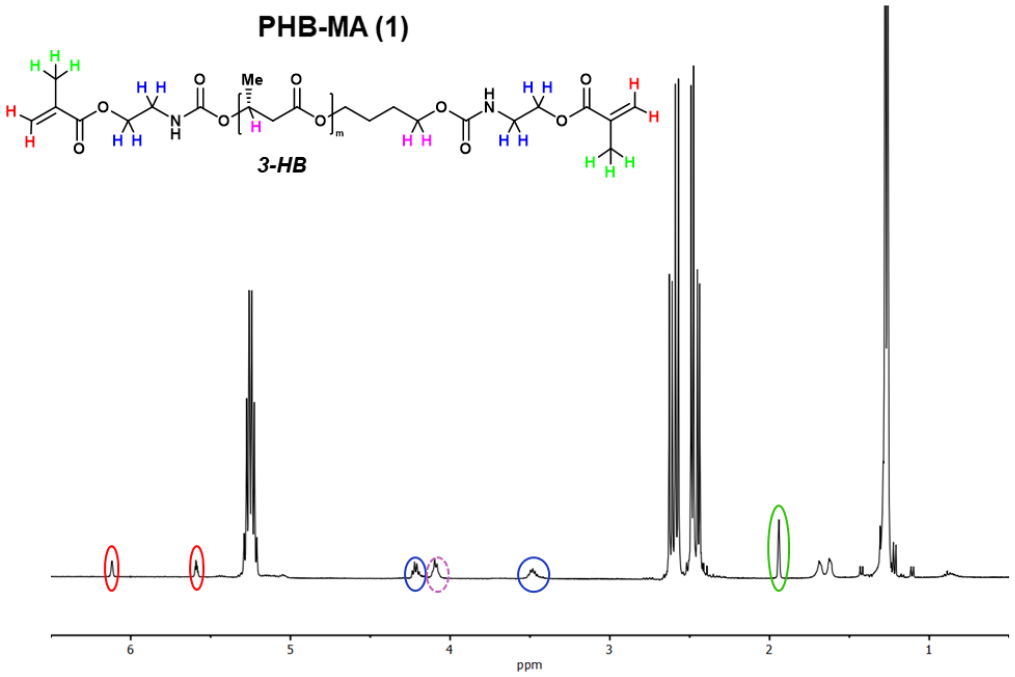

Figure 38. ^{1}H-NMR spectra of isolated PHB-MA (**1**).

Primary, NMR signals generated by the new ethyl methacrylate end-groups are unambiguously visible. Indeed, methylenic protons of the ethyl segment, blue circled in **Figure 38**, are observable. Even vinylic and methyl protons of methacrylate group, red and green circled respectively in **Figure 38**, are well distinguishable. Most important, shift of methine and methylenic polymer terminal protons signals, pink protons in **Figure 38**, confirms structure of prepared oligomers. Reasonably, functionalization does not affect oligoesters thermal properties and melting temperature remains unchanged (**Figure 39**).

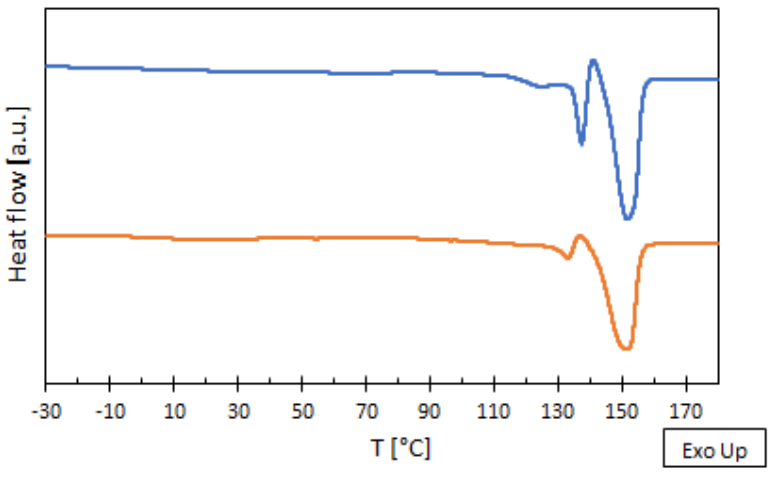

Figure 39. DSC thermogram (second heating) of starting PHB-diol (**1**) (blue line) and PHB-MA (**1**) (orange line).

Such a melting temperature (153 °C) clearly require utilization of an appropriate diluent to obtain a room temperature liquid PHB-based resin, suitable for vat photopolymerization. Therefore, by diluting PHB-MA (**1**) in 2-hydroxyethyl methacrylate (2-HEMA, **Figure 40**), a potential photoprintable resin is prepared

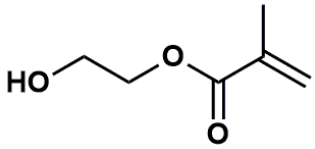

Figure 40. Chemical structure of 2-hydroxyethyl methacrylate.

2-HEMA is a monomer employable in photopolymerization that, being monofunctional, does not allow achievement of cross-linked macromolecular network through UV-irradiation. Thus, realization of a cross-linked polymer can be achieved only upon utilization of a cross-linking agent (**Figure 41**). Prepared bifunctional PHB-MA (**1**) is a potential candidate for such a role.

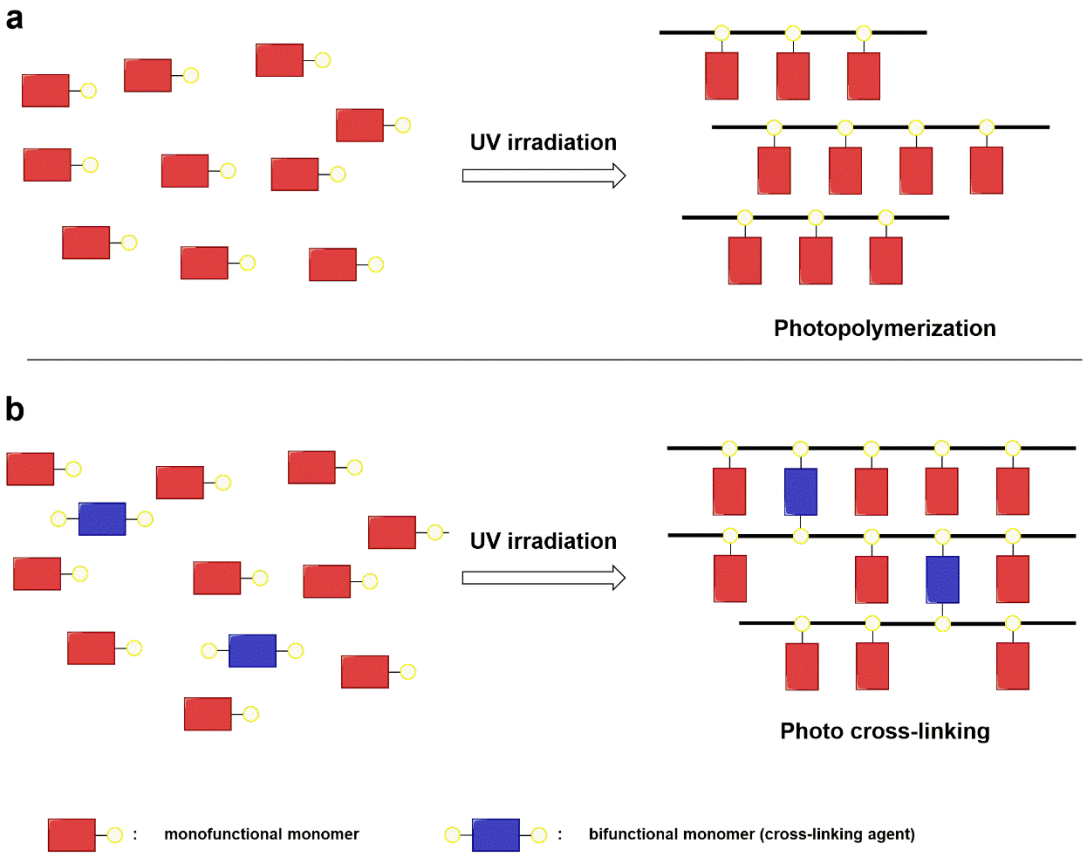

Figure 41. Schematic representation of a) photopolymerization of UV sensible monomers and b) photo cross-linking achievement due to bifunctional monomers.

Thus, a preliminary evaluation of prepared PHB-based oligoesters cross-linking ability in 3D printing conditions is attempted with the previously described resin. Obtainment of a

cross-linked object, characterized by insolubility and absence of melting, would clearly demonstrate PHB-MAs possible usage in such processes. Indeed, a 5wt% resin composed by PHB-MA (**1**) in 2-HEMA is prepared and, after photoinitiator addition, 2wt%, vat photopolymerized is attempted utilizing a stereolithography 3D printer. Due to the preliminary nature of the work, an extremely simple geometry is chosen and a square net is realized. Analyses carried out on the material reveal insolubly in chloroform, a good solvent for all the starting materials. In fact, a negligible weight-loss is observed after leaving the printed object in chloroform at room temperature for five days. Moreover, DSC analyses conducted on the printed object do not reveal occurrence of melting process (**Figure 42**).

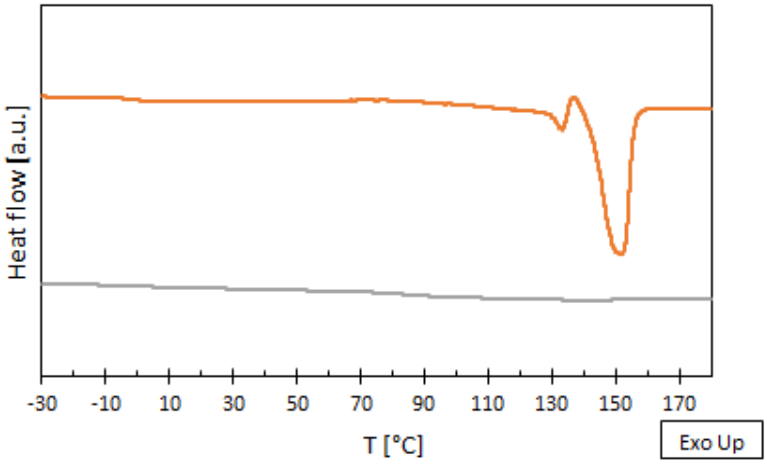

Figure 42. DSC thermogram (second heating) of starting PHB-MA (1) (orange line) and 3D printed object (grey line).

These preliminary results prove that PHB-MAs oligoesters can be effectively employed for realization of vat photopolymerized objects and encourage further investigations. However, before optimizing the printing process, possibilities to realize PHB-based macromonomers with a more effective and sustainable procedures are investigated. Indeed, chemical modifications that require utilization of expensive and toxic solvents have to be preferably avoided. This is more true dealing with sustainably produced materials as PHAs. Moreover, the inefficiency of the solution procedures in terms of reaction time and waste of reagent was previously pointed out. As a first step, individuation of a solvent-free procedure for realization of PHB-diols is achieved. As stated in the introduction, combination of relatively low temperature and fast reactive process could allow to react PHB in the melt without excessively degrade it. Thus, alcoholysis of PHB in the melt, performed with 1,4-butanediol, is conducted at 190°C. In

order to speed up the process and avoid excessive thermal degradation, titanium(IV) butoxide, $Ti(OBu)_4$, is used as transesterification catalyst (**Scheme 17**).

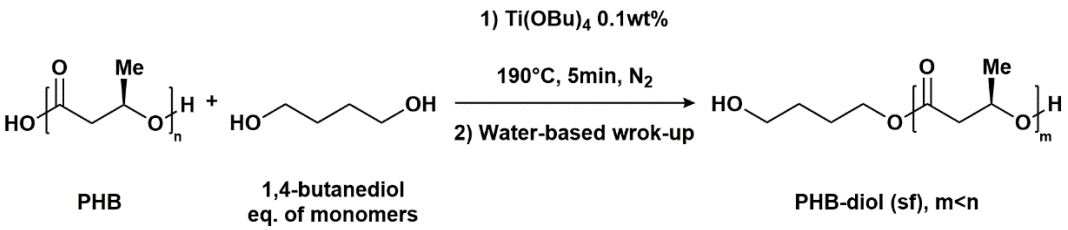

Scheme 17. Reaction condition for solvent-free preparation of PHB-diols.

As expected, utilization of catalyst unambiguously accelerate reaction and PHB-based oligoesters are obtained after just 5 minutes utilizing substoichiometric quantity of depolymerizing diol (see M_n in **Table 9**). Moreover, in addition to avoid utilization of expensive and toxic solvents, the proposed solvent-free methodology involves an extremely green work-up. A simple and room temperature water treatment allows to isolate PHB-diols and to hydrolyze traces of titanium catalyst (0.1wt%) to non-toxic titanium dioxide.

Reaction is conducted with various equivalent of diol and it is found out that such parameter has a huge effect on prepared PHB-diols structure. Indeed, it is reasonable retains that, at the begging of the alcoholysis, only PHB-diol **A** (see **Figure 43**) are formed. Nevertheless, proceeding of the reaction could results in establishment of a competition between diol and newly formed PHB-diol **A** in transesterifying high molecular weight PHB. Such competition leads to formation of PHB-diol **B** reported (**Figure 43**).

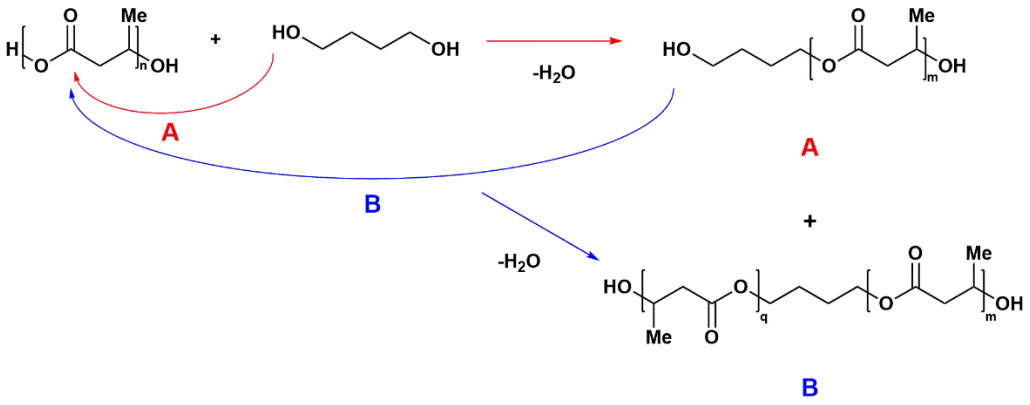

Figure 43. Schematic representation of PHB-diol **A** and PHB-diol **B** formation.

Formation of PHB-diol **B** have the effect to "consume" primary hydroxyl end-groups and, consequently, unbalance the overall hydroxyl terminals ratio. Thus, monitoring such a ratio could signalize occurrence of this process. For this reason, isolated PHB-diols,

prepared utilizing different equivalent of 1,4-butnaediol, are trifluoroacetylated following the previously established procedure (see **Figure 44**). After acquisition of ^{19}F-NMR spectra, ***OHV*** and hydroxyl rations ***OH^I/OH^{II}*** are calculated (**Table 9**).

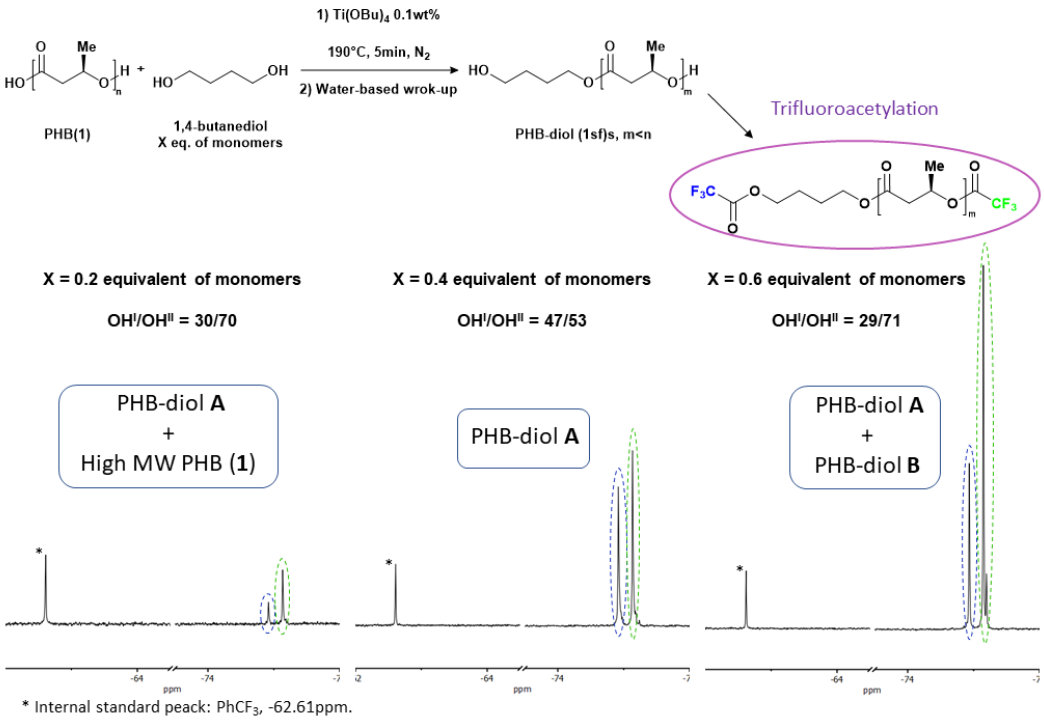

Figure 44. 19F-OHV recorded for prepared PHB-diol (**1sf**)s. Calculation of hydroxyl ratio (OH^I/OH^{II}) results in understanding structures.

Table 9. Properties of isolated PHB-diols in function of utilized amount of 1,4-butanediol.

Entry	1,4-butanediol (eq. of monomers)	M_n[a] [g·mol^{-1}]	OHV[b] [mol·g^{-1}]	OH^I/OH^{II}[b]	T_m[c] [°C]
0[d]	–	126 600	$0.10 \cdot 10^{-4}$	0/100	173
1	0.2	29 700	$1.10 \cdot 10^{-4}$	30/70	165
2	0.4	2 200	$8.91 \cdot 10^{-4}$	47/53	143
3	0.6	1 200	$13.9 \cdot 10^{-4}$	29/71	115

[a] Determined by GPC, [b] Determined by ^{19}F-NMR spectroscopy after PHB-diol hydroxyl groups trifluoroacetylation; [c] Determined by DSC second heat (heating and cooling rate 10°C/min): first heat to 195°C, cooling to -40°C; second heat to 195°C; [d] Starting PHB, not reacted.

Utilization of 0.2 monomers equivalent of 1,4-butanediol (entry **1**, **Table 9**) does not allow a complete transesterification. Indeed, a higher concentration of secondary hydroxyl groups in the isolated polymer can be explained by the persistence of high molecular weight PHB chains that does not undergo alcoholysis. Moreover, this hypothesis is supported by the DSC determined melting temperature (165°C), slightly lower then T_m of starting PHB (173°C, entry **0**, **Table 9**). Even the GPC valued number average molecular weight M_n is considerably higher with respect to the molecular

weight registered for the differently prepared analogues (entry **2** and **3**, **Table 9**). An opposite situation is encountered using 0.6 monomers equivalent of diol (entry **3**, **Table 9**). The observed high concentration of secondary hydroxyl end-groups (**Table 9**) is consistent with the presence of PHB-diol **B** (see **Figure 43**). Occurrence of such extra transesterifications is supported also by the very low determined T_m and M_n. (**Table 9**). On the other hand, utilization of 0.4 monomers equivalent of diol leads to a PHB-diol bearing an equal amount of primary and secondary hydroxyl groups. As for PHB-diol (**1**), obtainment of a dihydroxyl terminated oligoesters regularly structured (PHB-diol **A** in **Figure 43**) is confirmed by NMR spectroscopy (**Figure 45**).

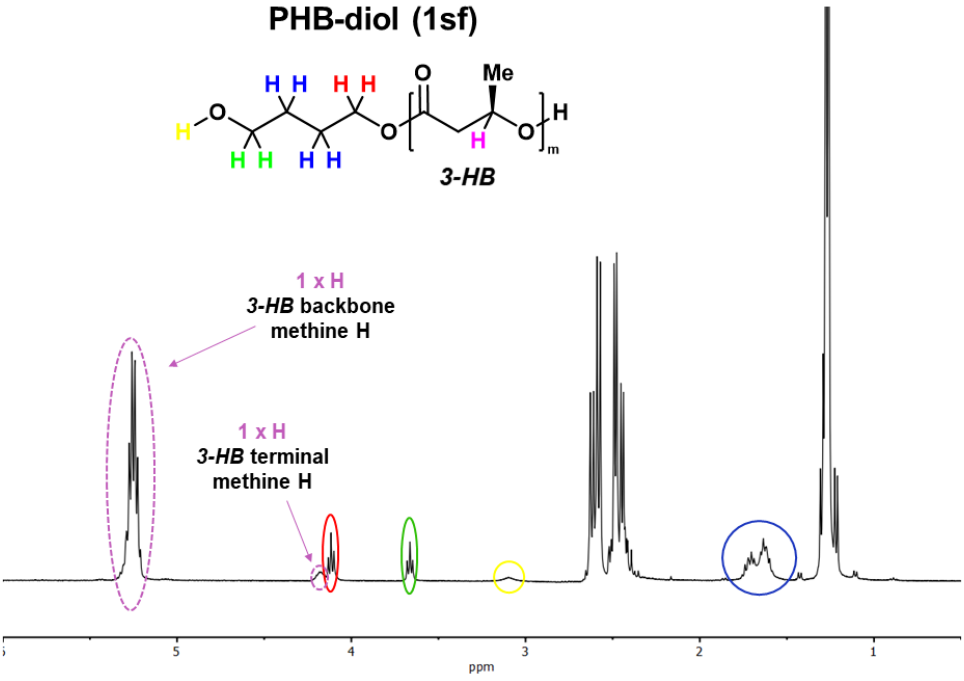

Figure 45a. ^{1}H-NMR spectrum of isolated PHB-diol (**1sf**) prepared in the optimized condition.

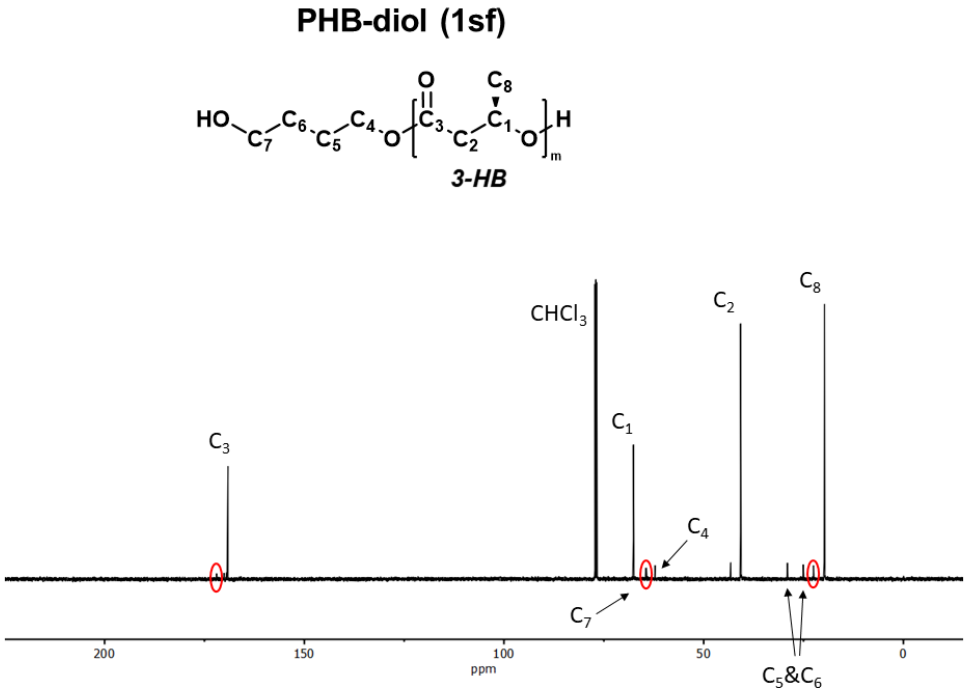

Figure 45b. ^{13}C-NMR spectrum of prepared PHB-diol (**1sf**). Presented spectrum, combined with HSCQ experiment (see **Figure 45c**), allows to assign carbon peaks and even identify signal produced by terminal group carbons (red circles, next to the signal of corresponding backbone analogous). Note that C_7 and terminal C_1 ^{13}C-NMR peaks has a very similar chemical shift (signals separation is not appreciable in reported spectrum.

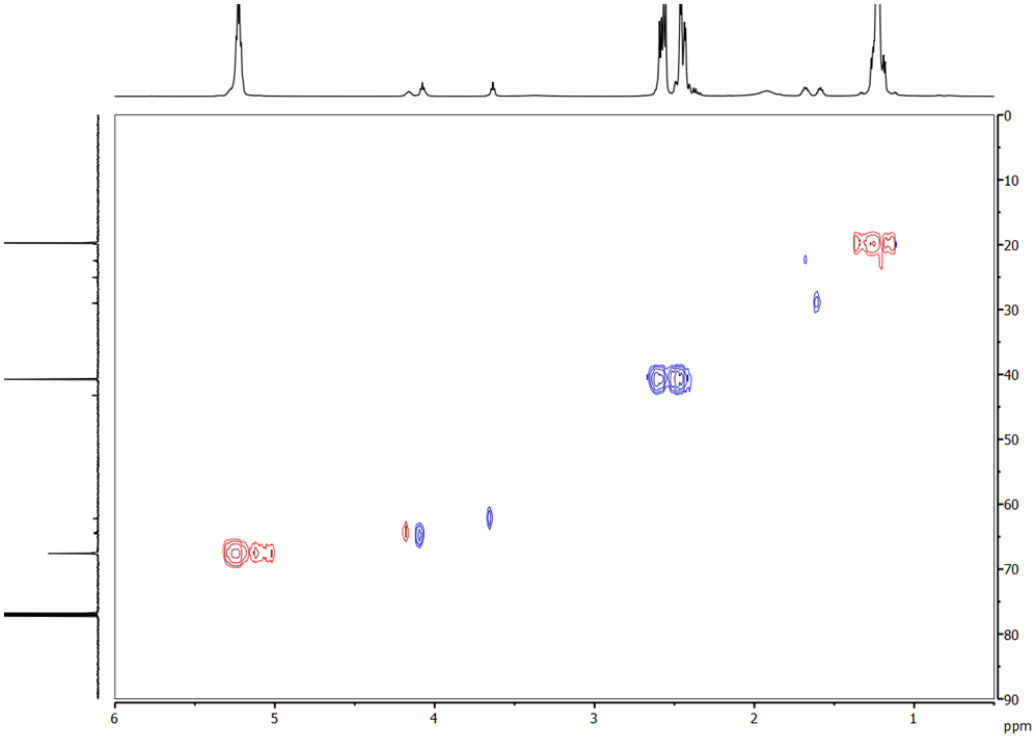

Figure 45c. HSQC spectrum of PHB-diol (**1sf**). HSQC experiments allow to distinguish secondary carbons (CH_2, red) from tertiary and primary carbons (CH and CH_3, blue). Correlating carbon and vicinal protons, such a technique is not able to identify quaternary carbons, as the carbonylic carbons. On the ^{13}C-NMR carbon axe, chloroform signal is observable (77.16ppm).

Once individuated reaction conditions to prepare PHB-oligomers 4-hydroxybutyl-terminated, *i.e.* PHB-diol **A** (**Figure 43**), possibility to modulate oligoesters molecular weight is investigated. Due to randomness of alcoholysis process, it is reasonable retain that varying starting PHB molecular weight results in preparation of PHB-diol **A** characterized by different molecular weight. Thus, keeping constant all reaction parameters, diverse PHB samples, characterized by different molecular weights, are reacted with 1,4-butanediol. In all the cases, a hydroxyl terminals ratio close to one is achieved, confirming obtainment of PHB-diol **A**. Moreover, as hypnotized, telechelic diols with lowering molecular weight are obtained and a sort of direct correlation among starting and final molecular weights seem to exist. Specifically, all the solvent-free prepared PHB-diols **A**, PHB-diol (**sf**), are reported in **Table 10** with the corresponding DSC and $\boldsymbol{OHV}$ analyses results. Analogously to previously in-solution prepared PHB-diols, even for PHB-diol **A** an $\boldsymbol{M_n}$ can be derived from the corresponding $\boldsymbol{OHV}$ according to **Equation 7**.

Table 10. Solvent-free prepared PHB-diol **A** and related properties.

Sample	Starting PHB[a]	OH^I/OH^{II}[b]	M_n[b] [mol·g^{-1}]	T_m[c] [°C]	T_c[c] [°C]	T_g[d] [°C]
PHB-diol (**1sf**)	PHB (**1**)	47/53	2200	143	66	-13
PHB-diol (**2sf**)	PHB (**2**)	43/57	1800	134	54	-19
PHB-diol (**3sf**)	PHB (**3**)	44/56	1600	133	51	-16

[a] Sample in molecular weight decreasing order, for $\boldsymbol{M_n}$ values see **Table 7**; [b] Ratio determined by ^{19}F-NMR spectroscopy after PHB-diol hydroxyl groups trifluoroacetylation; [c] Determined by DSC second heat (heating and cooling rate 10°C/min): first heat to 195°C, cooling to -40°C; second heat to 195°C; [d] Determined by DSC after a fast cooling from melt phase (195°C) and subsequent heat at 10°C/min to 195°C.

Reasonably, PHB-diols, being characterized by a low molecular weight, display lower glass transition temperature ($\boldsymbol{T_g}$, **Table 10**) with respect to high molecular weight counterparts (**Table 3**). Notwithstanding, the most relevant observation is the decrease in melting temperature $\boldsymbol{T_m}$. As previously stated, such an expected drop allows to react PHB-diols in the melt at temperature far enough from degradation condition. Indeed, end-capping process reported in **Scheme 16** could be easily conducted in solvent-free condition. Reaction, schematized in **Scheme 18**, is conducted on the oligoesters characterized by the lowest molecular weight, PHB-diol (**3sf**). Even in this case, kinetic of hydroxyl terminal derivatization is studied through FTIR (**Figure 46**). Probably, due to the high temperature achieved by solvent-free conditions, reaction is complete in just 10 minutes. Moreover, probably for the same reason, utilization of tin-based toxic catalyst is not necessary.

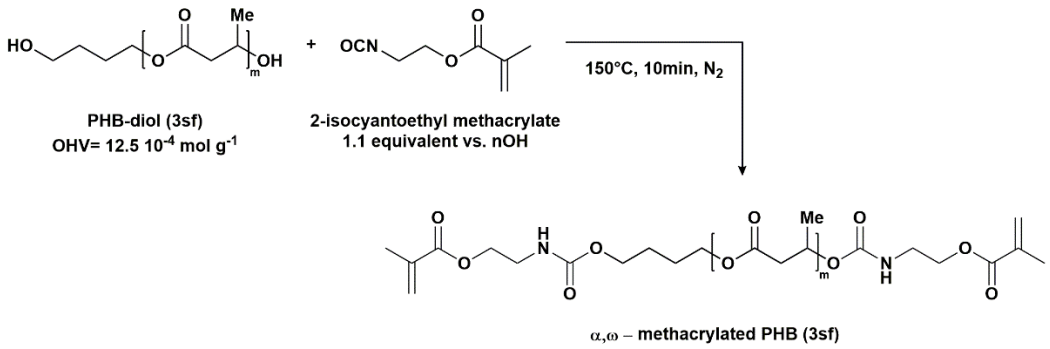

Scheme 18. Reaction condition for solvent-free end-capping of PHB-diol (**3sf**).

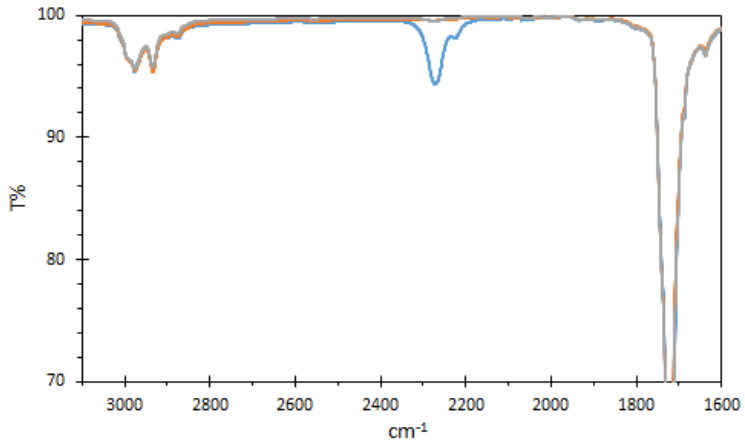

Figure 46. Kinetic study of PHB-diol (**3sf**) hydroxyl groups functionalization realized by FTIR spectroscopy (zoom on isocyanate peak region). Sample for analyses are collected at the beginning of the reaction (blue line), after 5 minutes (orange line) and 10 minutes (grey line). Decrease of isocyanate peak at 2227 cm^{-1} is clearly observable.

Excess of isocyante is removed applying vacuum and, even in this case, achievement of end-capping process is confirmed by ^{1}H-NMR (**Figure 47**).

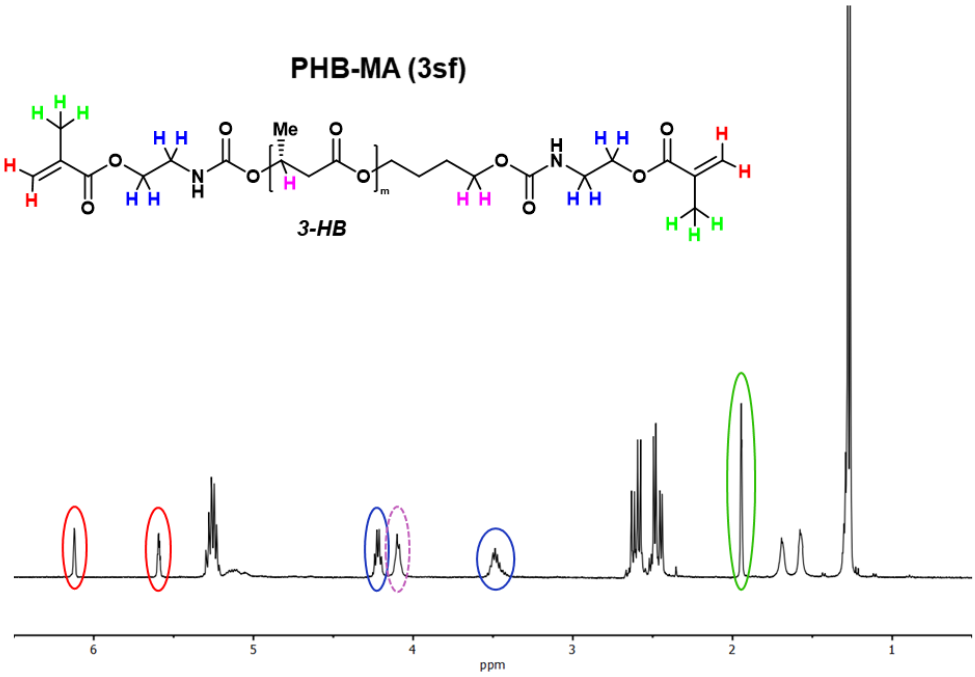

Figure 47. ^{1}H-NMR spectrum of prepared PHB-MA (**3sf**).

As for the in-solution prepared analogues (see **Figure 38**), peaks due to the newly introduced end-groups are observable. Moreover, the frequency shift that characterize methine and methylenic protons (pink protons in **Figure 47**) and disappearance of hydroxyl signals from the spectrum completely confirm accomplishment of the reaction.

Prepared PHB-MA (**3sf**) macromonomers is then diluted with propylene carbonate, a high boiling, non-toxic and non-reactive diluent. Due to the low molecular weight, a high concentrated resin, 60wt% of PHB-based macromonomers, was obtained at reasonable temperature (90°C). As a preliminary analysis, after addition of photoinitiator (2wt%), prepared resin is UV-irradiated to evaluate material response to light. As expected, recording FTIR spectra of the cured resin shows disappearance of carbon double bond signal of methacrylate moieties (1637 cm^{-1}, green circle in **Figure 48**) and allows to conclude that cross-linking took place.

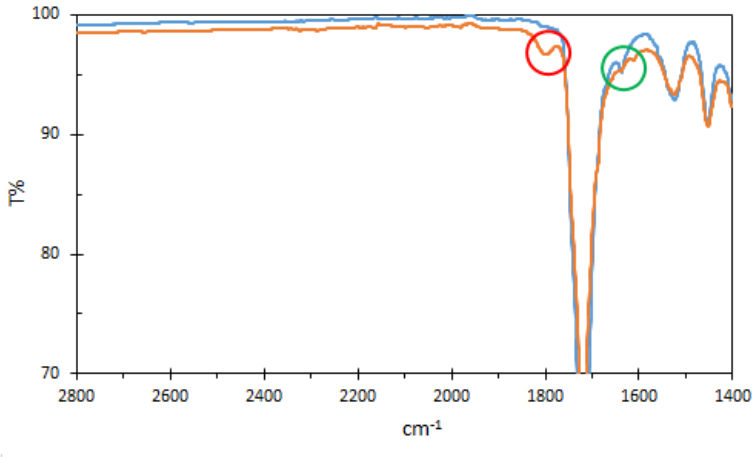

Figure 48. Comparison of FTIR spectra of PHB-MA (**3sf**) before (blue line) and after (orange line) UV irradiation carried out in presence of 2wt% of photoinitiator. Disappearance of double carbon bond signal of the methacrylic moieties is observable (green circle). Residual propylene carbonate is also visible (diluent carbonyl group signal, red circle).

4. Conclusions

Potential use of bacterially produced PHAs for the fabrication of advanced devices is investigated. Such biobased, bioproduced and biocompatible materials are fascinating candidates to be a real and sustainable alternative to nowadays widely spread petroleum-based polymers. The already intriguing biopolymers' properties can be further enhanced by incorporation of precise fillers into the polyester matrix to obtain advanced biocomposites. High abundancy and low cost of cellulosic fibers make this material an interesting biobased, biodegradable filler to enhance or even add potential functionalities to PHAs. Indeed, PHA-based reinforced with cellulosic fibrils were realized through well-established extrusion technology by utilization of the novel concept of cellulose polymeric dispersing agent. Collected SEM images highlighted good fibrils distribution and adhesion to thermoplastic matrix, but further studies are needed in this direction in order to evaluate MFC content effect on composites properties. On the other hand, utilization of well-known cells differentiation inducting fillers would result in preparation of devices suitable for tissue regeneration therapy. PHA biocompatibility and biodegradability allow usage of this polymer as a biomaterial and, after suitable preparation, osteoinductive inorganics filled scaffolds display a promising usage in bone tissue regeneration. Impressive properties have been displayed by the chemical modifications of enzymatic PHAs to explore opportunities offered by its derivatives and thus increasing the range of applications of PHAs.

An innovative analytical tool for characterizing PHAs and their derivates has been studied and validated by international standard techniques. This analytical method has been then employed to characterize low molecular weight di-hydroxyl terminated PHA-derivatives, which have been successfully used as a cross-linking agent in stereolithography 3D printing. Thus, efforts are made to identify a viable macromonomers preparation procedure that is more efficient than nowadays used methods and avoid the utilization of large excess of toxic solvents. It has to be underlined that versatility of the established procedure allows to prepare extremely diverse low molecular weight polyester derivatives concretely employable as PHA-based "building blocks" for the realization of advanced devices with even possibly tunable properties.

5. References

[1] G. Chen, Q. Wu; *Biomaterials* **2005**; 26; 6565.
[2] M. Lemoigne; *Ann Inst Pasteur* **1927**; 41; 148.
[3] A. Steinbüchel; *Macromol Biosci* **2001**; 1; 1.
[4] M.F. Chek, S. Kim, T. Mori, H. Arsad, M. Razip Samian, K. Sudesh, T. Hakoshima; *Sci Rep* **2017**; 7; 5312.
[5] L.-M. Ng, K. Sudesh; *J Biosci Bioeng* **2016**; 122; 550.
[6] Y. Elbahloul, A. Steinbüchel; *Appl Environ Microb* **2009**; 75; 643.
[7] M. Koller, R. Bona, E. Chiellini, E.G. Fernandes, P. Horvat, C. Kutschera, P. Hesse, G. Braunegg; *Bioresour Technol* **2008**; 99; 4854.
[8] A. Stanley, H.N. Punil Kumar, S. Mutturi, S.V.N. Vijayendra; *Appl Biochem Biotechnol* **2018**; 184; 935.
[9] A.B. Sathya, V. Sivasubramanian, A. Santhiagu, C. Sebastian, R. Sivashankar; *J Polym Environ* **2018**; 26; 3995.
[10] S.L. Riedel, C.J. Brigham, C.F. Budde, J. Bader, C.K. Rha, U. Stahl, A.J. Sinskey; *Biotechnol and Bioeng* **2013**; 110; 461.
[11] M. Koller, H. Niebelschütz, G. Braunegg; *Eng Life Sci* **2013**; 13; 549.
[12] N. Jacquel, C.W. Lo, Y.-H. Wei, H.S. Wu, S.S. Wang; *Biochem Eng J* **2008**; 39; 15.
[13] C. Samorì, F. Abbondanzi, P. Galletti, L. Giorgini, L. Mazzocchetti, C. Torri, E. Tagliavini; *Bioresource Technol* **2015**; 189; 195.
[14] C. Samorì, M. Basaglia, S. Casella, L. Favaro, P. Galletti, L. Giorgini, D. Marchi, L. Mazzocchetti, C. Torri, E. Tagliavini; *Green Chem* **2015**; 17; 1047.
[15] K.Srirangan, X. Liu, T.T. Tran, T.C. Charles, M. Moo-Young, C.P. Chou; *Sci Rep* **2016**; 6; 36470.
[16] G. Jiang, D.J. Hill, M. Kowalczuk, B. Johnston, G. Adamus, V. Irorere, I. Radecka; *Int J Mol Sci* **2016**; 17; 1157.
[17] C. Nielsen, A. Rahman, A.U. Rehman, M.K. Walsh, C.D. Miller; *Microbial Biotechnology* **2017**; 10; 1338.
[18] M. Koller, R. Bona, G. Braunegg, C. Hermann, P. Horvat, M. Kroutil, J. Martinz, J. Neto, L. Pereira, P. Varila; *Biomacromolecules* **2005**; 6; 561.
[19] S.S. Sawant; B.K. Bipinchandra, B.S. Kim; *Int J Biol Macromol* **2018**; 109; 1012.
[20] D.P. Tamboli, S.S. Gomare, S.S. Kalme, U.U. Jadhav, S.P. Govindwar; *Int Biodeter Biodegr* **2010**; 64; 755.
[21] M.W. Guzik, S.T. Kenny, G.F. Duane, E. Casey, T. Woods, R.P. Babu, J. Nikodinovic-Runic, M. Murray, K.E. O'Connor; *Appl Microbiol Biotechnol* **2014**; 98; 4223.
[22] F. Sabbagh, I.I. Muhamad; *Renewable and Sustainable Energy Reviews* **2017**; 72; 95.
[23] J. Asrar, J. C. Hill; *J Appl Polym Sci* **2002**; *83*, 457.
[24] E. Bugnicourt, P. Cinelli, A. Lazzeri, V. Alvarez; *eXPRESS Polymer Letters* **2014**; *8*, 791.
[25] D.B. Hazer, E. Kiliçay, B. Hazer; *Mater. Sci. Eng. C* **2012**; 32; 637.
[26] A. Ferre-Guell, J. Winterburn; *Biomacromolecules* **2018**; 19; 996.
[27] N. Zhila, E. Shishatskaya; *Int J Biol Macromol* **2018**; 111; 1019.
[28] F. Sabbagh, I.I. Muhamad; *Renew Sust Energ Rev* **2017**; 72; 95.
[29] M. Kunioka, A. Tamaki, Y. Doi; *Macromolecules* **1989**; 22; 694.
[30] Q. Ren, G. de Roo, J.B. van Beilen, M. Zinn, B. Kessler, B. Witholt; *Appl Microbiol Biotechnol* **2005**; 69; 286.
[31] W.M. Pachekoski, J.A.M. Agnelli, L.P. Belem; *Mater Res* **2009**; 12; 159.
[32] T. Lütke-Eversloh, K. Bergander, H. Luftmann, A. Steinbüchel; *Biomacromolecules* **2001**; 2; 1061.
[33] T. Lütke-Eversloh, A. Fischer, U. Remminghorst, J. Kawada, R.H. Marchessault, A. Bögershausen; M. Kalwei, H. Eckert, R. Reichelt, S.-J. Liu, A. Steinbüchel; *Nature Mater* **2002**; 1; 236.
[34] D.Y. Kim, T Lütke-Eversloh, K. Elbanna, N. Thakor, A. Steinbüchel; *Biomacromolecules* **2005**; 6; 897.
[35] M. Kunioka, Y. Doi; *Macromolecules* **1989**; 23; 1933.
[36] A.M. Silva; *Chem Phys Lett* **2007**; 439; 8.
[37] M. Kunioka, Y. Doi; *Macromolecules* **1990**; 23; 1933.
[38] D.M. Panaitescu, C.A. Nicolae, A.N. Frone, I. Chiulan, P.O. Stanescu, C. Draghici, M. Iorga, M. Mihailescu; *J Appl Polym Sci* **2017**; 134; 44810.
[39] I.T. Seoane, L.B. Manfredi, V.P. Cyras; *J Appl Polym Sci* **2018**; 46016.
[40] C. Wilkes, J. Summers, C. Daniels; *PVC handbook*; Hanser Publications; **2005**.
[41] M.G.A. Vieira, M.A. da Silva, L.O. dos Santos, M.M. Beppu; *Eur Polym J* **2011**; 47; 254.
[42] J. Li, T. Fukuoka, Y. He, H. Uyama, S. Kobayashi, Y. Inoue; *J Appl Polym Sci* **2005**; 97; 2439.
[43] K. Bahari, H. Mitomo, T. Enjoji, F. Yoshii, K. Makuuchi; *Polym Degrad Stabil* **1998**; 61; 245.

[44] S. Hong, Y. Lin, C. Lin; *J Appl Polym Sci* **2008**; 110; 2718.
[45] C. Chen, B. Fei, S. Peng, Y. Zhuang, L. Dong, Z. Feng; *J Appl Polym Sci* **2002**; 84; 1789.
[46] K. Chen, C.A. Wilkie, S. Vyazovkin; *J Phys Chem B* **2007**; 111; 12685.
[47] M. Erceg, T. Kovačić; I. Klarić; *Thermochimica Acta* **2009**; 485; 26.
[48] P. Polyák, E. Dohovits, G.N. Nagy, B.G. Vértessy, G. Vörös, B. Pukánszky; *Int J Biol Macromol* **2018**; 112; 156.
[49] L.S. Nair, C.T. Laurencin; *Prog Polym Sci* **2007**; 32; 762.
[50] R. Langer, D.A. Tirrell; *Nature* **2004**; 428; 487.
[51] P. Bailon, C. Won; *Expert Opin Drug Del* **2009**; 6; 1.
[52] F. Seidi, R. Jenjob, D. Crespy; *Chem Rev* **2018**; 118; 3965.
[53] G. Niu, A.B. Djaoui, D. Cohn; *Polymer* **2011**; 52; 2524.
[54] Y. Qiu, K. Park; Adv Drug Deliver Rev 2001; 53; 321.
[55] N.A. Chartrain, C.B. Williams, A.R. Whittington; *Acta Biomater* **2018**; 74; 90.
[56] F.P.W. Melchels, J. Feijen, D.W. Grijpma; *Biomaterials* **2010**; 31; 6121.
[57] J.M. Lee, S.L. Sing, M. Zhou, W.Y. Yeong; *Int J Bioprint* **2018**; 4; 151.
[58] X. Wang, M. Jiang, Z. Zhou, J. Gou, D. Hui; *Compos Part B* **2017**; 110; 442.
[59] J.R. Tumbleston, D. Shirvanyants, N. Ermoshkin, R. Janusziewicz, A.R. Johnson, D. Kelly, K. Chen, R. Pinschmidt, J.P. Rolland, A. Ermoshkin, E.T. Samulski, J.M. DeSimone; *Science* **2015**; 347; 1349.
[60] H.O.T. Ware, A.C. Farsheed, E. Baker, G. Ameer, C. Sun; *Procedia CIRP* **2017**; 65; 131.
[61] S. Schüller-Ravoo, J. Feijen, D.W. Grijpma; *Macromol Biosci* **2011**; 11; 1662.
[62] L. Shen, Y. Wang, Q. Zhao, F. Luo, J. Chen, M. Lu, L. Liang, K. Wu, J. Shi; *Polym Int* **2016**; 65; 1150.
[63] C.J. Bloomquist, M.B. Mecham, M.D. Paradzinsky, R. Janusziewicz, S.B. Warner, J.C. Luft, S.J. Mecham, A.Z. Wang, J.M. DeSimone; *J Control Release* **2018**; 278; 9.
[64] M. Zarek, M. Layani, I. Cooperstein, E. Sachyani, D. Cohn, S. Magdassi; Adv Mater 2016; 28; 4449.
[65] F. Rehfeldt, A.J. Engler, A. Eckhardt, F. Ahmed, D.E. Discher; *Adv Drug deliver Rev* **2007**; 59; 1329.
[66] F. Rengier, A. Mehndiratta, H. von Tengg-Kobligk, C.M. Zechmann, R. Unterhinninghofen, H.-U. Kauczor, F.L. Giesel; *Int J CARS* **2010**; 5; 335.
[67] F. Lin, J. Zheng, J. Yu, J. Zhou, M.L. Becker; *Biomacromolecules* **2013**; 14; 2857.
[68] Q. Zhang, V.N. Mochalin, I. Neitzel, I.Y. Knoke, J. Han, C.A. Klug, J.G. Zhou, P.I. Lelkes, Y. Gogotsi; *Biomaterials* **2011**; 32; 87.
[69] L.E. Ling, L. Feng, H. Liu, D. Wang, Z. Shi, J. Wang, W. Luo, Y. Lv; *J Biomed Mater Res A* **2015**; 103A; 1732.
[70] D. Steffens, D.I. Braghirolli, N. Maurmann, P. Pranke; *Drug Discov Today* **2018**; 23; 1474.
[71] J.M. Ferri, I. Gisbert, D. García-Sanoguera, M.J. Reig, R. Balart; *J Compos Mater* **2016**; 50; 4189.
[72] M. Titz, K.H. Kettl, K. Shahzad, M. Koller, H. Schnitzer, M. Narodoslawsky; *Clean Techn Environ Policy* **2012**; 14; 495.
[73] S. Heux, I. Meynial, M.J. O'Donohue, C. Dumon; *Biotechnology Advances* **2015**; 33; 1653.
[74] J. Ye; D. Hu, X. Che; X. Jiang, T. Li, J. Chen, H.M. Zhang, G. Chen; *Metab Eng* **2018**; 47; 143.
[75] S.A. Dahoumane, M. Mechouet, K. Wijesekera, C.D.M. Filipe, C. Sicard, D.A. Bazylinski, C. Jeffryes; *Green Chem* **2017**; 19; 552.
[76] R.A. Sheldon; *J R Soc Interface* **2016**; 13; 20160087.
[77] E. Champagne, S. Strandman, X. Zhu; *Macromol Rapid Comm* **2016**; 37; 1986.
[78] K. Żółtowska, E. Oledzka, M. Kuras, A. Skrzypzak, G. Nałęcz-Jawecki, M. Sobczak; Int *J Polym Mater Po* **2017**; 66; 768.
[79] R. Julio, J. Albet, C. Vialle, C. Vaca-Garcia, C. Sablayrolles; *Biofuels, Bioprod Bioref* **2017**; 11; 373.
[80] C. De Pretto, R. de Lima Camargo Giordano, P.W. Tardioli, C.B.B. Costa; *Waste Biomass Valor* **2018**; 9; 1703.
[81] S. Maina, V. Kachrimanidou, A. Koutinas; *Curr Opin Green Sustain Chem* **2017**; 8; 18.
[82] IUPAC; *Pure Appl Chem* **1996**; 68; 2287.
[83] C. Sanfilippo, A. Patti, M.A. Dettori, D. Fabbri, G. Delogu; *J Mol Catal B-Enzym* **2013**; 90; 107.
[84] R. Kourist, U.T. Bornscheuer; *Appl Microbiol Biotechnol* **2011**; 91; 505.
[85] M.D. Patil, G. Grogan, A. Bommarius, H. Yun; *Catalysts* **2018**; 8; 254.
[86] J.E. Kemnitzer, S.P. McCarthy, R.A. Gross; *Macromolecules* **1993**; 26; 1221.
[87] J.E. Kemnitzer, S.P. McCarthy, R.A. Gross; *Macromolecules* **1992**; 25; 5927.
[88] M.R. Timmins, R.W. Lenz, P.J. Hocking, R.H. Marchessault; *Macromol Chem Phys* **1996**; 197; 1193.
[89] P.J. Hocking, R.H. Marchessault, M.R. Timmins, R.W. Lenz, R. Clinton Fuller; *Macromolecules* **1996**; 29; 2472.
[90] Y. Hori, M. Suzuki, A. Yamaguchi, T. Nishishita; *Macromolecules* **1993**; 26; 5533.
[91] H. Wölfle, H. Kopacka, K. Wurts, P. Preishuber-Pflügl, B. Bildstein; *J Organomet Chem* **2009**; 694; 2493.

[92] D. Seebach, M. Züger; *Helv Chim Acta* **1982**; 65; 495.
[93] C. Gioa, M. Vannini, P. Marchese, A. Minesso, R. Cavalieri, M. Colonna, A. Celli; *Green Chem* **2014**; 16; 1807.
[94] D.S. Achilias, E. Panayotidou, I. Zuburtikudis; *Thermochimica Acta* **2011**; 514; 58.
[95] G. Siqueira, J. Bras, A. Dufresne; *Polymers* **2010**; 2; 728.
[96] H. Shaghaleh, X. Xu, S. Wang; *RSC Adv* **2018**; 8; 825.
[97] I. Siró, D. Plackett; *Cellulose* **2010**; 17; 459.
[98] N. Lavoine, I. Desloges, A. Dufresne, J. Bras; *Carbohyd Polym* **2012**; 90; 735.
[99] N. Lavoine, I. Desloges, A. Dufresne, J. Bras, *Carbohydrate Polymers* **2012**; 90; 735.
[100] A. Dufresne; *Mater Today* **2013**; 16; 220.
[101] M.E. Malainine, A. Dufresnea, D. Dupeyrea, M. Mahrouz, R. Vuong, M.R. Vignon; *Carbohydrate Polymers* **2003**; 51; 77.
[102] X. Qi, G. Yang, M. Jing, Q. Fu, F. Chiu; *J Mater Chem A* **2014**; 2; 20393.
[103] N. Lin, J. Huang, A. Dufresne; *Nanoscale* **2012**; 4; 3274.
[104] E.L. Hult, P.T. Larsson, T. Iversen; *Polymer* **2001**; 42; 3309.
[105] D. Sandquist; *Appita Journal* **2013**; 66; 156.
[106] S. Andreotti, E. Franzoni, M. Degli Esposti, P. Fabbri; *Materials* **2018**; 11; 165.
[107] E. Akaraonye, J. Filip, M. Safarikova, V. Salih, T. Keshavarz, J.C. Knowles, I. Roy; *Polym Int* **2016**; 65; 780.
[108] R. Grande, L.A. Pessan, A.J.F. Carvalho; *Carbohyd Polym* **2018**; 191; 44.
[109] D.F. Parra, J. Fusaro, F. Gaboardi, D.S. Rosa; *Polym Degrad Stabil* **2006**; 91; 1954.
[110] G. Wang, M. Jiang, Q. Zhang, R. Wang, X. Qu, G. Zhou; *Polym Degrad Stabil* **2018**; 153; 292.
[111] R.T.H. Chan, H. Marçal, R.A. Russel, P.J. Holden, L.J.R. Foster; *Int J Polym Sci* **2011**; 473045.
[112] Q. Fu, C. Duan, Z. Yan, Y. Li, Y. Si, L. Liu, J. Yu, B. Ding; *Macromol Rapid Commun* **2018**; 39; 1800058.
[113] A. Basu, K.R. Kunduru, E. Abtew, A.J. Domb; *Bioconjugate Chem* **2015**; 26; 1396.
[114] J.J. Vranckk, M.D. Hondt; *Innov Surg Sci* **2017**; 2; 189.
[115] V.V. Lunyak, A. Amaro-Ortiz, M. Gaur; *Front Genet* **2017**; 8; 220.
[116] S. Sayyar, D.L. Officer, G.G. Wallace; *J Mater Chem B* **2017**; 5; 3462.
[117] G. Jin, R. He, B. Sha, W. Li, H. Qing, R. Teng, F. Xu; *Mater Sci Eng B* **2018**; 92; 995.
[118] T. Lu, Y. Li, T. Chen; *Int J Nanomed* **2013**; 8; 337.
[119] T. Tsujimoto, N. Hosoda, H. Uyama; *Polymers* **2016**; 8; 66.
[120] J. Kent Leach, J. Whitehead; *Biomater Sci Eng* **2018**; 4; 1115.
[121] H. Lian, L. Zhang, Z. Meng; *Mater Design* **2018**; 156; 381.
[122] F.P.W. Melchels, J. Feijen, D.W. Grijpma; *Biomaterials* **2010**; 31; 6121.
[123] N.A. Chartrain, C.B. Williams, A.R. Whittington; *Acta Biomater* **2018**; 74; 90.
[124] E. Bugnicourt, P. Cinelli, A. Lazzeri, V. Alvarez; *Express Polym Lett* **2014**; 8; 791.
[125] F.P.W. Melchels, J. Feijen, D.W. Grijpma; *Biomaterials* **2009**; 30; 3801.
[126] J. Liu, J. Zhang, B. Zhang, X. Zhang, L. Xu, J. Zhang, J. He, C.-Y. Liu; *Cellulose* **2016**; 23; 2341.
[127] M.P.M. da Costa, M.C. Delpech, I.L. de Mello Ferreira, M.T. de Macedo Cruz, J.A. Castanharo, M.D. Cruz; *Polym Test* **2017**; 63; 427.
[128] M. Dannoux, P. Cassagnau, A. Michel; *Can J Chem Eng* **2002**; 80; 1075.
[129] Y. Aoyagi, K. Yamashita, Y. Doi; *Poly Degrad Stabil* **2002**; 76; 53.
[130] E. Le Roux; *Coordin Chem Rev* **2016**; 306; 65.
[131] T. Debuissy, E. Pollet, L. Avérous; *Eur Polym J* **2017**; 90; 92.
[132] I. Pesneau, M. Grégoire, A. Michel; *J Appl Polym Sci* **2000**; 79; 1556.
[133] T. Debuissy, E. Pollet, L. Avérous; *J Polym Sci Pol Chem* **2017**; 55; 1949.
[134] S. Amiya, K. Mathumara, T. Taniguchi; *Anal Sci* **1991**; 7; 1649.
[135] J.L Espartero, I. Rashkov, S.M. Li, N. Manolova, M. Vert; *Macromolecules* 1996; 29; 3535.
[136] J.H. Lee, Y. Okuno, S. Cavagnero; *J Magn Reson* **2014**; *241*; 18.
[137] J. Liu, L. Liu; *Macromolecules* **2004**; 37; 2674.
[138] B. Fortunato, F. Pilati; P. Manaresi; *Polymer* **1981**; 22; 655.
[139] H. Chen, J. Jia, W. Zhang, J. Kong; *Polymer Testing* **2014**; 35; 28.
[140] G.D.B. van Houwelingen, M.W.M. G. Peters, W.G.B. Huysmans; *Fresenius Z Anal Chem.* **1978**; *293*; 396.
[141] S. Al-AbdulRazzak, E.A. Lofgren, S.A. Jabarin; *Polym Int* **2002**; 51; 174.
[142] S.R.K. Chalasani, S. Dewasthale, E. Hablot, X. Shi, D. Gravier, R. Narayan; *J Am Oil Chem Soc* **2013**; *90*; 1787.
[143] V.L. Rendina, J.S. Kingsbury; *J Org Chem* **2012**; 77; 1181.
[144] T. Amari, K. Nishimura, K. Minou, A. Kawabata, Y. Ozaki; *J Polym Sci Part A* **2001**; 39; 665.

[145] A.M. Kenwright, S.K. Peace, R.W. Richards, A. Bunn, W.A. MacDonald; *Polymer* **1999**; 40; 2035.
[146] J.T. Gerig; Fluorine NMR **1997**; in *On-Line Biophysics Textbook* (Bloomfield, V., Ed.) Biophysical Society; Bethesda MD.
[147] W. He, F. Du, Y. Wu, Y. Wang, X. Liu, H. Liu, X. Zhao; *J Fluorine Chem* **2006**; 127; 809.
[148] V. Pourcelle, C.S. Le Duff, H. Freichels, C. Jérôme, J. Marchand-Brynaert; *J Fluorine Chem* **2012**; 140; 62.
[149] A. Moghimi, I. Omrani, M. R. Nabid, M. Mahmoodi; *European Polymer Journal* **2013**; *49*; 228.
[150] S.L. Manatt; *J Am Chem Soc* **1966**; 88; 1323.
[151] A. Spyros, D.S. Argyropoulos, R.H. Marchessault; *Macromolecules* **1997**; 30; 327.
[152] A. Athlan, C. Braud, M. Vert; *J Enviroment Polym Degrad* **1997**; 5; 243.
[153] M. Pierini, C. Di Bella, B. Dozza, T. Frisoni, E. Martella, C. Bellotti, D. Remondini, E. Lucarelli, S. Giannini, D. Donati; *J. Bone Joint Surg. Am.* **2013**; 95; 1101.
[154] C. Bellotti, C. Capanni, G. Lattanzi, D. Donati, E. Lucarelli, S. Duchi; *Springerplus* **2016**; 5, 1427.
[155] C.P. Rosenau, B.J. Jelier, A.D. Gossert and A. Togni, *Angewandte Chemie International Edition,* 2018, **57**, 9528.
[156] L.H. Kang, P.A. Armstrong, L.J. Lee, B. Duan, K.H. Kang, J.T. Butcher; *Ann Biomed Eng* **2017**; 45; 360.